

Copyright is owned by the Author of the thesis. Permission is given for a copy to be downloaded by an individual for the purpose of research and private study only. The thesis may not be reproduced elsewhere without the permission of the Author.

Investigation into the Inheritance and Biochemistry of Chondrodysplasia in Texel Sheep

A thesis presented in partial fulfilment of the requirements for the
Master of Science
at Massey University,
Palmerston North, New Zealand.

Timothy John Byrne

2005

Acknowledgements

Foremost I would like to express thanks to my supervisors, Professor Hugh Blair, Kathryn Stowell, and Professor Keith Thompson for their continued support and guidance throughout.

Thank you to the scholarship providers including Meat New Zealand and Gisborne Veterinary Club Charitable Trust for their interest in, and support of, the project, and to Palmerston North Medical Research Foundation for their funding.

I would like to acknowledge Graeme Poole and Susan Ellicott for their cooperation and contribution to aspects of the research.

I extend thanks to all the members of my lab-group and office. Those who contributed significantly to whom I would especially like to extend my appreciation include: John Tweedie, Mark Patchett, Rao Dukupati, Robyn Marston, Carole Flyger, Amram Williams, Kelly Senior, Henning Koehn, Natisha Magan, and Yuliana Yosaatmadja.

Lastly, and most importantly, I would like to thank my family and friends not yet mentioned.

Abstract

A skeletal chondrodysplasia characterized by dwarfism and angular deformity of the forelimbs has been recognized over four seasons in Texel and Texel cross lambs on three related properties. Some affected lambs have normal co-twins indicating that the disease is not dietary, but likely to be the result of a genetic disorder. This study reports on the inheritance and biochemistry of this newly discovered chondrodysplasia in Texel sheep. The outcome of a backcross trial between putative carrier ewes and affected rams provided evidence that indicated that the chondrodysplasia has an autosomal recessive mode of inheritance, and that it is likely to be caused by a single gene defect. Analysis of proteoglycan constituents of cartilage by SDS-PAGE, followed by sulfate-specific staining indicated that the biochemical abnormality lies in the level of sulfation of proteoglycans in the extracellular matrix of affected animals. It was also shown by SDS-PAGE that there were no differences in the major collagen constituents of cartilage between unaffected and affected animals. A candidate gene, the diastrophic dysplasia sulfate transporter, was determined based on its involvement in the process of sulfation of proteoglycans and its involvement in characterized human dysplasias, which resemble Texel chondrodysplasia both phenotypically and biochemically. PCR amplification and sequencing of 85.4 % of this gene revealed no nucleotide differences between the exonic DNA of normal, carrier, and affected animals. While this reduced the likelihood that this gene is causative in the chondrodysplasia, it does not eliminate it as a candidate, based on the fact that a mutation may exist in the region not sequenced, including the possibility of splice site mutations.

Abbreviations

ACG -1B	Achondrogenesis type 1B
AO2	Atelosteogenesis type 2
APS	Adenosine-phosphosulfate
ATP	Adenosine triphosphate
ATPSK2	Adenosine triphosphate sulfurylase/ Adenosine-phosphosulfate kinase 2 gene
bm	Brachymorphic
BSA	Bovine serum albumin
cDNA	Synthetic DNA, generated from RNA
cmd	Cartilage matrix deficiency
COL1	Collagen 1 protein domain
COL2A1	Collagen type II alpha 1 gene
COL3	Collagen 3 protein domain
COL9A1	Collagen type IX alpha 1 gene
COL9A2	Collagen type IX alpha 2 gene
COL9A3	Collagen type IX alpha 3 gene
COL10A1	Collagen type X alpha 1 gene
COL11A1	Collagen type XI alpha 1 gene
COL11A2	Collagen type XI alpha 2 gene
CSPGs	Chondroitin sulfate proteoglycans
DDSH	Dyssegmental dysplasia, Silverman- Handmaker type
Dmm	Disproportionate micromelia
DNA	Deoxyribose Nucleic Acid
dNTP	Deoxynucleoside triphosphate (dATP, dTTP, dCTP, dGTP)
DTDST	Diastrophic dysplasia sulfate transporter
DTT	Dithiothreitol

ECM	Extracellular Matrix
EDTA	Ethylene diamine tetra-acetic acid
FACIT	Fibril- associated with interrupted triple helices
FGFR3	Fibroblast growth factor receptor 3 gene
GAG	Glycosaminoglycan
GCG	Genetics Computer Group
HPLC	High performance liquid chromatography
Hspg2	Heparin sulfate proteoglycan gene 2
MED	Multiple epiphyseal dysplasia
ocd	Osteochondrodysplasia
OSMED	Oto-spondylo-megaepiphyseal dysplasia
PAPS	Phosphoadenosine-phosphosulfate
PCR	Polymerase chain reaction
PMSF	Phenylmethane-sulfonyl fluoride
QTL	Quantitative trait loci
SDSC	San Diego supercomputer center
SDS	Sodium dodecyl sulfate
SDS-PAGE	Sodium dodecyl sulfate polyacrylamide gel electrophoresis
SED	Spondyloepiphyseal dysplasia
SEDC	Spondyloepiphyseal dysplasia congenita
SEMD	Spondyloepimetaphyseal dysplasia
SMCD	Schmid metaphyseal chondrodysplasia
SMD	Spondylometaphyseal dysplasia
SJS	Schwartz-Jampel syndrome
SK2	Sulfate kinase 2 gene
TAE	Tris acetate EDTA
TCA	Trichloroacetic acid
TE	Tris –EDTA buffer
UV	Ultra-violet light

List of figures

	Page number
Figure 1: A structural model of aggrecan.	4
Figure 2: Chondrocyte sulfate activation pathway.	11
Figure 3: The collagen II:IX:XI heterofibril.	17
Figure 4: Clinical phenotype of lambs with the Texel Chondrodysplasia.	22
Figure 5: Focal loss of articular cartilage.	23
Figure 6: Transverse sections through the trachea.	24
Figure 7: Haematoxylin and Eosin stained physeal cartilage.	24
Figure 8: Haematoxylin and Eosin stained articular cartilage.	25
Figure 9: Haematoxylin and Eosin stained articular cartilage matrix.	25
Figure 10: Expected outcome from homozygous by carrier cross.	32
Figure 11: BSA standard curve used for determination of protein concentration of collagen and proteoglycan samples.	45
Figure 12: Analysis of collagen in control (C) and affected (A) animals.	47
Figure 13: Analysis of proteoglycans in control (C) and affected (A) animals.	48
Figure 14: Analysis of proteoglycan equal protein loading.	49
Figure 15: Position of PCR and sequencing primers on exon 2.	59
Figure 16: Positioning of PCR and sequencing primers on exon 3.	60
Figure 17: 1% agarose gel showing extracted genomic DNA.	64
Figure 18: 1% agarose gel showing the PCR products from amplification of exon 2.	65
Figure 19: 1% agarose gel showing PCR products from amplification of exon 3.	66
Figure 20: 1% agarose gel showing diagnostic digest of Exon 2 PCR fragment.	67
Figure 21: 1% agarose gel representing quantification of the PCR products of exon 2.	68
Figure 22: 1% agarose gel representing quantification of the PCR products of exon 3.	69
Figure 23: Alignment of the sequenced regions of exon 2.	70
Figure 24: Alignment of the sequenced regions of exon 3.	73
Figure 25: Complete alignment of exon 2 and exon 3 with the complete exonic sequence for the <i>Ovis aries</i> gene encoding sulfate transporter.	76

List of table

	Page number
Table 1: Results (number of offspring in affected and unaffected categories) and chi square analysis of a cross between an affected ram and carrier ewes (Pilot trial year 1).	33
Table 2: Scanning results and expected lamb production from mixed age ewes (Outcross trial year 1).	34
Table 3: Scanning results and expected lamb production from mixed age putative carrier and affected ewes (Pilot trial year 2).	35
Table 4: Scanning results and expected lamb production from ewe hoggets (Backcross trial year 2).	36
Table 5: Results (number of offspring in affected and unaffected categories) and chi square analysis of a cross between an affected ram and carrier ewes (Backcross trial year 2).	37
Table 6: Concentration of undiluted samples from control and affected animal collagen extracts.	46
Table 7: Concentration of undiluted samples from control and affected animal proteoglycan extracts.	46

Table of contents

Acknowledgements	ii
Abstract	iii
Abbreviations.....	iv
List of figures	vi
List of table	vii
Table of contents	viii
1 – Introduction and review	1
1.1 Bone growth and development	1
1.2 Cartilage and skeletal dysplasias.....	2
1.3 Proteoglycans and skeletal dysplasias	2
1.3.1 Manganese, proteoglycans, and skeletal dysplasias.....	5
1.3.2 Chondroitin sulfate proteoglycans.....	6
1.3.3 Heparan sulfate proteoglycans.....	8
1.3.4 Sulfate metabolism, proteoglycans, and skeletal dysplasias	10
1.4 Collagen and skeletal dysplasia	14
1.4.1 Collagen type II.....	15
1.4.2 Collagen type IX.....	17
1.4.3 Collagen type X.....	18
1.4.4 Collagen type XI.....	19
1.5 Sheep chondrodysplasias.....	20
1.6 Texel chondrodysplasia.....	21
1.7 Research aims.....	27
2 – Breeding trial.....	29
2.1 Introduction.....	29
2.2 Materials and methods.....	29
2.2.1 Materials for breeding trial	29
2.2.2 Animals	30
2.2.3 Mating	30
2.2.4 Data recording	31
2.2.5 Sample collection	31
2.2.6 Chi squared analysis.....	31
2.3 Pilot trial (year one).....	32
2.3.1 Parturition	32
2.3.2 Chi square	33
2.4 Outcross trial (year one).....	34
2.4.1 Pregnancy scanning.....	34
2.4.2 Parturition	34
2.5 Pilot trial (year two)	35
2.5.1 Pregnancy scanning.....	35
2.5.2 Parturition	35
2.6 Backcross (year two)	36
2.6.1 Pregnancy scanning.....	36

2.6.2	Parturition	36
2.6.3	Chi square	37
2.7	Discussion	38
3	– Biochemical analysis of collagens and proteoglycans	41
3.1	Introduction	41
3.2	Materials and methods.....	42
3.2.1	Materials for collagen analysis	42
3.2.2	Guanidine hydrochloride extraction	42
3.2.3	Protein quantification	43
3.2.4	Polyacrylamide gel electrophoresis.....	44
3.3	Results.....	44
3.3.1	Protein quantification	44
3.3.2	Collagen SDS – PAGE.....	46
3.3.3	Proteoglycan SDS – PAGE.....	48
3.4	Discussion	49
4	– DNA analysis	56
4.1	Introduction.....	56
4.2	Materials and methods.....	56
4.2.1	Materials for DNA extraction and analysis	56
4.2.2	DNA extraction.....	57
4.2.3	Sample preparation.....	57
4.2.4	Phenol chloroform extraction	57
4.2.5	DNA extraction from blood.....	58
4.2.6	Oligonucleotides.....	58
4.2.7	Exon two polymerase chain reaction and sequencing primers.....	59
4.2.8	Exon three polymerase chain reaction and sequencing primers.....	59
4.2.9	General PCR reactions	60
4.2.10	Column purification of DNA.....	61
4.2.11	DNA Quantification	61
4.2.12	Restriction endonuclease digests.....	61
4.2.13	Agarose gel electrophoresis	62
4.2.14	DNA sequencing	62
4.2.15	Sequence analysis.....	62
4.3	PCR.....	63
4.3.1	Genomic DNA extraction	63
4.3.2	Exon 2	64
4.3.3	Exon 3	65
4.3.4	Diagnostic digest	66
4.3.5	DNA quantification	67
4.4	Sequence analysis.....	69
4.4.1	Exon 2	69
4.4.2	Exon 3	71
4.4.3	Overall exon alignment.....	73
5	– Summary and future direction	77
	Reference list.....	81
	Appendix A	91

Appendix B	93
Appendix C	94
Appendix D	95
Appendix E	98
Appendix F	101
Appendix G	104

1 – Introduction and review

Molecular bases of skeletal dysplasias and associated dwarfism, along with the importance of extracellular matrix (ECM) in skeletal development, have become much better understood in recent years. It was previously thought that the extracellular matrix was a static structure with limited ability to influence tissue structure, function, development, or gene expression. However, it is now known that the ECM is a dynamic network of molecules secreted by cells.

The development of bone is linked to cartilage formation in that bone is formed from a cartilage template. Mutations or malfunctions in the molecules involved and in the steps by which cartilage matrix and endochondral bone is formed results in a range of skeletal diseases.

1.1 Bone growth and development

Most of the skeleton forms through a process called endochondral ossification which involves the replacement of a cartilage intermediate by bone, while a small number of skeletal elements, mainly the flat bones of the skull and lower jaw, form by a process known as intramembranous ossification, which involves the direct formation of bones from condensation of mesenchymal cells (Crombrugge *et al.*, 2001).

In endochondral skeletal elements, such as long bones, cells in the mesenchymal condensations differentiate into chondrocytes (cartilage cells). This process triggers collagen expression transition from type I to type II (French *et al.*, 1999) Chondrocytes deposit an extracellular matrix that is cartilage specific, undergo unidirectional proliferation that results in parallel columns of dividing cells and, after exit from the cell cycle become hypertrophic and die (Crombrugge *et al.*, 2001). Maturation into hypertrophic chondrocytes is marked by the expression of the proteoglycan aggrecan and collagen type X (French *et al.*, 1999). At this stage, the cartilage matrix becomes

mineralized and the septae between dead chondrocytes are removed by osteoclasts, leaving a scaffold of mineralized cartilage which serves as a framework for deposition of osteoid (bone matrix) by osteoblasts (Crombrughe *et al.*, 2001). Normal formation and mineralization of cartilage is therefore essential for subsequent formation of bone by endochondral ossification.

1.2 Cartilage and skeletal dysplasias

Cartilage serves as a multifunctional tissue in the vertebrate body. It is found in adult structures providing a flexible support in the nose, the trachea, the spine, and most notably in the joints of long bones in the form of articular cartilage (French *et al.*, 1999). Cartilage extracellular matrix (ECM) is composed primarily of type II collagen and large, link-stabilized aggregates of hyaluronic acid and chondroitin sulfate (Vertel *et al.*, 1993). The maturation and function of these complex macromolecules are dependent upon sequential processing events which occur during their movement through specific subcellular compartments in the constitutive secretory pathway (Vertel *et al.*, 1993). Diseases may arise as a consequence of errors in this process caused by genetic defects, nutritional deficiencies, or teratogens.

The skeletal dysplasias are a diverse group of disorders that have only recently begun to be understood at the molecular level (Francamano *et al.*, 1996). There has recently been a large increase in the number of identified genes involved in skeletal dysplasias, which has dramatically advanced this field.

1.3 Proteoglycans and skeletal dysplasias

The organisation of proteoglycans and glycosaminoglycans (GAGs) in the extracellular matrix of cartilage can affect the architecture and function of the tissue (Brennan *et al.*, 1983). Proteoglycans occur in the extracellular matrix as complex aggregates containing proteoglycan monomers, hyaluronic acid, and link proteins (Liu *et al.*, 1994) (Figure 1).

Secreted extracellular matrix proteins, especially GAGs and proteoglycans like chondroitin sulfate, dermatan sulfate, and keratan sulfate are a group of sulfated macromolecules, requisite for the differentiation and integrity of most tissues and organ systems in all eukaryotes. GAG-dependent functions can be loosely subdivided into two classes: the biophysical and the biochemical. The former term refers to functions that are dependent on the unique biophysical properties of GAGs – the ability to fill space, bind and organize water molecules, and repel negatively charged molecules (Brenig *et al.*, 2003), for which they provide a major role in the maintenance of cartilage. The more biochemical functions of GAGs are those that are mediated by specific binding of GAGs to other macromolecules, notably proteins. In recent years an enormous amount of information has been gathered on the binding of GAGs to proteins. This information has suggested numerous ways in which proteoglycans might participate in cell and tissue development and physiology.

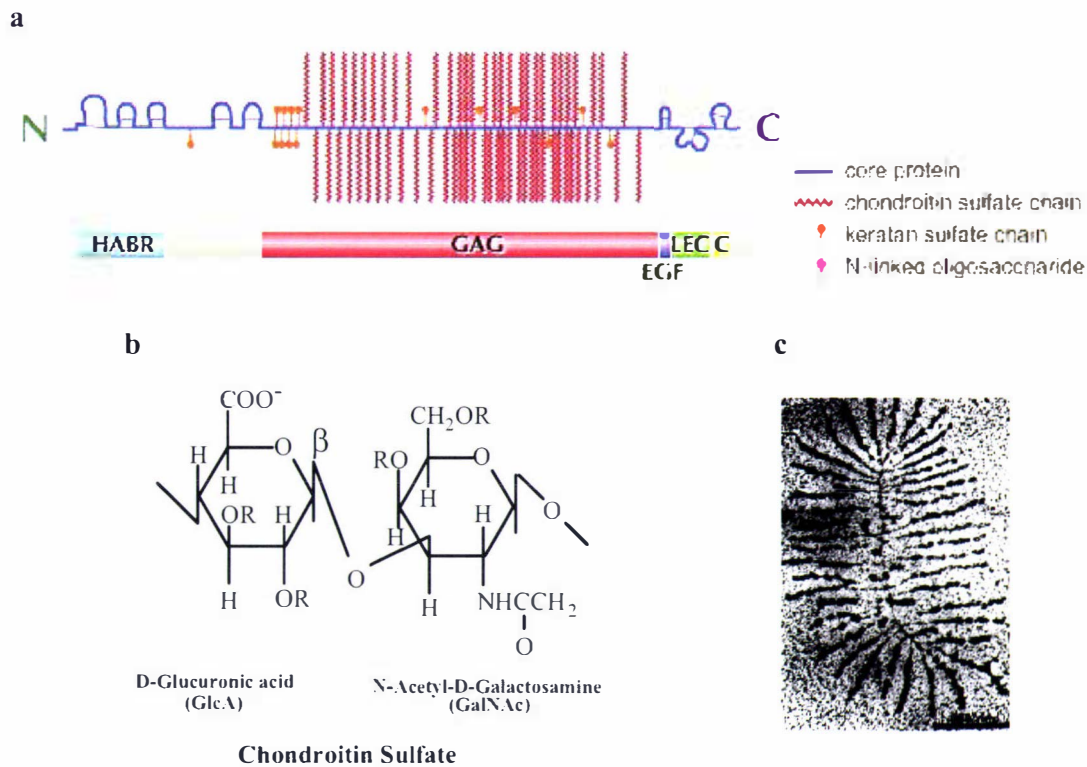


Figure 1: a) A structural model of aggrecan. The schematic representation shows the organization of peptide domains in aggrecan. HABR: hyaluronic acid-binding region; GAG: glycosaminoglycan-attachment domain; EGF: epidermal growth factor-like repeat; LEC: C-type lectin-like module; C: complement regulatory protein-like module. b) The repeating disaccharide unit that makes up chondroitin sulfate chains (every unit is composed of uronic acid (D-GlcA or L-IdoA) and amino sugar (D-GalNAc or D-GlcNH₂)) (courtesy of Cynthia Cresswell). c) Electron micrograph of hyaluronate (up to 4 μ m) coated with proteoglycans (aggrecan) (Yanagishita, 2005).

Proteoglycans are produced as a result of activation of a number of genes that proceeds with the differentiation of chondrocytes (Stirpe *et al.*, 1987), and with bone development (Brennan *et al.*, 1983). The proteoglycan monomer is comprised of a protein core to which numerous GAG side-chains are attached (Figure 1). The core can vary in size from approximately forty-thousand to greater than three-hundred and fifty-thousand Daltons (Lozzo and Murdoch, 1996). Cartilage proteoglycans may contain some one-hundred chondroitin sulfate side-chains attached to the protein core via a specific carbohydrate sequence. Interestingly, these side-chains are not distributed evenly along the protein core, but rather form clusters, especially close to the C-terminal portion of the protein core (Oldberg *et al.*, 1990) (Figure 1). Soft tissue proteoglycans, while sharing some structural features with the cartilage proteoglycans (such as an immunologically

identical hyaluronic acid-binding domain in the extracellular matrix of the aorta for example) differ from those of the cartilage (Oldberg *et al.*, 1990). This difference is associated primarily with structure in relation to the number of GAG side-chains. Polyclonal antibodies raised against aortic proteoglycans do not cross-react with the cartilage proteoglycans (Oldberg *et al.*, 1990). Thus it is quite clear that the cartilage proteoglycan represents a molecule specific for the tissue, albeit structurally similar to proteoglycans with a much wider tissue distribution.

1.3.1 Manganese, proteoglycans, and skeletal dysplasias

Manganese has been demonstrated to be essential element for many species of animals and is also essential for humans (Yang and Klimis-Tavantzis, 1998) for the biosynthesis and subsequent organisation of cartilage macromolecules. If manganese deficiency occurs during fetal development or early postnatal life, severe impairment of skeletal development may occur (Liu *et al.*, 1994). The primary effect is decreased endochondral bone growth, resulting in dwarfism (Valero *et al.*, 1990), as seen in thirty two full term Charolais calves that were born with shortened limbs and enlarged joints. Among the numerous functions of manganese, the most significant is its involvement in the polymerization and elongation of the GAG chains in connective tissue proteoglycans by way of manganese-activated glycosyltransferases, and sulfotransferases (Gundlach and Conrad, 1985). Thus, the effect of manganese in normal epiphyseal cartilage metabolism appears to be centered on its involvement in the biosynthesis of proteoglycans (Liu *et al.*, 1994). More directly, manganese has been described as the most efficient divalent metal ion for the activation of the sulfotransferases, enzymes responsible for the sulfation of GAG side-chains on proteoglycans (Yang and Klimis-Tavantzis, 1998). Maternal manganese deficiency is recognized as a cause of skeletal deformities, including shortening and twisting of the limbs, in new born calves and in other animal species (Thompson *et al.*, 2005).

1.3.2 Chondroitin sulfate proteoglycans

Aggrecan, a large chondroitin sulfate proteoglycan, is one of the major structural constituents of cartilage and contributes localized concentrations of negative charges that serve to increase the level of hydration and thereby provide an expanded tissue volume for bone replacement during long bone development (Vertel *et al.*, 1994). The drastic change in expression during differentiation from mesenchyme to cartilage, the loss of tissue integrity associated with proteoglycan degradation in several disease processes and, most importantly, the demonstration of abnormalities in proteoglycan production concomitant with the aberrant growth patterns exhibited by the cartilage matrix deficient mouse (Kimata *et al.*, 1981), and the nanomelic chicken (Stirpe *et al.*, 1987; Vertel *et al.*, 1993) provide the strongest evidence that the proteoglycan aggrecan is essential during differentiation and for maintenance of skeletal elements.

The lethal chick genetic disease, nanomelia, and the cartilage matrix deficient (cmd) mouse have greatly reduced proteoglycan (aggrecan) content in the ECM due to defective intracellular trafficking, leading to a dramatic reduction in the volume occupied by the extracellular matrix. The osteochondrodysplasia (ocd) rat shows histological anomalies in the epiphysis, also characterized by a decrease in the amount of GAGs in the ECM (Kikukawa and Suzuki, 1992). Early studies into the proteoglycan deficit in the cartilage of the nanomelic chicken by Argraves *et al.* (1981) revealed that the nanomelic mutation affects proteoglycans of cartilage only and that this defect was the result of a deficiency in proteoglycan core protein in that tissue. The chondrocytes of this homozygous recessive avian mutant nanomelia synthesize sulfated GAGs at levels which are ten percent of normal (Argraves *et al.*, 1981). Because non-cartilaginous proteoglycans synthesized by the mutant have normal core protein, this implies that tissue-specific proteoglycans possess different core proteins encoded in separate genes (Argraves *et al.*, 1981). Further studies demonstrated that the nanomelic chondrocytes produced a truncated aggrecan precursor, resulting from a premature stop codon in the aggrecan gene, which failed to be secreted (Luo *et al.*, 1996). As a result, the nanomelic chondrocytes assembled an ECM that consists of type II collagen but lacks aggrecan. Instead, the aggrecan precursor was localized intracellularly, within small cytoplasmic

structures corresponding to extensions of the endoplasmic reticulum, as determined by immunofluorescence and immunoelectron microscopy. Stirpe *et al.* (1987) presented evidence suggesting that the nanomelic mutation affects transcriptional regulation of the major proteoglycan core protein gene. It was noted by Vertel *et al.* (1994), in support of previous findings, that the truncated precursor was translated directly in cell-free reactions, indicating that the mutant truncated precursor does not arise post-translationally. The phenotypic result of this mutation is a chicken characterized by shortened and malformed limbs (Vertel *et al.*, 1993), associated with the anomalies in cellular trafficking and sorting, and with abnormal product retention in the chondrocytes of the nanomelic cartilage.

Results from Bingel *et al.* (1985) also showed a reduction in the amount of proteoglycan in growth plates of the Alaskan Malamute dog suffering from a chondrodysplasia, and stated that the extracellular matrices of dwarf growth plates contain proteoglycan monomers, which suggests a less mature extracellular cartilage matrix than that of age-matched normal controls. As observed in the nanomelic chicken, it was the high molecular weight proteoglycan, aggrecan, characteristic of cartilage that was absent from the dwarf Malamute cartilage matrix.

Mouse cartilage matrix deficiency (*cmd*) is an autosomal recessive phenotype caused by the absence of aggrecan (Krueger *et al.*, 1999). The phenotype in the homozygote becomes apparent a few days after birth and is characterized by disproportionate dwarfism, with a shortened trunk, limbs and tail, and a cleft palate (Kimata *et al.*, 1981). Kimata *et al.* (1981), using biochemical and immunofluorescent techniques, examined the collagen and proteoglycan constituents of fetal limb cartilage and discovered that while a normal amount of collagen II was found, the amount of proteoglycan was reduced. The addition of an exogenous substrate for chondroitin sulfate synthesis, followed by a direct assay for activity, indicated that *cmd* cartilage cells contained normal levels of the enzymes required for chondroitin sulfate synthesis (Kimata *et al.*, 1981). The ultrastructure pattern and greatly reduced cartilage matrix volume in the *cmd* mouse

are similar to that of the mutant in chicken, nanomelia. Hence it was suggested that the mutation resulted in the defective synthesis of the proteoglycan core protein.

The differential expression of two proteoglycans, the major cartilage proteoglycan isolated from a rat chondrosarcoma and a small molecular weight chondroitin sulfate proteoglycan isolated from rat yolk sac tumor, suggests that the synthesis of their core proteins is under separate genetic control, and therefore, these proteins are products of independent genes (Brennan *et al.*, 1983). Indeed, Brennan *et al.* (1983) confirmed these early observations by noting a lack of detectable cartilage-type proteoglycan in tissues of cmd/cmd mice, while the gene for the smaller proteoglycan was expressed at normal levels in a non tissue-specific manner. Completion of the mouse aggrecan gene structure and the identification of the defects that caused the occurrence of the cmd mouse phenotype by Krueger *et al.* (1999) revealed that a seven base-pair deletion in the coding region of the gene results in the incorporation of a premature stop codon, generating a truncated aggrecan protein, which ultimately resulted in the absence of functional aggrecan protein in the cartilage matrix and subsequent dwarfism (Brennan *et al.*, 1983).

1.3.3 Heparan sulfate proteoglycans

Perlecan, a large, multi-domain heparan sulfate proteoglycan is a component of all basement membranes and is expressed in cartilage and several other mesenchymal tissues during development (Costell *et al.*, 1999). It interacts with extracellular matrix proteins and cell adhesion molecules, growth factors and receptors, and influences cellular signaling (Arikawa-Hirasawa *et al.*, 1999).

Disruption of the gene encoding Perlecan (Hspg2) in mice (Arikawa-Hirasawa *et al.*, 1999) revealed a number of important functions of the molecule with respect to skeletal dysplasias. Approximately forty percent of Hspg2 *-/-* mice died at embryonic day ten with defective cephalic development (Arikawa-Hirasawa *et al.*, 1999). This resulted from defects in the basement membrane separating the brain from the adjacent mesenchyme (Costell *et al.*, 1999). The remaining Hspg2 *-/-* mice died just after birth,

with respiratory failure and had skeletal dysplasia characterized by disproportionate dwarfism with broad and bowed long bones, narrow thorax and craniofacial abnormalities (Arikawa-Hirasawa *et al.*, 1999). Homozygous null mice cartilage showed severe disorganization of the columnar structure of the chondrocytes and defective endochondral ossification. The Hspg2 ^{-/-} cartilage contained reduced and disorganized collagen fibrils and GAGs (Arikawa-Hirasawa *et al.*, 1999). The collagen fibrils were also shortened in length (Costell *et al.*, 1999). This suggests that perlecan has an important role in matrix structure, and may protect cartilage extracellular matrix from degradation (French *et al.*, 1999). Furthermore, proliferation of chondrocytes was reduced and the prehypertrophic zone was diminished in homozygous mice with a null mutation (Arikawa-Hirasawa *et al.*, 1999).

Mutations in the perlecan gene in humans cause two classes of skeletal disorders: the relatively mild Schwartz-Jampel syndrome (SJS) and severe neonatal lethal dyssegmental dysplasia, Silverman-Handmaker type (DDSH) (Arikawa-Hirasawa *et al.*, 2002). SJS is a non-fatal autosomal recessive skeletal dysplasia characterized by varying degrees of myotonia and osteochondrodysplasia, with which the patients survive (Arikawa-Hirasawa *et al.*, 2002). The phenotype includes features such as a short stature (dwarfism), a fixed facial expression, sometimes low set ears, and myopia (Arikawa-Hirasawa *et al.*, 2002). Skeletal abnormalities include metaphyseal and epiphyseal dysplasias, joint contractures, and vertebral malformations (Costell *et al.*, 1999). Patients with differing mutations present resulted in various forms of perlecan, and therefore helped define the molecular basis involved in the difference in phenotypic severity between DDSH and SJS. Heterozygous mutations with SJS produced either truncated perlecan protein or significantly reduced levels of wild-type perlecan. Another case had a homozygous seven kilobase deletion that resulted in reduced amounts of nearly full-length perlecan. Unlike DDSH, SJS mutations result in different forms of perlecan in reduced levels that are secreted to the ECM and are likely partially functional (Arikawa-Hirasawa *et al.*, 2002). Perlecan null bones show mild changes in epiphyseal cartilage, but severe abnormalities in the growth plate, indicating that perlecan is

important in proper organisation and function of matrix components (Arikawa-Hirasawa *et al.*, 2002).

Interestingly, the skeletal abnormalities observed in the perlecan null mice resemble the phenotype of the *COL2A1*-deficient mice (mutation in the type II collagen gene) and Dmm (disproportionate micromelia) mice. This was supported by Aszódi *et al.* (1998) who stated that the ultrastructure of the perlecan null mice cartilage lacked a typical collagen network, and that the reduced amount and the shortening of the collagen fibrils suggests that perlecan plays a role in maintaining the collagen network (Costell *et al.*, 1999).

1.3.4 Sulfate metabolism, proteoglycans, and skeletal dysplasias

The role of sulfate in metabolism is paramount. Sulfate groups are found as structural features on various types of biological molecules, such as proteins, proteoglycans, lipids, and polysaccharides. Much of the sulfate in biological systems is used in the posttranslational modification of GAGs, the repeating disaccharide chains that are covalently linked to protein cores to constitute the family of proteoglycans (Kimura *et al.*, 1998). Proteoglycans are synthesized by most cells as cellular or ECM components. Studies into the synthesis and sulfation of proteoglycans have shown that sulfate groups on proteoglycans may be derived from both intracellular catabolism of cysteine and other thiols and from the extracellular fluid (Rossi *et al.*, 2003).

In connective tissue disorders such as osteogenesis imperfecta and chondrodysplasias, defects may involve the abnormal synthesis, processing, translocation, and assembly of ECM components caused by defective controlling enzymes (Vertel *et al.*, 1994).

Ion uptake and inhibition studies have indicated that in chondrocytes, sulfate ions are taken up by an anion-exchange mechanism driven by the chloride gradient; intracellular chloride ions are released, while sulfate ions are taken up by the cell (Kamiski, 2001). The molecule or enzyme responsible for this exchange, the first in the sulfate activation pathway, is the transmembrane chloride/sulfate antiporter (NCBI accession #

NM_000112) designated diastrophic dysplasia sulfate transporter (DTDST) of the cell membrane (Rossi and Superti-Furga, 2001), which is homologous to the hepatocanicular sulfate transporter Sat-1 (Satoh *et al.*, 1998). The sulfate activation pathway can be seen in Figure 2. Chondrocytes appear to be mostly dependent on extracellular sulfate for proteoglycan sulfation (Ito *et al.*, 1982). Thus a high rate of synthesis of proteoglycans seems to correlate with dependence on uptake of extracellular sulfate and the inactivation of the sulfate exchanger leads to intracellular sulfate depletion and to the synthesis of undersulfated proteoglycans (Rossi and Superti-Furga, 2001). Proof that this carrier-mediated transport of sulfate across the cell membrane is a key step for proteoglycan sulfation *in vivo* comes from a family of recessively inherited chondrodysplasias in humans, which show a continuous spectrum, that include diastrophic dysplasia, multiple epiphyseal dysplasia (MED), atelosteogenesis type 2 (AO2), and achondrogenesis type 1B (ACG -1B) (Rossi *et al.*, 2003). Heterozygous individuals appear to be asymptomatic (Rossi and Superti-Furga, 2001).

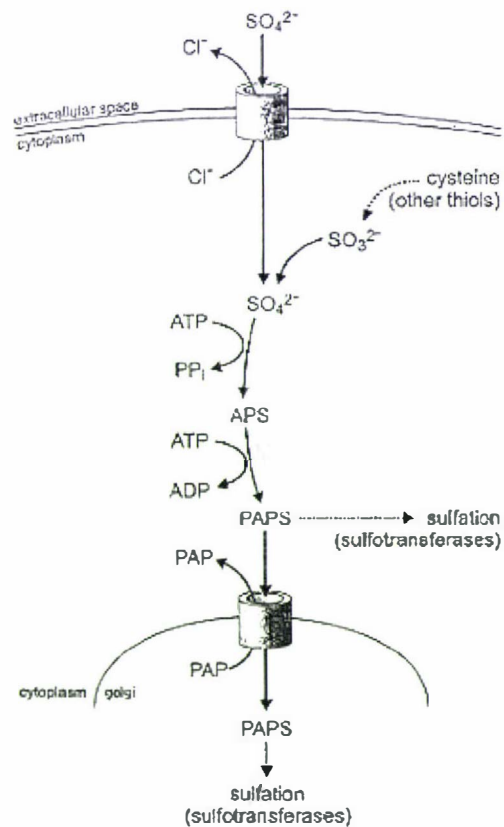


Figure 2: Chondrocyte sulfate activation pathway (Superti-Furga, 2001).

Mutations detected in DTDST in patients include point mutations causing amino acid substitutions, premature stop codons or defective splicing, and base deletions altering the reading frame (Rossi *et al.*, 2003). Genotype-phenotype correlations are recognizable within the spectrum produced by mutations in the DTDST, with mutations predicting a truncated protein or a non-conservative amino acid substitution in the transmembrane domain of DTDST giving the severe phenotype, and non-transmembrane amino acid substitutions and splice site mutations giving a milder phenotype (Kamiski, 2001).

Cartilage from patients with the most severe form of the chondrodysplasia, ACG -1B, is softer than control cartilage and has distinctive histological features such as coarsened collagen fibers and a peculiar ringlike pericellular arrangement of collagen fibers, probably associated with the loss of the regulatory effect of proteoglycans on collagen fibrillogenesis (Corsi *et al.*, 2001). The cartilage contains less inorganic sulfate and less sulfated disaccharides (Rossi and Superti-Furga, 2001). ACG -1B is characterized by severe hypodysplasia of the spine, the rib cage, and the extremities, with a relatively preserved head (Rossi and Superti-Furga, 2001). Further signs include a flat face, a short neck, with the soft tissue of the neck thickened. The thorax is narrow and the abdomen is protruberant. The limbs are severely shortened and the fingers and toes short and stubby. In addition, the feet and toes are rotated inwards (Superti-Furga, 2001). This form of the disease, resulting in severe skeletal underdevelopment, is invariably lethal immediately after, and sometimes even before birth.

Phenotypic manifestations of the milder diastrophic dysplasia include a short stature, joint contractures, cleft palate, and classic clinical signs such as the so-called hitch-hiker thumb, and cystic swelling of the external ears (Rossi *et al.*, 1998). There are at least two methods by which impairment of DTDST function may result in skeletal dysplasia. The first involves changes in composition, architecture, and mechanical properties of the ECM in cartilage; the second, somewhat hypothetical, may involve secondary changes in the fibroblast growth factor signaling pathway in chondrocytes that depends in part on heparan sulfate proteoglycans (Kamiski, 2001).

Brachymorphic (*bm*) is a spontaneously occurring, recessively inherited mouse mutation. The homozygous phenotype is characterized by a dome-shaped skull, and an abnormally short and thick tail, in addition to shorter than normal, but not wider, limb bones (Epstein *et al.*, 1988, Superti-Furga, 2001). In histological and ultra-structural studies Orkin *et al.* (1977) reported a defective cartilage matrix that contains normal collagen fibrils, but proteoglycan aggregate granules that are smaller than normal and present in reduced numbers, particularly in the columnar and hypertrophic zones of the growth plate. It was also noted that the ECM stains poorly with stains specific for sulfated GAGs.

Biochemical analysis confirmed that *bm* cartilage contains normal levels of GAGs but with disaccharides, namely chondroitin sulfate proteoglycan side-chains, which are indeed significantly undersulfated (Sugahara and Schwartz, 1979). The reduced incorporation of sulfate in brachymorphic cartilage is associated with limited phosphoadenosine-phosphosulfate (PAPS) availability, the universal donor for post-translational protein sulfation in all cell types (ul Haque *et al.*, 1998), because of a reduction predominantly in adenosine-phosphosulfate kinase activity (Kimura *et al.*, 1998). This undersulfation of GAGs was shown to be linked with mutations in the gene *SK2* (sulfate kinase 2 gene), by its colocalization with the locus for the autosomal recessive murine phenotype brachymorphism (Kimura *et al.*, 1998). Missense mutations in the *SK2* coding sequence of *bm* mice that alters highly conserved amino acid residues, namely mutations in the functional motif in the kinase domain of mouse *SK*, designated the BM-motif, destroys APS-kinase activity and therefore the ability of *SK2* to synthesize PAPS (Singh and Schwartz, 2003). Thus, undersulfated, non-functional proteoglycan side-chains resulted in a dwarfing disease, by their affect on the composition of the ECM of cartilage (Superti-Furga, 2001).

Ul Haque *et al.* (1998) studied a large inbred family with a distinct form of recessively inherited spondyloepimetaphyseal dysplasia (SEMD) and mapped a gene associated with this dwarfing condition to chromosome 10q23-24, a region syntenic with the locus for the brachymorphic mutation on mouse chromosome 19. Two orthologous genes, *ATPSK2* and *Atpsk2*, encoding novel ATP sulfurylase/APS kinase orthologues in the respective regions of the human and mouse genomes, have been identified.

In addition to human and mouse mutations in the DTDST, analysis of a population of Holstein cattle showed two polymorphisms within the coding region of the bovine DTDST (NCBI accession # AJ223615). Two alleles were identified, resulting from two polymorphisms at different positions. The first exchange, at position 1417 of the cDNA, is silent, while the second results in an amino acid exchange at position 520 of the sulfate transporter protein. Both polymorphisms are detectable by restriction enzyme cleavage, with the silent polymorphism abolishing a restriction site and the polymorphism at position 1559 creating a site (Brenig *et al.*, 2003). Sulfate uptake studies revealed that the resultant amino acid substitution (Ile520Ser) caused a threefold reduction in sulfate uptake in the cells. Thus, this is a functional mutation and could conceivably lead to an undersulfation of GAGs and proteoglycans. Whether the amino acid exchange in the bovine DTDST will be causative for a chondrodysplastic disorder in cattle, for which the effect may only be subtle, remains unclear (Brenig *et al.*, 2003).

The cartilage-specificity of the human and mouse phenotypes provides further evidence of the critical role of sulfate activation in the maturation of cartilage ECM molecules and the effect of defects in this process on the architecture of cartilage and skeletogenesis.

1.4 Collagen and skeletal dysplasia

There are various forms of collagen involved in the formation of functional cartilage tissue including: the fibrillar collagens; types I, II, III, V, and XI; the non-fibrillar collagens which are divided into network-forming, types IV, VIII, and X; and fibril-associated with interrupted triple helices (FACIT), types IX, XII, XIV, XVI, and XIX. Also included in the non-fibrillar collagens are beaded-filament-forming collagen, type VI; collagen of anchoring fibrils, type VII; and collagens with a transmembrane domain, types XIII and XVII. Collagens types XV and XVIII, not yet in a named family are an additional form of the non-fibrillar type (Kuivaniemi, 1997).

Biomechanically, articular cartilage can be regarded as a hierarchically organized material, in which collagen contributes to the tensile properties and withstands shear

force, while proteoglycans are primarily responsible for the viscous osmotic resistance during compression (Hytinen *et al.*, 2001). The three dimensional collagen network of the matrix is thought to be crucial for the mechanical properties of articular cartilage, during joint loading and cartilage deformation (Hytinen *et al.*, 2001). The collagen framework of the ECM of developing hyaline cartilage is assembled primarily from three cartilage-specific collagens: type II; type IX; and type XI as well as type X collagen. These collagen molecules copolymerize into heterotypic fibrils (Figure 3) and become cross-linked intermolecularly (Fernandes *et al.*, 2003). The spatial organisation of type II collagen is regulated by the covalently linked type IX and XI collagens, and possibly also by proteoglycans (Ichimura *et al.*, 2000).

The list of collagen genes with defined mutations that cause chondrodysplasia syndromes, in humans in particular, is growing rapidly and includes collagens II, IX, X, and XI (Ichimura *et al.*, 2000).

1.4.1 Collagen type II

The collagen type II molecule is a long, thin rod consisting of three α polypeptides that are wrapped into a triple helix (Figure 3). The triple helical conformation is possible because every third amino acid is glycine. Therefore, the sequence of each α chain of approximately one thousand amino acids can be expressed as $(\text{Gly-X-Y})_n$, where X and Y represent amino acids other than glycine and n varies according to collagen type. Many of the X- and Y-position amino acids are ring amino acids proline and hydroxyproline that give stability to the triple-helix (Kuivaniemi *et al.*, 1997). It is therefore not surprising that mutations in the *COL2A1* gene that replace arginine codons at Y-positions 75, 519, and 789 in the triple-helical domain with codons for cysteine (an amino acid not normally found in the triple-helical domain of type II collagen from any species) are the only amino acid substitutions in this domain that cause a disease phenotype (Kuivaniemi *et al.*, 1997).

A variety of cartilage disorders have been shown to be caused by other mutations in the *COL2A1* gene for type II procollagen. Heterozygous mutations in the type II collagen gene (*COL2A1*) made articular cartilage softer, altered the collagenous network, reduced subchondral bone volume, and altered its microstructure (Hytinen *et al.* 2001). Eyre *et al.* (1991) stated that the presence of the mutant (cysteine for arginine at residue 519 of the triple helical domain of the protein mentioned above) collagen II protein molecules in the extracellular collagen reduces the durability of the articular cartilage and manifests as the disorder, severe primary osteoarthritis (OA) in humans. The same mutation was also found to cause osteochondrodysplasia in transgenic mice carrying the human *COL2A1* gene (Sahlman *et al.*, 2004). Hytinen *et al.* (2001) also reported that normal type II collagen fibril formation is disturbed if mutated pro-collagen II chains are synthesized and several reports have shown that *COL2A1* gene mutations can cause the development of osteoarthritis and mild to severe chondrodysplasias (Fernandes *et al.*, 1998, Tiller *et al.*, 1995, So *et al.*, 2001). This spectrum of chondrodysplasias includes Stickler syndrome, Kniest dysplasia (Weis *et al.*, 1998), spondyloepiphyseal dysplasia congenita (SEDC), spondyloepimetaphyseal dysplasia (SEMD), achondrogenesis type II, and hypochondrogenesis. Individuals affected with these disorders exhibit abnormalities of the growth plate, nucleus pulposus, and vitreous humor, all of which contain type II collagen (Tiller *et al.*, 1995).

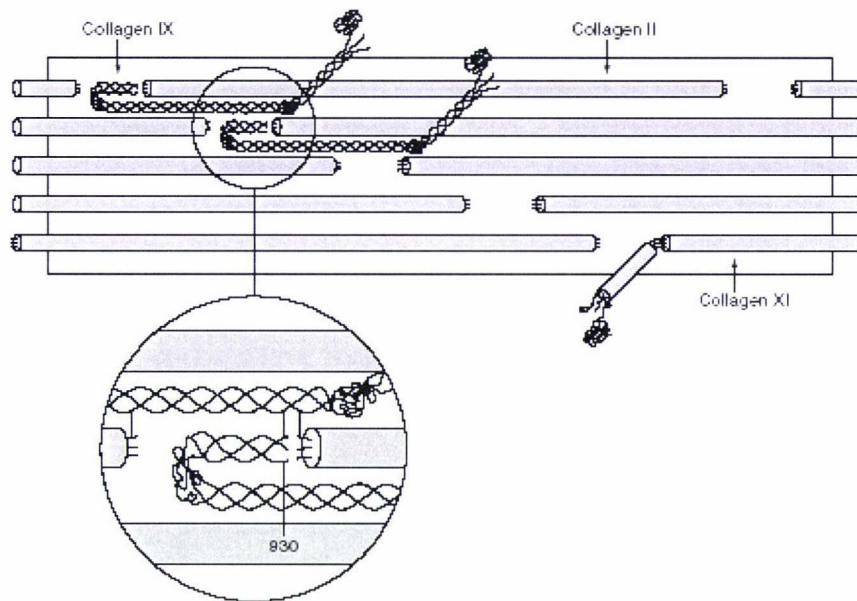


Figure 3: The collagen II:IX:X1 heterofibril. A molecular model of the collagen IX fold and interaction site with collagen II microfibrils that can account for the known cross-linking sites between collagen II and collagen IX molecules (Eyre, 2002)

1.4.2 Collagen type IX

Collagen IX is a heterotrimeric non-fibrillar collagen consisting of three different α chains, $\alpha 1$ (IX), $\alpha 2$ (IX), and $\alpha 3$ (IX), that are encoded by three distinct genes, *COL9A1*, *COL9A2*, and *COL9A3* (Paassilta *et al.*, 1999). It is located on the surface of type II collagen-containing fibrils in articular cartilage and covalent cross-links between types IX and II stabilize the interaction (Kuivaniemi *et al.*, 1997).

MED is a common epiphyseal dysplasia characterized by mild to moderate short stature, early-onset of osteoarthritis (OA) mainly in the hip and knee joints, and abnormally small and/or irregular epiphysis (Nakashima *et al.*, 2005). In a family with a form of MED, the disorder was linked to the gene *COL9A2* and the molecular defect shown to be a heterozygous exon-skipping mutation within the $\alpha 2$ (IX) chain (Muragaki *et al.*, 1996), while both Paassilta *et al.* (1999) and Bonnemann *et al.* (2000) reported an inversion mutation in intron 2 of the $\alpha 3$ (*COL9A3*) locus in a family with autosomal dominant

MED. All the type IX collagen mutations reported cause exon skipping that results in the loss of the COL3 domain of the protein (Nakashima, 2005).

1.4.3 Collagen type X

Collagen X, a short-chain collagen whose expression is largely restricted to the hypertrophic chondrocytes of growth plate cartilage (Chan *et al.*, 1999), has been suggested to be involved in the formation of hexagonal network structures and may be important in regional ECM organization by interacting with other matrix components (Bateman *et al.*, 2003). The molecule is a homotrimer of three $\alpha 1$ (X) chains (Kwan *et al.*, 1997).

The localization of collagen X to the hypertrophic chondrocytes of growth plate cartilage, which distinguishes them as those destined for replacement by bone and marrow, predicts that collagen X plays a role in endochondral ossification-associated events. Thus, disruption of the collagen X gene in transgenic mice resulted in a disorganized lattice network of the matrix in these mice. Interestingly, collagen X disruption resulted in an altered distribution of GAGs and proteoglycans, confirmed by a paucity of staining for hyaluronan and heparan sulfate proteoglycans (Jacenko *et al.*, 2001). Phenotypically, collagen X deficient mice showed a reduction in thickness of the growth plate resting zone and articular cartilage, altered bone content, and atypical distribution of matrix components (Kwan *et al.*, 1997). It was therefore proposed that collagen X plays a role in the normal distribution of matrix vesicles and proteoglycans within the growth plate matrix

Mutations in the human collagen X gene (*COL10A1*) produce a disease known as Schmid metaphyseal chondrodysplasia (SMCD) in humans (Ikegawa *et al.*, 1997, Bonaventure *et al.*, 1995, Sawai *et al.*, 1998). The null collagen X mice have a phenotype which partly resembles SMCD in humans with respect to abnormal trabecular bone architecture (Kwan *et al.*, 1997).

Spondylometaphyseal dysplasia (SMD), which shows a significant phenotypic overlap with SMCD, comprises a heterogeneous group of heritable skeletal dysplasias characterized by modifications of the vertebral bodies of the spine and metaphyses of the tubular bones, and has been shown to be caused by a missense mutation in the *COL10A1* gene (resulting in the protein substitution Gly595Glu) in a SMD diseased family (Ikegawa *et al.*, 1998).

1.4.4 Collagen type XI

Collagen XI is essential for the normal cohesiveness of cartilage and important for the formation of the fine network of collagen cartilage fibrils and the regulation of fibril diameter (Li *et al.*, 1995). Like collagen IX, type XI collagen is a heterotrimer composed of $\alpha 1$ (XI), $\alpha 2$ (XI), and $\alpha 3$ (XI) chains (Melkoniemi *et al.*, 2000). The $\alpha 3$ (XI) chain is a more extensively posttranslationally modified product of the *COL2A1* gene, which codes for the $\alpha 1$ chain of type II collagen (Li *et al.*, 2001). Because of this close structural and functional similarity between collagen types XI and II, mutations in the genes coding for either of them result in partially overlapping phenotypes (Spranger, 1998).

Alterations of type XI collagen caused by mutations of the encoding genes *COL11A1* and *COL11A2* lead to Stickler dysplasia type 2 (Richards *et al.*, 1996), Marshall syndrome, Weissenbacher-Zweymuller syndrome, heterozygous oto-spondylo-megaepiphyseal dysplasia (OSMED), and homozygous OSMED, respectively, in humans (Melkoniemi, 2000). In mice a mutation, resulting in a frameshift, in the *COL11A1* gene produces the autosomal recessive chondrodysplasia (cho) mouse (Olsen, 1995). The OSMED phenotype is highly homogenous and results from homozygosity or compound heterozygosity for *COL11A2* mutations, most of which are predicted to cause complete absence of $\alpha 2$ (XI) chains (Melkoniemi, 2000).

1.5 Sheep chondrodysplasias

The earliest recorded chondrodysplasia among domestic sheep was recognized in New England during the late 18th century (Landauer and Chang 1949). The sheep were known as Ancon or Otter mutants at the time, but are breeds now believed to be extinct.

Characterized by short limbs, awkward gait and crooked forelegs, but the possession of a normal skull and axial skeleton, the mutant reappeared in a farm flock in Norway (Landauer and Chang, 1949). A third instance of a spontaneous mutation giving rise to the achondroplastic dwarf, Ancon, in Merino sheep occurred in America in 1962.

Breeding data from subsequent mating involving an affected ram confirmed it to be an inherent form of dwarfism, and also strongly indicated it to be a simple recessive trait (Shelton, 1968).

Several other sporadic occurrences of dwarfism have arisen, including one reported by Wray *et al.* (1971), which described an achondroplastic syndrome in South Country Cheviot sheep, characterized by ectrodactyly, achondroplasia of the head with protruding eyes, shortened forelimbs, and short ears and tail. It was reported that the syndrome was unlikely caused by nutritional factors or drug use, because no such cases were seen in other breeds of sheep on the two farms where it occurred.

A further, lethal, chondrodysplasia characterized by short, plump lambs, with a shortened nose and cleft palate, short pad-like limbs, a narrow thorax, and swollen abdomen, was noted in lambs born to mixed-breed ewes crossed with Suffolk rams (Duffell *et al.*, 1985). There were also significant histological lesions restricted to the skeleton, lungs, trachea, and thyroid.

The most common inherited chondrodysplasia of sheep is the semi-lethal condition “spider syndrome”, which is inherited by a single autosomal recessive gene (Oberbauer *et al.*, 1995). It was identified as a skeletal disease affecting domestic lambs of black-faced breeds, including purebred Suffolk sheep and Suffolk crosses and the Hampshire breed (Vanek *et al.*, 1989) in America. The disease first arose in New Zealand in Suffolk sheep

in 1992, and was described by West *et al.* (1995). At birth, affected lambs may be grossly abnormal or may appear normal but then develop an abnormal conformation at four to six weeks of age (Rook *et al.*, 1988). Affected animals are characterized by abnormally shaped bones of the axial and appendicular skeleton, including a humped and twisted spine (kyphosis and scoliosis); limbs that are crooked, relatively fine-boned, and unlike typical chondrodysplasias, disproportionately long and spider-like (Vanek *et al.*, 1986). Other skeletal abnormalities may include certain facial deformities, such as angular deviation with or without shortening of the maxilla and a pronounced “roman nose” (Thompson *et al.*, 2005). The gene and defect involved has been defined as a restriction enzyme polymorphism in fibroblast growth factor receptor 3 gene (FGFR3) (Cockett *et al.*, 1999). There is now a commercial test available for this gene defect.

The literature provides numerous examples of monofactorial dominant and recessive hereditary types that cause dwarfism in cattle. The genetic defects cause either a proportionate or disproportionate type of dwarfism, and act as lethal or sub-lethal. Two well-known examples of chondrodysplasia or achondroplasia are the single locus incompletely dominant “bull-dog” form in Dexter cattle (Cavanagh *et al.*, 2002), for which there is now a genetic test, and the autosomal recessive “Snorter” found in the Hereford and Angus breeds (Jones and Jolly, 1982).

1.6 Texel chondrodysplasia

Chondrodysplastic Texel sheep were first recognized in a commercial sheep breeding and lamb fattening property running approximately 1100 mixed-breed ewes, including Texel, Perendale, and White-faced Marsh breeds, on improved pasture in Southland. Terminal sire rams used included those with Perendale, Polled Dorset, Texel/Romney, Texel/Suffolk, and Texel/Perendale breeding (Thompson *et al.*, 2005).

The Texel progeny affected by the chondrodysplasia, both male and female, appear to be normal at birth but as early as ten days of age show evidence of reduced growth rate, shortened legs and neck, angular forelimb deformities, and progressive exercise intolerance. Affected animals usually had a wide-based stance (Figure 4). A further

characteristic seen in some affected lambs was a tendency for them to walk backwards, which was most evident particularly when the mother was stationary (see attached cd). Results on development of morphological changes and further histological analysis form part of a more detailed study, and will be reported separately.



Figure 4: Clinical phenotype of lambs with the Texel Chondrodysplasia. a) Normal lamb (right) alongside its affected co-twin (left) at approximately 5 weeks of age. b) 3 week-old affected lamb beginning to show signs of reduced growth rate and a wide stance. c) 5-week old lamb with evidence of angular forelimb deformity. d) 4-week old lamb with extremely shortened stature and neck.

Phenotypically, the chondrodysplasia has a spectrum of severity, both morphologically and histologically, with some animals dying as young as two weeks of age and other, less severely affected animals living to breeding age. Thus, there are varying degrees of

disproportionate dwarfism. Morphologically, postmortem analysis of the joints of a number of severely affected individuals revealed widespread loss of articular cartilage and exposure of subchondral bone on the weight bearing surfaces of the leg bones (Figure 5). This signifies the occurrence of a breakdown in the cartilage structure and function.

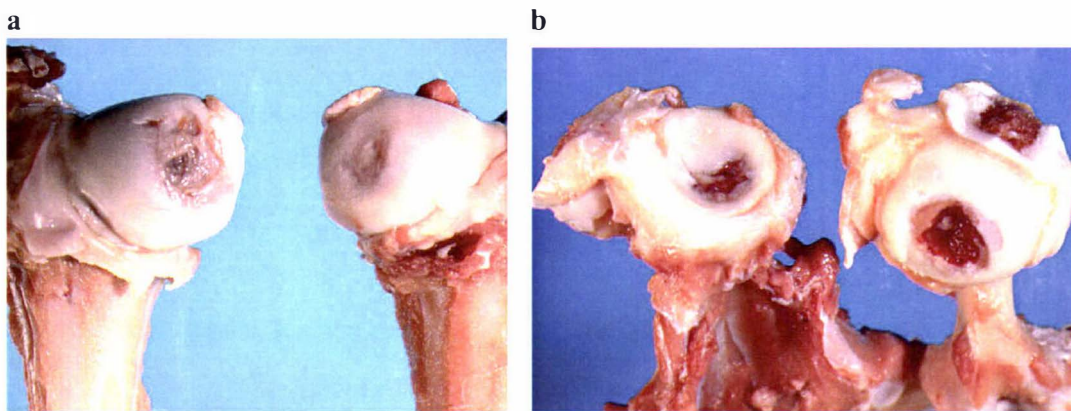


Figure 5: Focal loss of articular cartilage on weight-bearing surfaces of the femoral heads (a) and shoulder joint (b) in a severely affected 3-month old lamb (photographs courtesy of Keith Thompson).

In some lambs there was an exaggerated convex curvature of the ribs and costal and costal cartilages, resulting in these lambs having a “barrel-chested” appearance, and presumably contributing to the wide based stance seen in certain individuals.

Existing articular, epiphyseal, and physeal cartilages were thicker than normal, indicating impaired or delayed endochondral ossification. The trachea is flaccid, abnormally kinked, and has thickened cartilaginous rings with a narrow lumen (Figure 6). For this reason severely affected animals are prone to respiratory distress, sometimes causing sudden death, presumably due to tracheal collapse (Thompson *et al.*, 2005).

In addition, chondrocytes in articular and physeal cartilage were rounded and loosely packed (Figure 9), with disruption of the normal columnar alignment of proliferating chondrocytes (Figure 7) and a conspicuous absence of hypertrophic chondrocytes, as in normal cartilage. These characteristics are variable. Multiple foci of chondrolysis were observed in articular cartilage, resulting in the development of large clefts in some areas (Figure 9). The cartilage extracellular matrix surrounding the chondrocytes had a fibrillar appearance (Figure 8).



Figure 6: Transverse sections through the trachea of a normal lamb (left) and an affected Texel lamb. The cartilage from the affected animal is noticeably thicker, and the trachea lumen is narrowed (photographs courtesy of Keith Thompson).

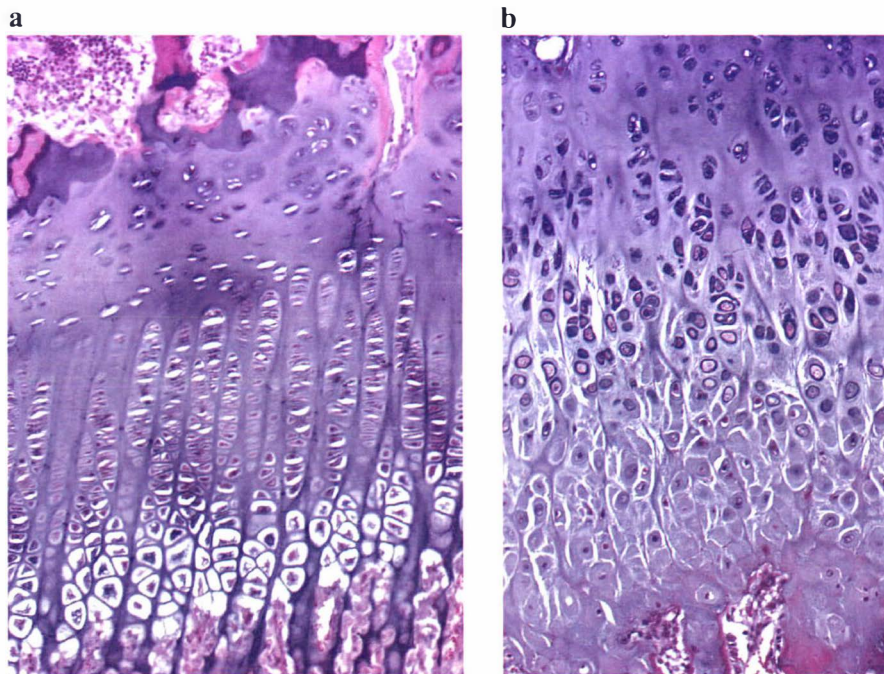


Figure 7: Haematoxylin and Eosin stained hyaline cartilage from a normal (a) and an affected (b) animal. Loss of the columnar structure of the hyaline cartilage is seen in the affected lamb. The chondrocytes are noticeably disorganized when compared to those from an unaffected animal (photographs courtesy of Keith Thompson).

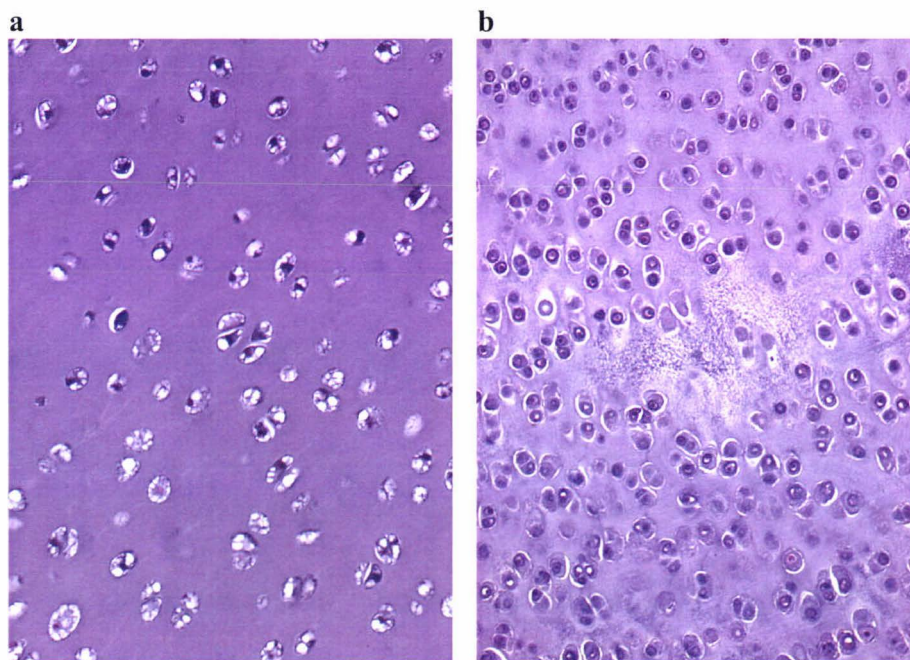


Figure 8: Haematoxylin and Eosin stained histological slides of articular cartilage from a normal (a) and an affected (b) animal. Regions of rarefied cartilage, and the appearance of coarse fibrillar strands, can be seen developing in the affected animals' cartilage as a result of chondrolysis (photographs courtesy of Keith Thompson).

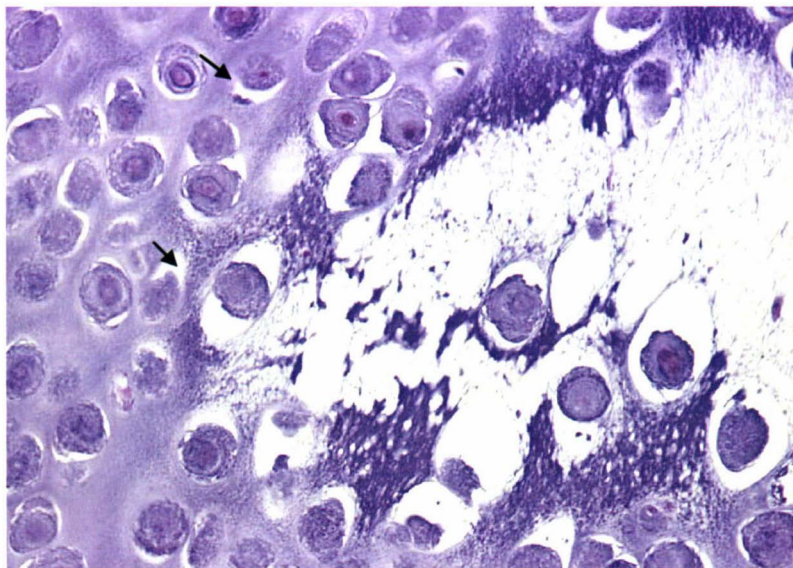


Figure 9: Haematoxylin and Eosin stained articular cartilage matrix, revealing large clefts caused by fusion of multiple points of chondrolysis in an affected animal. Chondrocytes can also be seen surrounded by concentric rings (arrows) (photograph courtesy of Keith Thompson).

Valero *et al.* (1990) studied chondrodystrophy in calves associated with manganese deficiency and noted that affected calves had collapsed tracheas and thickened tracheal cartilage, similar to those seen in Texel chondrodysplasia. Manganese deficiency also results in a reduction in the cartilage hexosamine concentration, a major component of glycosaminoglycan side-chains (Liu *et al.*, 1994).

The phenotype of chondrodysplasia in Texel sheep shows some resemblance to disorders caused by mutations in the gene encoding the large chondroitin sulfate proteoglycan, aggrecan. This similarity is related to the loss of tissue integrity associated with the proteoglycan degradation, due to the truncated protein being retained in the chondrocytes and therefore not in the cartilage matrix. The result of these mutations has been seen phenotypically in mice and chickens.

Mutations in the gene encoding perlecan, a large heparan sulfate proteoglycan, produce a skeletal dysplasia characterized by disproportionate dwarfism in mice, as seen in affected Texel sheep. SJS and DDSH are diseases in humans that result from perlecan gene mutations. While there are characteristics of these diseases seen in Texel chondrodysplasia, several features are not seen in sheep such as myotonia and abnormal facial expressions.

Characteristics of diseases associated with major collagen constituents; collagen types II, IX, X, and XI, respectively which show similarities to Texel chondrodysplasia imply that there is a possibility that a collagen defect may be causative in the Texel chondrodysplasia. It is predicted that collagen X plays a role in endochondral ossification (Jacenko *et al.*, 2001). The fact that a characteristic of the chondrodysplasia in Texel sheep is possible delayed endochondral ossification, suggests a collagen X gene defect may be responsible for the occurrence of this disease. Disruption of the collagen X gene in mice resulted in a disorganized lattice network in the ECM, and altered distribution of matrix components in line with what is observed in the Texel sheep with this form of chondrodysplasia.

Defective sulfate metabolism is another possible mechanism by which the Texel chondrodysplasia may have arisen. Defective sulfate transport has been shown to result in the production of unsulfated proteoglycans, in humans, mice and cattle, which are defective in the maintenance of cartilage ECM integrity. Diseases associated with defective sulfate metabolism have a range of severity, depending on the mutation or the individual. Characteristics similar to those related to the Texel chondrodysplasia include a short stature and joint contractures. The observed chondrodysplasia shows similarities with a number of the dysplasias in which there is current knowledge. Thus the hypothesis is that the chondrodysplasia in Texel sheep is inherited in an autosomal recessive manner and is the result of a mutation in a gene associated with the production and/or processing of proteoglycans.

1.7 Research aims

At the outset of this research the information available regarding the disease included observations of the animals' phenotype, as well as the gross lesions and histological anomalies. No disease of this nature had been observed in the Texel breed before, so the main aim of this research was to characterize the disease in terms of inheritance and biochemical and genetic abnormalities. Thus, the research began with a breeding trial, not only to provide the data to establish the mode of inheritance, but also to provide samples for further research. Affected animals produced from the breeding trial provided articular cartilage tissue for purification of proteoglycans and collagen and subsequent biochemical analysis of these cartilage constituents. Blood samples taken from unaffected, assumed carrier, and affected animals would be used for isolation of DNA and genetic analysis of the disease.

The specific objectives of this research were as follows:

- Carry out a series of breeding trials, involving outcross and backcrossing components.

- Determine the phenotype of the chondrodysplasia biochemically by protein fractionation and subsequent analysis by polyacrylamide gel electrophoresis (SDS-PAGE).
- Identify a candidate gene by histological and biochemical comparison to other diseases.

2 – Breeding trial

2.1 Introduction

The aim of this trial was to determine the mode of inheritance of chondrodysplasia in Texel sheep. An autosomal recessive mode of inheritance was considered most likely for several reasons. The dams and sire producing the affected progeny were well-grown and appeared clinically normal, with the rams having been purchased from the same breeder for several years (Thompson *et al.*, 2005). While some of the affected lambs born during the 2002 season had pigmented faces, they were most likely sired by a Texel/Suffolk cross ram that was no longer on the property (Thompson *et al.*, 2005). Parentage was confirmed for all dwarf lambs available for testing on the Southland property in the 2002 season using DNA fingerprinting (hoof-printing), a service provided by *Signagen*® based on microsatellite markers, and showed that all affected lambs born had been sired by the same ram (Thompson *et al.*, 2005). Approval was obtained from the Massey University Animal Ethics Committee and the trial was conducted in two parts, over two years, to cover two breeding seasons.

2.2 Materials and methods

2.2.1 Materials for breeding trial

Ear tags and flexitag taggers used were obtained from Allflex New Zealand Limited, Palmerston North, New Zealand. Identification spray, super sprayline stock marker, was a product of Donaghys Industries, Christchurch, New Zealand. Scales used for weighing were purchased from Tru-test, Auckland, New Zealand. The raddle (Mating Mark) used was a product of Stockguard Laboratories (Ltd) New Zealand, Hamilton, New Zealand.

2.2.2 Animals

A number of animals were made available from the Southland farm where the condition arose, and these were transported to Massey University for the study. The flock transported included six affected rams, five affected ewes, seventeen putative carrier ewes, and a number of younger animals including eight rising two-tooth ewes, and eleven lambs. Several of the younger animals had to be euthanased prior to the breeding season in year one of the trial due to the progression of the chondrodysplasia, and therefore not all of the animals mentioned above were included in the first mating season. This did however allow for sample collection. Animals were provided with pasture and water *ad lib*, as the availability of the season permitted.

To begin the trial a small flock of suspected carrier and affected mixed age ewes were mated to affected rams, in a pilot trial, to produce lambs to monitor the growth characteristics of the diseased animals. This also allowed further sample and data collection for biochemical and genetic analysis. An outcross trial conducted was the beginning of the inheritance analysis.

2.2.3 Mating

5 mildly affected two-tooth ewes and 20 mixed age putative carrier ewes were mated with an affected ram (pilot trial), over a five week period. The ram was affected, determined by clinical phenotype, and had also been selected based on parentage to previously recorded affected animals born in Southland. During this five week period, the ram was harnessed and the colour of the raddle was changed after two and a half weeks, in order to determine the cycle in which conception took place for each ewe. In the first year of the study (2003) an outcross trial was also undertaken with 221 unrelated, unaffected ewes, being crossed to 3 affected rams, with the aim of producing daughters for backcrossing to their sires. The daughters (F1 generation), of which there were 125, were then mated to their sires in the subsequent breeding season (backcross) (2004).

2.2.4 Data recording

Newly born lambs were caught in the paddock, tagged to their mother (where possible) and sprayed with the corresponding tag number on their sides, to allow identification and monitoring from a distance. The birth date was recorded and used along with the date of disease symptom development to give a time course of the morphological progression of the disease. Photographs were taken of lambs as they grew. Data were collected on a daily basis for new born lambs and included weight, sex, birth rank, dam number, and morphological measurements, which consisted of crown-rump length, front leg length, back leg length, and girth.

2.2.5 Sample collection

The offspring from the affected ewes were of primary interest for tissue sample collection from birth. Samples from deceased and euthanased animals included articular, physeal, and tracheal cartilage samples, some of which were frozen for biochemical analysis, and some of which were stored in 10% buffered formalin for histological analysis. Tissue samples including muscle and spleen, and blood samples were collected to provide DNA for genetic analysis. Control (i.e. normal) tissue was collected from an external source in the earlier stages of lambing because affected and unaffected lambs could not be distinguished reliably during the first ten days of life. After identification of affected animals, control samples were taken from within the existing flock from animals that were not affected by the disease (carriers).

2.2.6 Chi squared analysis

The chi square test allows a comparison of a collection of categorical data with a known theoretical distribution i.e. does the observed result deviate from the expected result due to chance (Eck and Ryan, 2005). Based on a cross between carrier ewes (represented genetically by Aa) and an affected ram (represented genetically by aa), and an autosomal recessive mode of inheritance, the expected outcome is described in Figure 10.

		Ewes Heterozygous	
		A	a
Rams	a	Aa	aa
Homozygous	a	Aa	aa

Figure 10: Expected outcome from homozygous by carrier cross.

Thus, half of the progeny are expected to be affected (represented by aa above) and half unaffected (represented by Aa above), giving an expected proportion of 0.5.

The chi square value is calculated as follows:

$$\text{Chi square (affected)} = \sum \frac{(\text{observed} - \text{expected})^2}{\text{expected}}$$

The chi square value is interpreted as follows; acceptance of the hypothesis (calculated probability is greater than 0.05, $P > 0.05$) means the difference in the proportions (in this case expected proportion of 0.5) is likely to be by chance (unlikely to get exactly a 0.5 proportion in the lambs). Rejection of the hypothesis (calculated probability is less than 0.05, $P < 0.05$) means the data are sufficiently different from the 0.5 proportion and it is likely that a proportion other than 0.5 more accurately reflects the actual data.

2.3 Pilot trial (year one)

2.3.1 Parturition

38 lambs were born over a 58 day period (24th Aug – 20th Oct, 2003), with the majority (34) being born in the first 31 days (24th Aug – 23rd Sept, 2003). This produced a 152% lambing rate ($(38 \div 25) * 100$). 7 lambs died at birth or soon after. It was not known whether these deaths were the result of the disease. 5 lambs were born to the 5 affected

ewes, while the remainder were born to carrier ewes (appendix A). The identification of disease was based on the clinical signs described in section 1.6, and on postmortem analysis of affected individuals. This diagnosis (observation for occurrence of clinical signs) was carried from birth onwards, to ensure that the earliest manifestations of the condition were seen.

2.3.2 Chi square

In the use of the chi square test lambs mothered by affected ewes were not included in the analysis because all offspring produced were affected, therefore removing the need to test these animals. The lambs which died at birth, or soon after, were not included in the analysis because the disease state of these animals could not be obtained. These two categories accounted for 12 lambs. The observed results for the 26 offspring produced by the carrier and a summary of the chi square analysis are represented in Table 1.

	Affected	Carrier	Total
Expected (E)	13	13	26
Observed (O)	15	11	26
O – E	2	-2	0
(O – E)²	4	4	8
(O – E)² / E	0.308	0.308	0.616

Table 1: Results (number of offspring in affected and unaffected categories) and chi square analysis of a cross between an affected ram and carrier ewes.

$$\text{Chi square } (X^2) = 0.616$$

Entering the Chi square distribution table with 1 degree of freedom the chi square value of 0.616 results in a corresponding probability of $0.5 < P < 0.1$ (between 50 and 10%).

This suggests acceptance of the hypothesis, that the ratio of affected to unaffected lambs is 50:50, ($0.50 < P < 0.10$) and the difference in the data from a 50:50 split is likely to be due to chance.

2.4 Outcross trial (year one)

2.4.1 Pregnancy scanning

The two hundred and twenty one mixed age ewes were pregnancy scanned six and a half weeks (46 days) after the last day of mating. Based on the results of this scan the ewes were expected to produce the lambs as shown in Table 2.

Rank	Ewes	Lambs expected
No lamb	10	0
Single	114	114
Twins	95	190
Triplets	2	6
Total	221	310

Table 2: Scanning results and expected lamb production from mixed age ewes.

The ewes scanned at a rate of one hundred and forty lambs per one hundred ewes ($310/221 * 100$) (140.3%).

2.4.2 Parturition

The 221 ewes in the outcross trial produced 214 (lambing rate of 97.3%) of which 95 were males. The lambs were born over a 39 day period (2nd Sept – 10th Oct). Thus, 119 females (214 – 95) produced from these ewes (214 – 95) as well as 6 ewe hoggets from the pilot trial were available for backcross to their sires in year two.

2.5 Pilot trial (year two)

2.5.1 Pregnancy scanning

Pregnancy scanning of the twenty two mixed age ewes was carried out six and a half weeks (46 days) after the end of mating. Based on the results of pregnancy diagnosis the mixed age ewes were expected to produce the lambs as in Table 3.

Rank	Ewes	Lambs expected
No lamb	2	0
Single	5	5
Twins	13	26
Triplets	2	6
Total	22	37

Table 3: Scanning results and expected lamb production from mixed age putative carrier and affected ewes.

The animals scanned at a rate of one hundred and sixty eight lambs per one hundred ewes ($37 \div 22 * 100$) (168.2%). For the full details of scanning results see appendix B.

2.5.2 Parturition

The 22 mixed age ewes gave birth to 26 lambs over a 26 day period (26th Sept – 21st Oct, 2004). This equates to a rate of one hundred and eighteen lambs per one hundred ewes ($26 \div 22 * 100$) (118.2%). A number of lambs were lost at birth or shortly after. Refer to appendix C for full details of parturition.

2.6 Backcross (year two)

2.6.1 Pregnancy scanning

Two of the hoggets died before mating and therefore only 123 hoggets could be used. Pregnancy scanning of the 123 hogget ewes was carried out six and a half weeks (46 days) after the end of mating. Based on the results of pregnancy diagnosis the mixed age ewes were expected to produce lambs as in Table 4.

Rank	Ewes	Lambs expected
No lamb	45	0
Single	68	68
Twins	10	20
Triplets	0	0
Total	123	88

Table 4: Scanning results and expected lamb production from ewe hoggets.

The animals scanned at a rate of seventy two lambs per one hundred ewes ($88 \div 123 * 100$) (71.5 %). For full details of scanning results see appendix D.

2.6.2 Parturition

The 123 hoggets gave birth to 83 lambs over a 32 day period (26th Sept – 27th Oct, 2004) (lambing rate of 66.7 %) (Appendix E). Of these lambs 23 died at birth and 14 died within the first 14 days of life, therefore the disease status of these animals was not able to be recorded by clinical phenotype alone. There are several reasons for these high mortality rate and deviation from the expected outcome based on scanning. The season was particularly good in terms of pasture growing conditions and the hoggets were fed very well in the later part of gestation. This resulted in some large lambs which caused a number of dystocia cases, causing lamb death. Several lambs also died due to exposure. For this reason these 37 animals are excluded from the chi square analysis. There may be

the opportunity to categorize these animals as affected or not affected based on histological data, which is part of an ongoing study.

2.6.3 Chi square

The observed proportion of affected lambs (p) is 0.478 (22/46), while the expected proportion (p) is 0.5.

The observed results for the 46 offspring (83 – 37), for which disease status was observed, produced by the carrier hogget ewes and a summary of the chi square analysis, are represented in Table 5.

	Affected	Carrier	Total
Expected (E)	23	23	46
Observed (O)	22	24	46
O – E	-1	1	0
(O – E)²	1	1	8
(O – E)² / E	0.043	0.043	0.087

Table 5: Results (number of offspring in affected and unaffected categories) and chi square analysis of a cross between an affected ram and carrier ewes.

$$\text{Chi square } (X^2) = 0.087$$

Entering the Chi square distribution table with 1 degree of freedom the chi square value of 0.087 results in a corresponding probability of $0.5 < P$ (greater than 50 %). This suggest acceptance of the hypothesis, that the ratio of affected to unaffected lambs is 50:50, and the difference in the data from a 50:50 split is likely to be due to chance. This outcome provides further support that the disease is inherited in an autosomal recessive manner. No general directions were found in the literature regarding how small a sample may be and still be suitable for a chi square test of goodness of fit. However, caution should be exercised with sample sizes of n less than 50 in interpreting results (Sokal and Rohlf, 1969). Therefore caution has to be taken when interpreting these results.

$$\begin{aligned} 95\% \text{ confidence} &= \text{mean} \pm 1.96 \sqrt{p(1-p)/n} \\ &= 0.5 \pm 1.96 \sqrt{0.5(1-0.5)/46} \\ &= 0.5 \pm 1.96 \sqrt{0.5(0.5)/46} \\ &= 0.5 \pm 1.96 \sqrt{0.25/46} \\ &= 0.5 \pm 1.96 \sqrt{0.0054} \\ &= 0.5 \pm 1.96 (0.0737) \\ &= 0.5 \pm 0.144452 \end{aligned}$$

Based on this outcome, the 95% confidence interval for an expected proportion (p) of 0.5, with a population size of 46, is between 0.355548 and 0.644452. The calculated proportion of 0.478 is within this range, and therefore it is 95% likely that this value represents the actual expected proportion of 0.5. From this it can be determined that the null hypothesis, that there is a difference in the expected and observed proportions (meaning that 0.478 is significantly different from 0.5), is rejected.

2.7 Discussion

The animals born over the two year period were assessed for development of the condition and monitored as they grew. The pilot trial provided an opportunity to assess the technical aspects of lamb numbering and monitoring. The outcome of this trial indicated an autosomal recessive disease, and this was supported by the results from the successive breeding season.

Several threads of evidence suggest that the condition under study is a new recessively inherited chondrodysplasia of the Texel breed. In all affected animals there were Texel genes on both dam and sire sides of the pedigree, and some affected individuals had normal co-twins. No causative plant agents or potential teratogens were identified and because affected lambs were successfully bred at Massey University this excludes any cause relating to the Southland property, such as a mineral deficiency. Parentage testing results, identifying one ram as the sire of all affected lambs from the 2002 season, gave further evidence for a genetic aetiology.

Given that the Texel breed in New Zealand is based on a relatively small number of founder animals, it is not surprising that the defective gene became widespread before detection. As a result of the continued use of a carrier ram by the farmer, carrier ewes eventually became part of the flock and were mated to carrier rams, producing affected progeny (Thompson *et al.*, 2005). Key observations that support an autosomal recessive mode of inheritance include the following: no normal lambs were born to a cross between affected parents; affected lambs have been produced from a cross between normal parents; a cross between a normal parent and an affected parent produces both normal and affected progeny; and no third phenotype has been identified at this stage.

The proportions of normal and affected lambs, from the putative carrier ewes crossed with an affected ram in the pilot trial (year one) provide support for the hypothesis that the chondrodysplasia was indeed caused by a single autosomal recessive gene. In addition to this, proportions of normal and affected lambs in the backcross trial in year two, with a larger number of animals, were consistent with the expected proportions assuming autosomal recessive inheritance. Equal numbers of lambs of each sex, 11 males and 11 females, affected with the chondrodysplasia were born in the backcross trial, indicating that the inheritance is not sex-linked.

It is not uncommon for animal chondrodysplasias to be inherited in an autosomal recessive mode. One such example is the 'spider' syndrome disease in Suffolk sheep. While the aetiology of the few recognized sheep chondrodysplasias is limited, one which is well characterized is 'spider' syndrome. Evidence suggested that 'spider' lamb syndrome was caused by a single autosomal recessive gene. Directed test-breeding of presumed homozygous rams and presumed heterozygous ewes supported this prediction (Oberbauer *et al.*, 1995). The genetic cause has been attributed to a polymorphism in fibroblast growth factor receptor 3 gene (FGFR3). In the case of the Ancon mutant and other reported forms of chondrodysplasia a genetic aetiology was suspected but not proven in all cases. The Ancon Merino sheep, which occurred in America in 1962, was shown to be a simple recessive trait (Shelton, 1968).

Mutations in the chondroitin sulfate gene aggrecan produce the nanomelic chicken (Argraves *et al.*, 1981) and the cartilage matrix deficient mouse (Krueger *et al.*, 1999), which are diseases inherited in an autosomal recessive manner. Chondrodysplasia in the Alaskan Malamute is an autosomal recessive trait, and is characterized by disproportionate dwarfism (Minor and Famum, 1988). In addition the 'snorter' dwarf in Hereford and Angus breed of cattle is also an autosomal recessive trait. To imply that Texel chondrodysplasia is inherited in an autosomal recessive would not be unreasonable being that other animal chondrodysplasias are commonly inherited by a single autosomal recessive gene.

Human forms of chondrodysplasia are also commonly inherited in an autosomal recessive manner. The family of chondrodysplasias caused by sulfate transporter mutations (Rossi and Superti-Furga, 2001) are all inherited in this fashion, and show many phenotypic similarities to Texel chondrodysplasia, and thus provided a major focus for this study.

3 – Biochemical analysis of collagens and proteoglycans

3.1 Introduction

In order to examine the genetic cause of Texel chondrodysplasia, an insight was needed into the biochemical differences underlying the abnormal characteristics of the cartilage matrix in affected animals.

Collagen and the collagen network are integral parts of the cartilage ECM, providing the tensile properties allowing it to withstand shear force and establishing the mechanical properties of the matrix during joint loading and cartilage deformation. Histological examination of articular cartilage in affected animals showed gross abnormalities. As type II collagen is the major constituent of articular cartilage and because collagen types IX and XI are important for the spatial organisation of type II collagen, a first step in the analysis was to determine whether there was any significant difference in type II, type IX, and type XI collagen in the articular cartilage from unaffected and affected animals.

Based on phenotypic similarity, particularly at the histological level, between the observed chondrodysplasia in Texel sheep and the chondrodysplasias, ACG -1B and MED, in humans, it was postulated that a similar biochemical mechanism may be associated with the Texel disease. The biochemical mechanism involved in the human disorder is related to the chloride/sulfate antiporter (DTDST). Mutations in the gene, encoding this transport protein, have been shown to be responsible for the ACG -1B and MED phenotypes, by disrupting the sulfate activation pathway (Figure 2). Sulfation requires active transport of inorganic sulfate into the cell, conversion into the “active” high energy form of PAPS, translocation of PAPS across the Golgi membrane, and transfer of sulfate from PAPS, via a multitude of sulfotransferases, to the recipient biomolecules. The sulfate activation pathway consists of two activities, ATP-sulfurylase, which catalyzes synthesis of APS from ATP and SO_4^{-2} , and APS kinase, which phosphorylates APS in the presence of another molecule of ATP to form PAPS. In

contrast, when these two sulfate-activating activities were purified from rat chondrosarcoma they were found to exist as a bifunctional enzyme, which uses a channeling mechanism to transfer the intermediate APS efficiently from the sulfurylase to the kinase active site (Kurima *et al.*, 1998). Ultimately, mutations in the transporter gene result in a depletion of the PAPS donor molecule and therefore the abnormality seen in the proteoglycan constituents of cartilage from ACG -1B and MED patients, is related to the level of sulfation of the glycosaminoglycan side-chains in the proteoglycan macromolecules.

Thus a further step in analysis of the biochemical cause of Texel chondrodysplasia was to investigate the level of sulfation of the proteoglycan constituent of the cartilage, in affected animals and compare this to the level of sulfation in unaffected animals.

3.2 Materials and methods

3.2.1 Materials for collagen analysis

Guanidine hydrochloride, Crystalline N-Ethylmaleimide, Collagen Type II (Bomstein and Traub nomenclature) from chicken sternal cartilage, and Toluidine Blue O were purchased from Sigma – Aldrich Chemical Company, MO, USA. Coomassie Brilliant Blue R stain was purchased from GIBCOBRL, Invitrogen Corporation, Invitrogen NZ Limited, Penrose, Auckland, New Zealand. The acrylamide: bis-acrylamide (ratio 29.1:0.9) ready-to-use solution (Acrylogel 3 solution) was a product from BDH Laboratory Supplies, Poole, England. Precision Plus Protein™ Standards All Blue and Bradford protein assay kit were obtained from BioRad, Hercules, CA, USA.

3.2.2 Guanidine hydrochloride extraction

100 mg (wet weight) of each cartilage sample, five from normal animals and four from affected animals, were finely minced using an Ultra-turrax T25 blender (Janke and Kunkel, IKA-Labortechnik) in 10 mL (100 µL/mg of wet tissue) of a guanidine

hydrochloride solution (4.0 M guanidine hydrochloride, 50 mM tris-chloride, and 1 mM each of phenylmethane-sulfonylfluoride (PMSF), N-ethylmaleimide, and EDTA). The samples were then left for 48 hours at 8°C with continuous stirring.

The sample was then centrifuged at 3000 rpm (1864 g) for 10 minutes and the supernatant removed and placed in dialysis tubing for purification of proteoglycans. Four proteoglycan extracts from normal animals and four from affected animals were treated as follows. The supernatants were then dialysed for 24 hours against 150 mM NaCl, 50 mM tris-chloride pH 7.4, 0.1 % triton X-100, and 1 mM each of protease inhibitors phenylmethane-sulfonylfluoride (PMSF), N-ethylmaleimide, and EDTA at 4°C. The dialysis was repeated three times to maximize the purity of the proteoglycans.

The residue, containing collagen, was washed with phosphate buffer saline (PBS) (0.14 M NaCl, 0.003 M KCl, 0.002 M KH_2PO_4 , 0.01 M Na_2HPO_4 pH 7.4) and further extracted with the same volume of 0.5 M acetic acid containing 1 mg pepsin/mL.

Pepsin extracts were lyophilized overnight using a freeze dryer (Kenetics Thermal Systems) and reconstituted in 0.8 mL of sample buffer containing 2.0 M urea, and excluding DTT (15 % (w/v) glycerol, 6 % Sodium dodecyl sulfate (SDS), 0.125 % Tris-HCl pH 6.8) (Superti-Furga, 1994).

3.2.3 Protein quantification

The protein concentration of collagen and proteoglycan extracts was determined using the Bradford protein assay dye reagent concentrate (BioRad) according to manufacturer's instructions. The concentrated reagent was diluted 1:5 in water, and then 200 μL was added to bovine serum albumin (BSA) (0.2 mg/ μL) standards (diluted to a range of 0-2.5 μg in water). The collagen samples assayed included a 1:2 dilution in water, while serial dilutions of the proteoglycan samples were made to give dilutions of 1:2, 1:5, and 1:10 in water. A 5 μL aliquot of each dilution was loaded in triplicate into a hard plastic 96-well microtitre plate (Nunc), and left to develop colour at room temperature for a minimum of 10 minutes, at which time absorbance was read at 595 nm. A protein

standard curve was constructed using the standard amounts of BSA and the amount of protein present in each sample was estimated.

3.2.4 Polyacrylamide gel electrophoresis

Collagen extracts were diluted 10 x and dissolved and denatured by boiling for 3 minutes with 5 μ L of 2 x loading buffer (40 % w/v sucrose, 0.25 % bromophenol blue). Aliquot volume was determined by results of the Bradford assay, and 7 μ g of protein from each sample were then separated on 5 % acrylamide gels containing 0.5 M urea under non-reducing conditions (Steinmann *et al.*, 1984). A stock solution of 1 % (w/v) Coomassie Brilliant Blue R in ethanol was diluted with 20 volumes of 12 % (w/v) trichloroacetic acid (TCA), and gels were stained overnight. Gels were then bathed in 12 % TCA until clear, and then photographed to visualize collagens (Superti-Furga, 1994).

Aliquots (containing 7 μ g of protein as determined by Bradford assay above) of proteoglycan extract were boiled for 3 minutes with 5 μ L of 2 x loading buffer (40 % w/v sucrose, 0.25 % bromophenol blue), and samples were separated by SDS – PAGE on a discontinuous gel system with 2.5 % stacking gel and a 3 % - 7 % step-separating gel under reducing conditions. All gels were prepared and electrophoresed in Mini-PROTEAN[®] II Cell (BioRad) vertical gel units. Visualisation of proteoglycans was achieved by staining in 7.5 % acetic acid with 0.2 % toluidine blue for 60 minutes. Gels were then partially destained in 7 % acetic acid / 30 % methanol and placed in water to enhance metachromasia. Proteoglycan gels were subsequently stained with 1 % (w/v) Coomassie Brilliant Blue R to stain for equal protein loading (Superti-Furga, 1994).

3.3 Results

3.3.1 Protein quantification

The overall protein concentration of the collagen and proteoglycan sample extracts was determined using the BSA standard curve (Figure 11). This information was used to

ensure that an equivalent amount of protein was loaded and electrophoresed on the polyacrylamide gels for analysis.

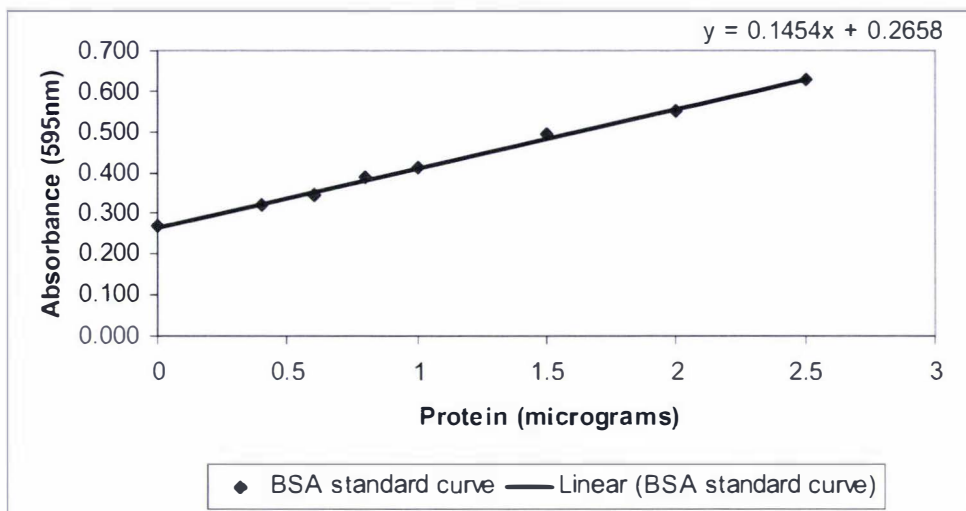


Figure 11: Typical BSA standard curve used for determination of protein concentration of collagen and proteoglycan samples.

From the quantification data the following protein concentrations were observed for control (C) and diseased (A) animals. Average protein concentration was calculated from each of the triplicate dilutions, and then the concentration of the undiluted sample for collagens (Table 6) and proteoglycans (Table 7) calculated. For data on collagen and proteoglycan quantification see appendix F.

Sample	Concentration (mg/mL)
C1	0.571
C2	0.637
C3	0.769
C4	0.656
C5	0.756
A1	0.609
A2	0.608
A3	0.625
A4	0.552

Table 6: Concentration of undiluted samples from control (C) and affected (A) animal collagen extracts.

Sample	Concentration (mg/mL)
C1	0.415
C2	0.376
C3	0.693
C4	0.449
A1	0.489
A2	0.518
A3	0.394
A4	0.412

Table 7: Concentration of undiluted samples from control (C) and affected (A) animal proteoglycan extracts.

3.3.2 Collagen SDS – PAGE

Throughout sample collection from affected individuals and to a lesser extent during mincing, cartilage appeared softer and was easier to sever than control hyaline cartilage, and was also noticeably opaque.

This feature bears resemblance to cartilage from patients with Achondrogenesis type II (Superti-Furga, 1994), which is caused by a genetic defect in collagen type II (Dertinger *et al.*, 2005).

SDS-PAGE analysis of pepsin-extracted collagens from control and affected lamb's cartilage revealed no differences in the mobility of collagen II, collagen IX, or collagen XI (Figure 12) between control (C) and affected (A) animal extracts. There also appears to be no difference in the composition of the cartilage with respect to the relative amounts of these tissue components, shown by the fact that the samples (both control and affected) appear to have equivalent amounts of each of the three collagen species noted, with an equal amount of protein loaded into the wells.

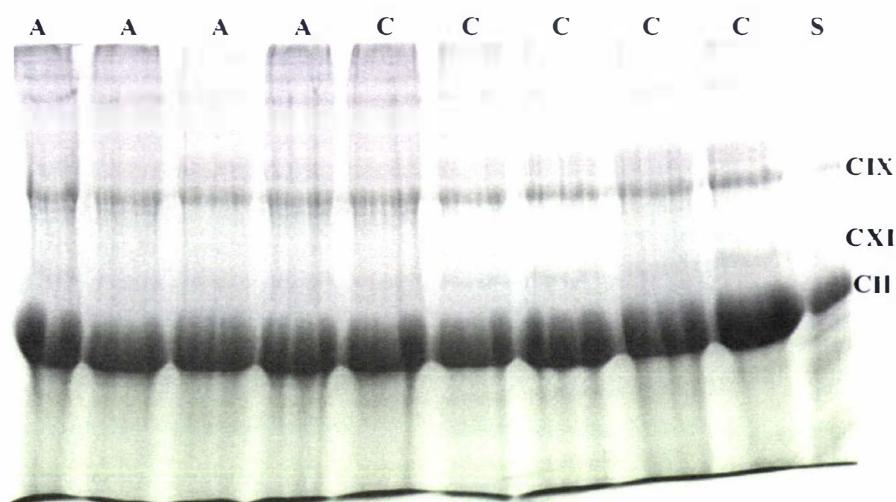


Figure 12: Analysis of collagen in control (C) and affected (A) animals. 5 % SDS gel containing 0.5 M urea. The gel was electrophoresed in 1x electrode buffer until the dye front reached the bottom of the gel. Cartilage guanidine extracts show equivalent Coomassie brilliant blue staining of control and affected animal collagen extracts. **S** represents a collagen type II standard. It can be seen that there are no difference between samples from the two groups. **CII** = collagen II; **CXI** = collagen XI; **CIX** = collagen IX

3.3.3 Proteoglycan SDS – PAGE

The SDS-PAGE gel below (Figure 13) represents proteoglycan samples taken from minced articular cartilage of unaffected (control) and affected animals. In control animal samples (C), and to a much lesser extent in affected animal samples (A), toluidine blue – positive material of high molecular weight, most of which barely enters the gel (and probably corresponding to aggrecan), is seen. Figure 14 represents the proteoglycan gel stained with Coomassie Brilliant Blue R. The gel shows staining which is equal between control and affected samples indicating that the amount of protein loaded in each well was the same.

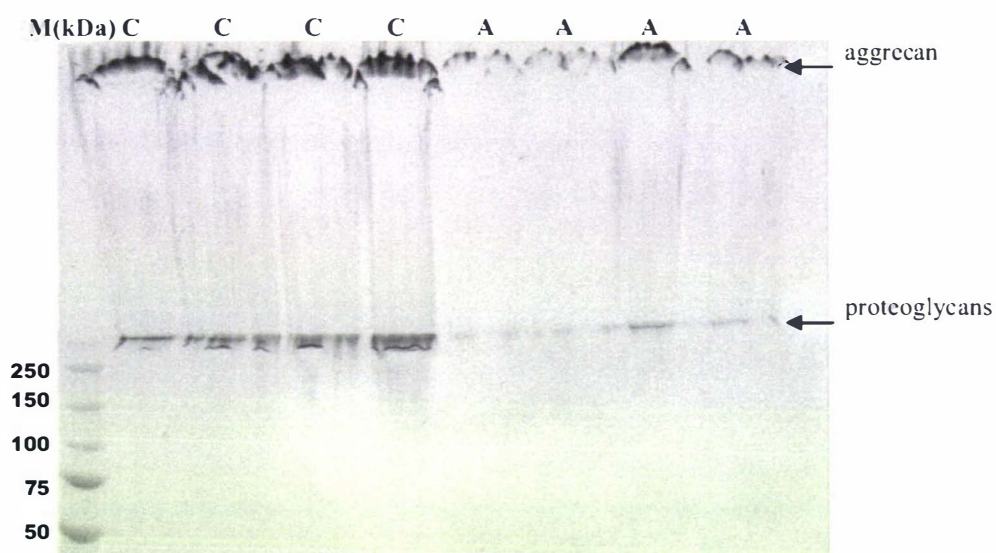


Figure 13: Analysis of proteoglycans in control (C) and affected (A) animals. Cartilage guanidine extracts separated by SDS-PAGE on a 3 % - 7 % step-separating gel. The gel was electrophoresed in 1x electrode buffer for 1.5 hours at 200V. The gel was stained with Toluidine blue O, a stain with high affinity for sulfated molecules, and shows differential sulfate staining of control and affected animal proteoglycan extracts, indicating a difference in the level of sulfation of these proteoglycans. **M** = protein standard marker.

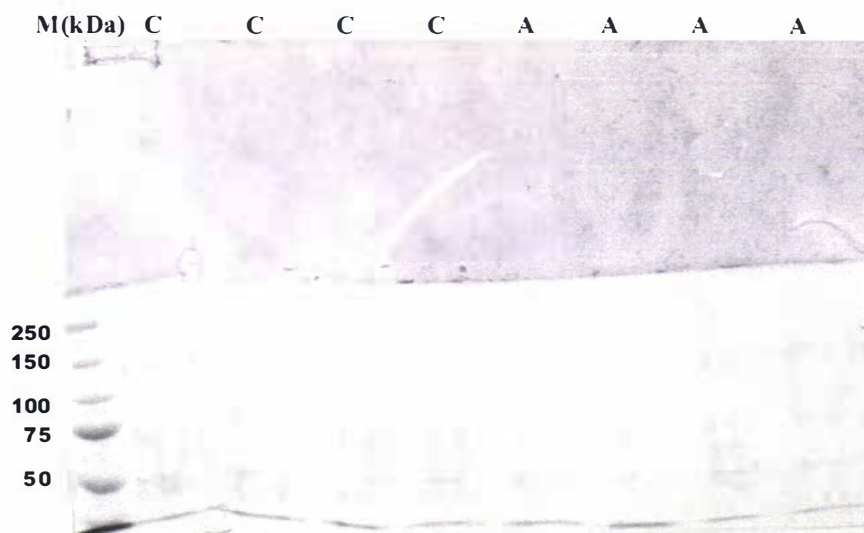


Figure 14: Cartilage guanidine extracts separated by SDS-PAGE on a 3 % - 7 % step-separating gel. The gel is the same as in figure 13 stained with Coomassie Brilliant Blue R, showing equivalent loading of control (C) and affected (A) animal proteoglycan extracts. **M** = protein standard marker.

3.4 Discussion

In mammals, collagen accounts for about two-thirds of the dry weight of adult articular cartilage. The tissue's material strength depends on the extensive cross-linking of the collagen and the apparent zonal changes in fibrillar architecture with tissue depth (Eyre, 2001). Identification of the molecular defect in patients with type II collagen disorders is therefore usually a challenge, not only because cartilage is relatively acellular, but because of the relatively large size and complexity of the *COL2A1* gene and its main expression in cartilage (Mortier *et al.*, 2000), along with its high degree of interaction with other cartilage components. However, differences in collagen constituents, namely collagen II, have been noted in the spondyloepiphyseal dysplasias (SED), and the spondyloepimetaphyseal dysplasias (SEMD) (Murray *et al.*, 1989) as well as Kniest dysplasia (Weis *et al.*, 1998) in humans, by way of collagen analysis using SDS-PAGE. Results revealed that in all patients in the study groups, the type II collagen exhibited a slower electrophoretic mobility when compared with that from controls, indicating some structural alteration in type II collagen from these individuals. This electrophoretic

mobility dissimilarity was not observed in Texel chondrodysplasia between control and affected animal samples, when subjected to SDS-PAGE.

Collagen extracts from patients with either achondrogenesis II-hypochondrogenesis or severe spondyloepiphyseal dysplasia congenita (SEDC) when subjected to SDS-PAGE, similarly showed slowly migrating $\alpha 1$ (II) chains when compared with the control extracts (Mortier *et al.*, 2000). An analogous investigation was carried out by Eyre *et al.* (1991) who studied a dominantly inherited form of osteoarthritis associated with a mild chondrodysplasia, for which linkage studies showed that the condition was co-inherited with an allele for the type II collagen gene, and also produced results that illustrated a slight retardation in the mobility of patient's $\alpha 1$ (II) chain, when compared to that of the control human $\alpha 1$ (II) chain. These characteristics were not seen when comparisons were made between control and affected collagen extracts from the Texel chondrodysplasia. In transgenic mice harbouring collagen II pro- α -chains containing a Gly574Ser mutation, pepsin - extracted collagen, from embryo cartilage, was analyzed electrophoretically and showed predominantly type II collagen, as expected, in both wild-type and transgenic tissue. Equivalent amounts of wet tissue were used in extraction; however less $\alpha 1$ (II) collagen was extracted from the rib cage of the transgenic embryos compared with that from wild-type littermates. The relative amount of $\alpha 1$ (II) collagen in the transgenic cartilage was quantified from gel band intensities and shown to be reduced to 0.30 of wild-type (Maddox *et al.*, 1997). The same study also noted that the ratio of the $\alpha 1$ (XI) and $\alpha 2$ (XI) to the $\alpha 3$ (II) and $\alpha 1$ (II) bands, which co-migrate, appeared to be consistent between littermates, demonstrating that the composition of the fibrils was normal, although the amount of type XI collagen present in the transgenic tissue was less than in wild-type. Overall, the major collagen components present in rib cage cartilage, those being type II and type XI were present in reduced quantities in transgenic mouse tissue. As an internal control type I collagen, present in adjacent non-cartilaginous tissue, was at wild-type levels. In collagen analysis from Texel chondrodysplastic and control tissue, not such differences were seen in quantity or mobility of extracts from unaffected and affected extracts, providing further support that collagen defects are not the underlying cause of Texel chondrodysplasia.

The “spider syndrome” clinical phenotype is quite different from that observed in the currently studied chondrodysplasia. “Spider lambs” have long, spindly legs and various other deformities associated with the vertebral column and face (Vanek *et al.*, 1986), while lambs with the current chondrodysplasia have disproportionate dwarfism and short legs. Indeed, no other reports describing dwarfism in sheep resemble the Texel chondrodysplasia in terms of clinical signs, gross lesions, and histopathology (Thompson *et al.*, 2005). Nakano *et al.* (1994) reported that eroded proximal humeral articular cartilage from a lamb with “Spider syndrome” contained a lower concentration of collagen when compared to adjacent visually normal cartilage, a characteristic not observed in the current Texel chondrodysplasia. SDS-PAGE analysis of collagen extracted in the native state from spider-affected cortical bone revealed that it is comprised of type I collagen which is normal in its primary structure (Troyer *et al.*, 1988). It would be interesting to determine the biochemical structure of the type I collagen in bones from Texel chondrodysplastic individuals and observe whether it was different from that of normal animals. This would involve pulverizing and demineralization of bone samples, and then limited pepsin degradation. The samples would then be subjected to interrupted electrophoresis on 5 % acrylamide gels using the technique of Sykes *et al.* (1976).

These notable differences, particular in structure, apparent in the collagen species from a wide range of skeletal dysplasias in humans, mice, and sheep, were not seen in the currently studied Texel chondrodysplasia, suggesting that the Texel chondrodysplasia does not result from a mutation involving any of the three main collagen constituents of mature cartilage.

While type IX and type XI collagens are quantitatively minor components of hyaline cartilage, they are essential for the normal structural integrity of the tissue (Ichimura *et al.*, 2000). In a study examining the iliac crest growth cartilage from a patient with diastrophic dysplasia, SDS-PAGE revealed a pronounced excess of the COL1 domain of the molecule in pepsin extracts, suggesting an abnormality in structure or metabolism of type IX collagen (Diab *et al.*, 1994). While no analysis of individual domains was

carried out in the present study, no difference is seen in the electrophoretic mobility of the overall type IX molecule (Figure 12).

As discussed, cartilage from ACG- 1B patients has distinguishing histological features including coarsened collagen fibers and a concentric pericellular arrangement of the matrix around chondrocytes. This is thought to be a result of the loss of the regulatory effect of proteoglycans on collagen fibrillogenesis (Corsi *et al.*, 2001). Similar histological features are seen in Texel chondrodysplasia (Figure 9), therefore indicating that the same biochemical mechanism may be involved.

Superti-Furga (1994) investigated the metabolic activation of sulfate in a patient with ACG- 1B. It was reported that when guanidine extracts of control cartilage were separated by SDS-PAGE and the gels stained with toluidine blue, a cationic dye which has affinity for sulfated proteoglycans, metachromatic staining of sulfated proteoglycans was seen by virtue of their polyanionic nature. However, this staining was not seen in samples taken from patients with ACG- 1B. The noticeable difference in sulfate staining between control and ACG- 1B patients could indicate that proteoglycans are either reduced in quantity, or have some defect in sulfation. The quantity of proteoglycans was shown to be unchanged in these patients, as it was reported that synthesis of the core protein, as well as initiation and elongation of the GAG side chains was normal. Rossi *et al.* (1996) also reported lack of toluidine blue staining, consistent with the hypothesis that patient's proteoglycans were not correctly sulfated and thus less negatively charged, rather than reduced in quantity. Results indicated that both the large chondroitin sulfate proteoglycans (CSPGs), such as aggrecan, and the small CSPGs synthesized by ACG- 1B chondrocytes bear glycosaminoglycan chains which are of normal length but not correctly sulfated. Texel chondrodysplasia has a resemblance to ACG- 1B, and recessive MED (DTDST chondrodysplasias), in terms of staining behaviour of proteoglycans after SDS-PAGE, providing support for the chondrodysplasia being caused by a defect in the uptake or activation of sulfate in chondrocytes. The degree of proteoglycan undersulfation *in vivo*, was evaluated in extracted chondroitin sulfate proteoglycans from cartilage of twelve patients with sulfate transporter

chondrodysplasias. High Performance Liquid Chromatography (HPLC) analysis indicated that the amount of non-sulfated disaccharide was elevated in patients' samples (Rossi *et al.*, 1998).

Impaired sulfation of glycosaminoglycan side chains could in theory be due to reduced availability of the sulfate donor, PAPS, by a defective PAPS synthesis enzyme as seen in the Brachymorphic mouse (ul Haque *et al.*, 1998), or by reduced activity of the transferase activities transferring sulfate from PAPS to endogenous acceptors (a defect in sulfate metabolism). This theory was resolved for ACG- 1B patients by Superti-Furga *et al.* (1996), who showed, by sulfate uptake studies, that the disease was not caused by a defect in the metabolic activation of sulfate, but was the result of impaired sulfate uptake, and therefore the DTDST was responsible for the sulfation defect.

It is not known whether the Texel chondrodysplasia is caused by a reduction in available sulfate as a result of a defect in the enzymes responsible for the synthesis of PAPS or the sulfotransferases responsible for the transfer of sulfate to acceptor molecules. However, the similarities seen in the microscopic lesions in abnormal articular cartilage, the biochemical behaviour of proteoglycans between children with ACG- 1B and lambs with Texel chondrodysplasia, and the absence of collagen differences, indicate that it is likely to be a defect in the sulfation of glycosaminoglycans, rather than a defect on collagen formation.

As mentioned in section 1.6, the chondrodysplasia in Texel sheep shows variable expression; it is therefore of interest to note that the recessively inherited MED is characterized by a markedly variable phenotype, with short to normal stature, and variable epiphyseal dysplasia, features that resemble those described for the present chondrodysplasia, and provide further support for the disease being the result of a mutation in the DTDST (Mäkitie *et al.*, 2003).

The distinct variation in severity of phenotype, clinically, and histologically within affected animals is unusual for a genetic disease. This variation probably reflects the presence of different biochemical pathways, or modifying enzymes, capable of modifying

gene expression, such as the ability to utilise cytoplasmic thiols or sulphur containing amino acids, rather than the presence of more than one defective gene (Thompson *et al.*, 2005)

In cartilage from ACG- 1B patients the matrix is distinctly abnormal and is characterized by rarefaction of ground substance (matrix), as is seen with the Texel chondrodysplasia. In a study characterizing chondrodystrophy in calves associated with manganese deficiency (Valero *et al.*, 1990), it was seen that affected calves had many characteristics similar to those seen in Texel chondrodysplasia, including the presence of large amounts of rarefied cartilage, and joint laxity resulting in varus forelimb deformities.

The observed chondrodysplasia also shows phenotypic similarities to those caused by manganese deficiency with respect to shortening and twisting of the limbs, reduced endochondral bone formation, resulting in dwarfism, and in particular similarities associated with the collapsed trachea and the general disorganization of cells in the growth plate cartilage (Liu *et al.*, 1994). The major role of manganese in cartilage metabolism is its involvement as a co-factor in the biosynthesis of glycosaminoglycan chains, which constitute a large part of proteoglycans, through activation of glycosyltransferases and sulfotransferases (Gundlach and Conrad, 1985, Leach, 1971). It is therefore not unreasonable, if indeed the disease is associated with manganese, to suggest that the observed chondrodysplasia may be the result of a mutation that renders an enzyme involved in GAG synthesis such as a glycosyltransferase, or involved in GAG sulfation such as a sulfotransferase, incapable or impaired in the utilization of manganese. Thus a phenotypic overlap between manganese deficiency and the Texel chondrodysplasia may have been created by way of an enzyme mutation, which could be associated with inability to utilize manganese but results in a disease that is characteristic of a sulfate metabolism defect, rather than a direct deficiency issue. Dietary manganese deficiency can be ruled out as the ewe flock had been grazed on improved pasture throughout pregnancy, with only a small percentage of animals on the property affected (Thompson *et al.*, 2005).

Differences observed in the sulfate staining behaviour between unaffected and affected animal proteoglycan extracts, along with the absence of any significant collagen species anomalies in affected animal extracts when compared to unaffected animal pepsin extracts, indicates that the chondrodysplasia is likely associated with proteoglycan sulfation and not a collagen defect. This is supported by histological and biochemical similarities between Texel and human and mouse chondrodysplasias resulting from sulfation defects.

4 – DNA analysis

4.1 Introduction

The chloride/sulfate antiporter DTDST plays an important role in proteoglycan synthesis in the extracellular matrix of bone and cartilage. As suggested in section 1.3.4 the DTDST gene encoding the chloride/sulfate antiporter of the cell membrane is involved in a number of chondrodysplastic disorders in humans with the degree severity determined by the position and type of mutation in the gene. It is hypothesized that the DTDST gene might be a candidate for Texel chondrodysplasia.

A reduction was observed in the level of sulfation of cartilage proteoglycans from animals affected by the chondrodysplasia. In addition phenotypic similarities exist between several of the human diseases, achondrogenesis type IB and multiple epiphyseal dysplasia, caused by mutations in the DTDST gene and the observed Texel chondrodysplasia. Therefore the exonic DNA sequence of the sheep DTDST gene, in diseased animals, was investigated for the presence of any mutations that may be causative in the disease. A comparison of the gene (exonic) sequence from unaffected animals was then made. This involved PCR (polymerase chain reaction) amplification of the exonic sequences of the gene in several separate reactions, and subsequent DNA sequence analysis.

4.2 Materials and methods

4.2.1 Materials for DNA extraction and analysis

Wizard™ Genomic DNA purification kit was a product of Promega. Phenol used for DNA extraction was obtained from USB Corporation, Cleveland, OH, USA. Custom PCR and Sequencing primers were ordered from Invitrogen life technologies Corporation, Auckland or Sigma Genosys, NSW, Australia. Agarose was purchased from Invitrogen

life technologies Corporation, Auckland. *Taq* DNA Polymerase and Proteinase K were purchased from Roche Diagnostics, Mt Wellington, Auckland. The restriction enzyme used in this project (*Kpn* I) were obtained from Invitrogen life technologies Corporation, Auckland or Amersham Biosciences, Auckland.

4.2.2 DNA extraction

DNA extraction was required to obtain samples for parentage analysis to determine paternity and therefore enable a ram, which is known to produce affected progeny, to be mated to diseased and carrier ewes in the first part of the breeding trial. The samples available at the time from affected lambs were muscle tissue, and these therefore were used to obtain the initial DNA sample used to determine parentage. Blood samples, taken throughout the project, were used for genetic analysis of the disease.

4.2.3 Sample preparation

Muscle tissue samples were taken from two lambs, designated 33047A and 33047B, respectively. Lamb 33047A had died at two days of age, while lamb 33047B died at three weeks of age with severe histological lesions. Muscle was frozen in liquid nitrogen and then pulverized using a rock crusher that had been cooled to -196°C . 10 mL of TE9 buffer (500 mM Tris, 20 mM EDTA, 10 mM NaCl pH 9.0) containing 1 mL of 10% SDS (BDH Laboratories) and 125 μL of 40 $\mu\text{g}/\mu\text{L}$ proteinase K (Roche Diagnostics) was then added to the muscle samples to aid in protease degradation. After incubation for 48 hours at 50°C , the solution was forced through an eighteen gauge needle three times, using finger pressure, to shear the tissue fragments.

4.2.4 Phenol chloroform extraction

DNA was extracted by adding an equal volume of tris-equilibrated phenol and chloroform followed by vigorous vortexing for 3 minutes. The sample was then centrifuged at 3,000 rpm (RTH-750 rotor) (1864 g) for 10 minutes and the supernatant removed. This was repeated three times. Extraction of final aqueous phase was

performed using an equal volume of chloroform, and vigorous vortexing for 3 minutes. The sample was then centrifuged for 10 minutes at 3,000 rpm and the upper phase transferred to a sterile 15 mL NUNC tube for ethanol precipitation. DNA was precipitated from samples by adding 1/3 sample volume of 10 M ammonium acetate, followed by 2.5 volumes of cold 95% ethanol. Samples were then incubated at -70°C for at least two hours, followed by centrifugation at 13,000 rpm (a-4-38 rotor) for 1 hour at 4°C. The DNA pellet was then washed in 70% ethanol and centrifuged again at 13,000 rpm for 5 minutes at 4°C. After drying and re-suspension of the DNA pellet in 250 µL of renaturation solution (10 mM Tris-HCl, 1 mM EDTA pH 8.0) (Wizard genomic DNA kit), 3.5 µL samples were analysed on 1% agarose gel, and sample concentration was determined by spectrophotometry using absorbance at 260 nm and 280 nm.

4.2.5 DNA extraction from blood

Blood samples of 10 mL volume taken from control, carrier, and affected animals were stored with 14 mg/mL EDTA and frozen at -70°C until required for DNA analysis. DNA was extracted using the Wizard™ Genomic DNA Purification Kit (Promega). Determination of successful extraction and quantification of samples was determined by subjecting 5 µL of the DNA to agarose gel electrophoresis.

4.2.6 Oligonucleotides

Oligonucleotide primers were designed to both PCR amplify and sequence the exonic region of the sulfate/chloride antiporter (see appendix H for primer sequences), based on the *Ovis aries* cDNA (NCBI accession # Y18558), using the primer design computer software, Amplify 1.0 (<http://engels.genetics.wisc.edu/amplify/index.html>). Oligonucleotides were synthesized by Sigma Genosys, NSW, Australia, and provided as a dry stock. Each was reconstituted in TE buffer (10 mM Tris-HCl pH 8.0, 0.1 mM EDTA) to a concentration of 10 µg/ µL and stored at -20°C. Oligonucleotides were serially diluted in TE to a concentration of 50 ng/ µL for PCR reactions.

4.2.7 Exon two polymerase chain reaction and sequencing primers

A forward polymerase chain reaction primer was designed to the sequence in the 5' region of exon 5 (exon2-for) and a reverse primer (exon2-rev) designed to the region which corresponded to the 3' end of exon two. The positioning of these primers can be seen in Figure 15. Refer to appendix G for primer sequences. The primers used to sequence exon two were the same as those used in the PCR reaction (exon2-for/exon2-rev).

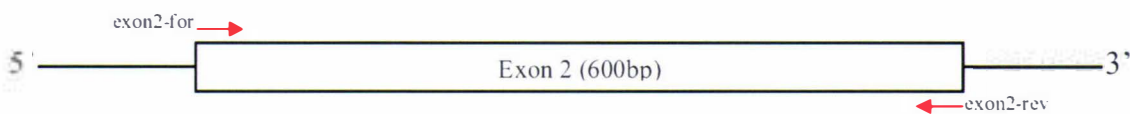


Figure 15: Position of PCR and sequencing primers on exon 2. Using these PCR primers the fragment is expected to be 600 base pairs in length.

4.2.8 Exon three polymerase chain reaction and sequencing primers

A forward polymerase chain reaction primer was designed to the sequence in the 5' region of exon 3 (exon3-for) and a reverse primer (exon3-rev) designed to the region which corresponded to the 3' end of exon 3. The primer sequences can be seen in appendix G. In order to obtain the full sequence for exon three several sequencing reactions were required using different primers. This involved the use of the PCR primers as well newly designed sequencing primers. Individual reactions were set up with either a primer that was designed to anneal to the 5' end of the fragment (exon3-for/exon3-for1), to a region in the centre of the fragment (exon3-for2/exon3-rev2), or to the 3' end of the fragment (exon3-rev/exon3-rev1) (see appendix G for primer sequences). The positioning of the primers can be seen in Figure 16.

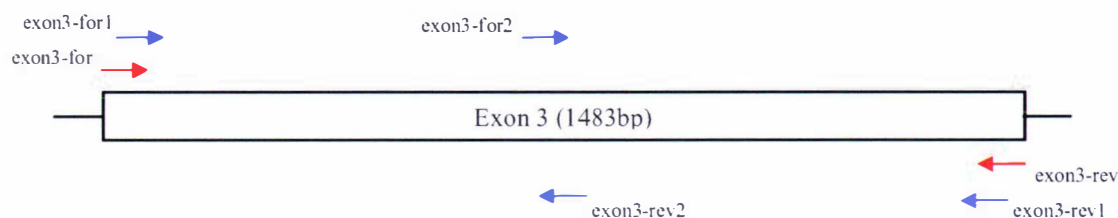


Figure 16: Positioning of PCR (—▶) and sequencing (—▶) primers on exon 3. The PCR primers were also used for sequencing. Using these PCR primers the fragment is expected to be 1483 base pairs in length.

The fragment, for each of the control, carrier, and diseased animal samples, was therefore sequenced in both directions (on both strands) in a number of separate reactions.

4.2.9 General PCR reactions

Each PCR reaction contained 5 μL (50 $\text{ng}/\mu\text{L}$) of each primer, 5 μL (3 mM) dNTPs (a mixture of dATP, dTTP, dCTP, and dGTP), 5 μL 10 x PCR buffer (100 mM Tris-HCl, 500 mM KCl pH 8.3, Roche), 0.5 μL *Taq* polymerase (5 U/ μL , Roche), 2 μL of DNA template (approximately 2 $\text{ng}/\mu\text{L}$) and dH_2O to make a total reaction volume of 50 μL . *Taq* polymerase was added last and the reaction mixed thoroughly followed by addition of a drop (approximately 25 μL) of mineral oil. All PCR was carried out in 0.5 mL tubes on a Corbett FTS – 320 thermal sequencer (Corbett Research) programmed as shown below.

Thermocycling conditions for PCR

	95°C for 5 minutes.	
Denaturing	95°C for 30 seconds	}
Annealing	55°C for 30 seconds	
Extension	72°C for 30 seconds	
		30 cycles

72°C for 4 minutes

A negative control (no DNA template) was also included with each PCR reaction to ensure no contamination of samples. A 5 μL aliquot of each reaction was analyzed for correct amplification by agarose gel electrophoresis, and restriction enzyme digest.

4.2.10 Column purification of DNA

DNA was purified from PCR using the QIAquick PCR purification kit (Qiagen). This involves DNA binding to a silica column in the presence of high salt, and at a pH of less than 7.5. The samples were mixed with the buffer as supplied to provide optimum conditions for binding, and applied to the column. During centrifugation at 13,000 rpm DNA binds to the silica, whilst contaminants pass through. The column was then washed with ethanol containing buffer, and DNA eluted in a low salt buffer.

4.2.11 DNA Quantification

The concentration of DNA samples was estimated by gel electrophoresis. 5 μL of the query DNA with 10 % loading dye was loaded on a 1 % agarose gel (incorporating 2 μL of 10 mg/mL ethidium bromide), along with 5 μL of each quantification standard (5 ng/ 5 μL , 10 ng/ 5 μL , 20 ng/ 5 μL , 50 ng/ 5 μL , 100 ng/ 5 μL), and electrophoresed for 1 hour in 1 x TAE at 100V. DNA was visualized by exposure to UV light and the intensity of fluorescence emitted from the query DNA was compared to that of the known standards, thereby indicating the concentration of the query DNA. The standards were generated from linearized plasmid DNA (pBluescript SK-II).

4.2.12 Restriction endonuclease digests

Restriction digests were carried out in 1 x digestion buffer (as recommended by manufacturer of individual enzymes) in a 30 μL total volume. For complete digestion, 1 unit of enzyme was used per 5 μg of DNA, and samples incubated at the optimal temperature as recommended by manufacturer for 1 hour.

4.2.13 Agarose gel electrophoresis

Agarose gel electrophoresis was carried out using Mini SubTM DNA Cell (BioRad) gel boxes, in 1 x TAE (0.04 M Tris-Acetate, 1 mM EDTA pH 8.0). Agarose was dissolved in 1 x TAE, and 2 μ L of ethidium bromide solution (10 mg/mL) per 50 μ L of gel was added once the gel had cooled. Agarose was then poured into a gel tray with combs in place and left to set. DNA loading dye (40 % (w/v) sucrose, 0.25 % (w/v) bromophenol blue) was added to samples which were applied to the wells of gel submerged in 1 x TAE. Current (120V) was applied to the gel, with the DNA migrating toward the positive terminal. Once the bromophenol blue dye front reached the bottom of the gel, the current was switched off, and DNA visualized under UV light.

4.2.14 DNA sequencing

DNA to be sequenced was pre-mixed at a concentration of 1 ng of DNA per 100 base pairs, with 3.2 pmol of primer in a 15 μ L total reaction volume. Pre-mixed DNA and primer samples were submitted to the Allan Wilson Centre Genome Service, where the DNA was sequenced using the BigDye[®] Terminator v3.1 Kit (Applied Biosystems) and samples were analysed using the ABI3730 Genetic Analyzer (Applied Biosystems). The resulting sequence data was edited manually and used in alignments.

4.2.15 Sequence analysis

Sequences were analyzed and contiguous sequences created by sequence analysis software provided by either GCG (Wisconsin Genetics Computer Group, Version 9.1, USA) or Biology Workbench (San Diego Supercomputer Centre, University of California, USA). Various functions were used in GCG to carry out certain processes, including: sequence uploading (pico, Gelenter), fragment assembly (Gelstart), generating contiguous sequences (Gelmerge), sequence alignment and graphic output (Gelassemble). Firstly, a directory was created within the program using the command line 'Gelstart'. This command initializes the fragment assembly system and enables the GCG network to recognize and build individual projects. Each sequence was entered individually into the directory using 'pico' and 'Gelenter' commands to allow storage within the created

directory. Each set of sequences was then assembled into consensus sequences using 'Gelmerge'. 'Gelmerge' automatically recognizes overlapping sequences between individual fragments and creates aligned assemblies. Finally, 'Gelassemble' allowed viewing of the consensus sequences created. The web-based tool, SDSC Biology Workbench (Subramaniam, 2005) which allows searching of many protein and nucleic acid sequence databases was also used. This website allows database searching integrated with access to a wide variety of analysis and modeling tools. The functions used included analyzing a nucleotide sequence for restriction enzyme sites (TACG), and aligning sequences using optimal global sequence alignment (ALIGN). Alignments were created using the gap and best-fit algorithms.

4.3 PCR

4.3.1 Genomic DNA extraction

Genomic DNA extracted from control (N), carrier (C), and affected (A) blood samples can be seen in Figure 17. These samples were diluted in dH₂O before being used as a template for PCR.

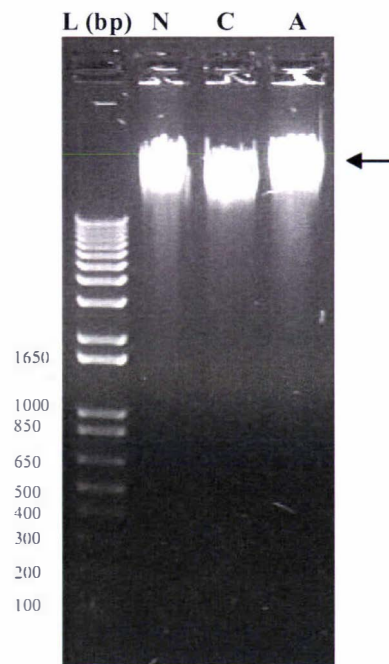


Figure 17: 1% agarose gel electrophoresed in 1x TAE buffer until the bromophenol blue dye front reached the end of the gel. 5 μ L of each DNA extract were loaded in the wells. The bands (arrow) show extracted genomic DNA. L = 1 kb plus ladder; N = normal animal DNA sample; C = carrier animal DNA sample; A = affected animal DNA sample.

4.3.2 Exon 2

The melting temperatures of the forward and reverse primers are 64° C and 60° C respectively. The following thermocycling conditions were set for the reaction.

Thermocycling conditions for PCR

95° C for 5 minutes.

Denaturing	95° C for 30 seconds	} 30 cycles
Annealing	58° C for 30 seconds	
Extension	72° C for 30 seconds	

72° C for 4 minutes

PCR products were successfully produced from each of the normal, carrier, and affected animal DNA samples, as shown below. The bands represent a six hundred base pair fragment (Figure 18).

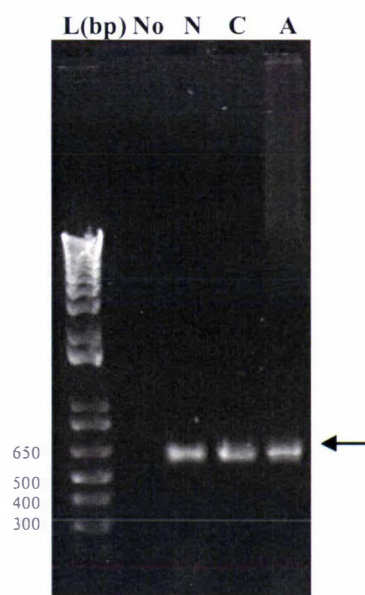


Figure 18: 1% agarose gel showing the PCR products produced from amplification of exon 2. 5 μ L of each product was loaded and the gel electrophoresed in 1x TAE until the dye front reached the end of the gel. **L** = 1kb plus Ladder; **No** = pcr blank; **N** = normal animal DNA; **C** = carrier animal DNA; **A** = affected animal DNA. The bands produced represent a fragment of 600bp in size (arrow).

4.3.3 Exon 3

The melting temperature of the forward and reverse primers designed for Exon 3 is 56° C. Therefore the PCR conditions were altered accordingly and the following thermocycle was used.

Thermocycling conditions for PCR

	95°C for 5 minutes.	
Denaturing	95°C for 30 seconds	} 30 cycles
Annealing	54°C for 30 seconds	
Extension	72°C for 30 seconds	
	72°C for 4 minutes	

Products that represent fragments of one thousand four hundred and eighty three base pairs are present for each of the DNA samples (Figure 19).

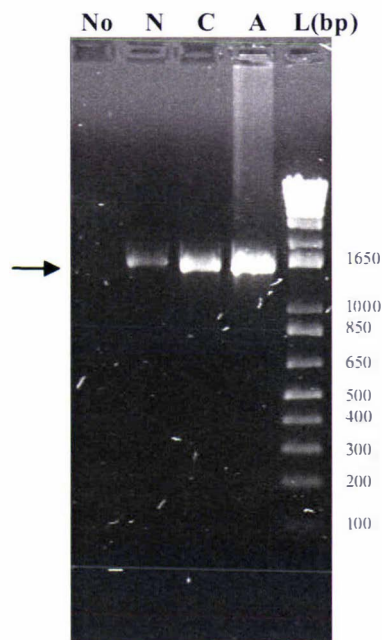


Figure 19: 1% agarose gel electrophoresed in 1 x TAE until dye front near end of gel, showing bands representing PCR products from exon 3. L = 1 kb plus DNA Ladder; No = pcr blank; N = normal animal DNA; C = carrier animal DNA; A = affected animal DNA. The bands represent a product of 1483bp in size (arrow).

4.3.4 Diagnostic digest

The specificity of restriction enzymes for their cut sites allows for their use in diagnostic digests of PCR products, and therefore determination that the product is the desired amplified fragment, based on the presence of fragments of a known size after digestion.

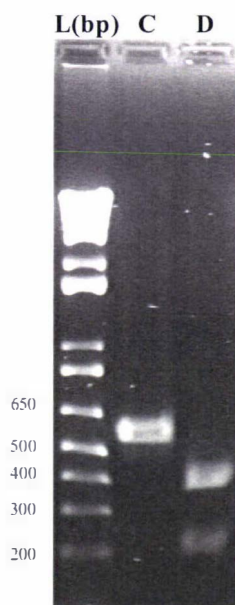


Figure 20: 1% agarose gel showing diagnostic digest of exon 2 PCR fragment. 5 μ L of each product was loaded and the gel electrophoresed in 1x TAE until the dye front reached the end of the gel. It can be seen that after digestion (lane D) two fragments appear of sizes 205 and 395bp, respectively, indicating successful digestion of the band, and confirmation of the correct fragment. **L** =1kb plus DNA ladder; **C** = negative control; **D** = digested DNA.

Figure 20 shows the digestion of a 600 base pair – exon 2 fragment into fragments of 205 and 395 base pairs, respectively, using *Kpn I*. This provides confirmation that this amplified DNA region is the one expected. Rather than subjecting exon 3 fragments to digestion, direct sequencing was carried out to determine that the amplified region was indeed exon 3 of the DTDST.

4.3.5 DNA quantification

DNA quantification was determined, and the information used to ensure that the correct concentration of PCR product was included in each of the sequencing reactions. Quantification agarose gels can be seen in Figure 21 for exon 2 and Figure 22 for exon 3. Results indicated that the concentration of the PCR products for exon 2 normal, carrier, and affected animals were approximately 20 ng/5 μ L, 10 ng/5 μ L, and 5 ng/5 μ L, respectively. The quantification gel for exon 3 indicates that the approximate

concentrations of pcr products for exon 3 are 10 ng/5 μ L for each of the normal, carrier, and affected animals. These gels are representative, and a number of pcr reactions were carried out, and quantified, in order to get enough products for all sequencing reactions.

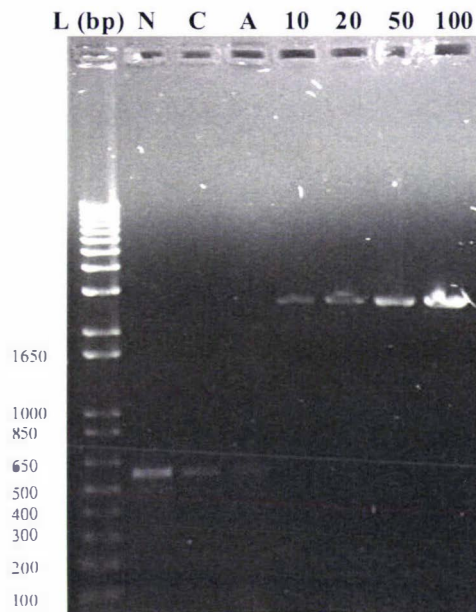


Figure 21: 1 % agarose gel representing quantification of the PCR products of exon 2. 5 μ L of each product was loaded and the gel electrophoresed in 1x TAE until the dye front reached the end of the gel. **N** = PCR product from control animal; **C** = PCR product from carrier animal; **A** = PCR product from affected animal. **10, 20, 50, 100** represent DNA concentration standards of 10 ng/5 μ L, 20 ng/5 μ L, 50 ng/5 μ L, and 100 ng/5 μ L, respectively. It can be seen that PCR product from the control (N) animal has a concentration of approximately 20 ng/5 μ L, while the carrier (C) and affected (A) samples have a concentration of approximately 10 ng/5 μ L, and slightly less than this, respectively

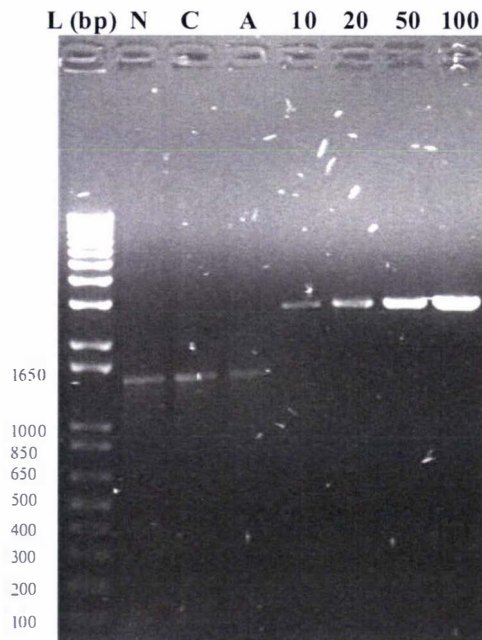


Figure 22: 1 % agarose gel representing quantification of the PCR products of exon 3. 5 μ L of each product was loaded and the gel electrophoresed in 1x TAE until the dye front reached the end of the gel. N = PCR product from control animal; C = PCR product from carrier animal; A = PCR product from affected animal. 10, 20, 50, 100 represent DNA concentration standards of 10 ng/5 μ L, 20 ng/5 μ L, 50 ng/5 μ L, and 100 ng/5 μ L, respectively. It can be seen that PCR products from the control (N), carrier (C) and affected (A) animal samples have a concentration of approximately 10ng/5 μ L.

4.4 Sequence analysis

4.4.1 Exon 2

Forward and reverse sequences were obtained for each of the affected, carrier, and control (normal) PCR products by direct sequencing of exon 2, on both strands (refer to appendix H for sequence output). The two sequence products for each animal group were then combined to create a consensus sequence, which were then aligned for a comparison of the coding sequence. The sequence shown below represents 96.8 %, 97.3 %, and 98.5 % of the control, carrier, and affected PCR product, respectively.

From Figure 23 it can be seen that there are no base pair polymorphisms in the sequences across the length of the aligned region.

```

Name: Ex2Affected      = Exon 2 Affected consensus   Len:   591
Name: Ex2Carrier       = Exon 2 Carrier consensus     Len:   584
Name: Ex2Normal        = Exon 2 Control consensus      Len:   581

Ex2Affected           1                               50
CATCTGGGAT CCATGTGGAG CATGAAGAGG AATCACGTAA TGACTTCTGG
Ex2Carrier            CATCTGGGAT CCATGTGGAG CATGAAGAGG AATCACGTAA TGACTTCTGG
Ex2Normal             ~~~~TGGGAT CCATGTGGAG CATGAAGAGG AATCACGTAA TGACTTCTGG

Ex2Affected           51                               100
CAGTTTGAGT CCAGTAATCT TTTTAGACAC CCTAGGATCC ATTTGGAGCC
Ex2Carrier            CAGTTTGAGT CCAGTAATCT TTTTAGACAC CCTAGGATCC ATTTGGAGCC
Ex2Normal             CAGTTTGAGT CCAGTAATCT TTTTAGACAC CCTAGGATCC ATTTGGAGCC

Ex2Affected           101                              150
TCAAGAGAAA TCAGATAATA ACCTCAAGAA GTTTGTATC AAAAAACTAG
Ex2Carrier            TCAAGAGAAA TCAGATAATA ACCTCAAGAA GTTTGTATC AAAAAACTAG
Ex2Normal             TCAAGAGAAA TCAGATAATA ACCTCAAGAA GTTTGTATC AAAAAACTAG

Ex2Affected           151                              200
AGAAGAGTTG CCAGTGTAGT TCAACCAAAG CCAAAAATAC CATTTTGGT
Ex2Carrier            AGAAGAGTTG CCAGTGTAGT TCAACCAAAG CCAAAAATAC CATTTTGGT
Ex2Normal             AGAAGAGTTG CCAGTGTAGT TCAACCAAAG CCAAAAATAC CATTTTGGT

Ex2Affected           201                              250
TTCCTTCCTG TTTTGCAGTG GCTCCCAAAA TATGATCTGA AGAAAAACAT
Ex2Carrier            TTCCTTCCTG TTTTGCAGTG GCTCCCAAAA TATGATCTGA AGAAAAACAT
Ex2Normal             TTCCTTCCTG TTTTGCAGTG GCTCCCAAAA TATGATCTGA AGAAAAACAT

Ex2Affected           251                              300
TTTAGGAGAT ATGATGTCTG GCTTGATTGT GGGCATCTTA TTGGTGCCCC
Ex2Carrier            TTTAGGAGAT ATGATGTCTG GCTTGATTGT GGGCATCTTA TTGGTGCCCC
Ex2Normal             TTTAGGAGAT ATGATGTCTG GCTTGATTGT GGGCATCTTA TTGGTGCCCC

Ex2Affected           301                              350
AATCCATTGC TTATTCTCTC TTGGCTGGCC AAGAACCTAT CTATGGTCTG
Ex2Carrier            AATCCATTGC TTATTCTCTC TTGGCTGGCC AAGAACCTAT CTATGGTCTG
Ex2Normal             AATCCATTGC TTATTCTCTC TTGGCTGGCC AAGAACCTAT CTATGGTCTG

Ex2Affected           351                              400
TACACATCTT TTTTGGCCAG CCTCATTAT  TTCATTTTGG GTACTCCCG
Ex2Carrier            TACACATCTT TTTTGGCCAG CCTCATTAT  TTCATTTTGG GTACTCCCG
Ex2Normal             TACACATCTT TTTTGGCCAG CCTCATTAT  TTCATTTTGG GTACTCCCG

Ex2Affected           401                              450
TCACATCTCT GTGGGCATTT TTGGAATACT GTGCCTTATG ATTGGTGAAG
Ex2Carrier            TCACATCTCT GTGGGCATTT TTGGAATACT GTGCCTTATG ATTGGTGAAG
Ex2Normal             TCACATCTCT GTGGGCATTT TTGGAATACT GTGCCTTATG ATTGGTGAAG

Ex2Affected           451                              500
TAGTTGACCG AGAACTATAC ATAGCTGGCT ATGACTGT  CCATGCCGCT
Ex2Carrier            TAGTTGACCG AGAACTATAC ATAGCTGGCT ATGACTGT  CCATGCCGCT
Ex2Normal             TAGTTGACCG AGAACTATAC ATAGCTGGCT ATGACTGT  CCATGCCGCT

Ex2Affected           501                              550
TCAAATGAGA GTCATTAGT AAACCAGATG TCAAACCAGA CATGTGACAG
Ex2Carrier            TCAAATGAGA GTCATTAGT AAACCAGATG TCAAACCAGA CATGTGACAG
Ex2Normal             TCAAATGAGA GTCATTAGT AAACCAGATG TCAAACCAGA CATGTGACAG

Ex2Affected           551                              591
AAGTTGCTAT GCAATTACAG TTGGCAGCAC TGTAACCTTT G
Ex2Carrier            AAGTTGCTAT GCAATTACAG TTGGCAGCAC TGTA~~~~~ ~
Ex2Normal             AAGTTGCTAT GCAATTACAG TTGGCAGCAC TGTA~~~~~ ~

```

Figure 23: Alignment of the sequenced regions of exon 2 from normal (Ex2Normal), carrier (Ex2Carrier), and affected (Ex2Affected) animals. There are no base pair polymorphisms present in any of the sequences.

4.4.2 Exon 3

Several sequencing products were obtained from the PCR products of exon 3. As with exon 2, the exon 3 fragment was sequenced directly in the forward and reverse direction (both strands), which included two, three, or four reactions in the forward direction and two, three, or four reactions in the reverse direction, respectively. Thus, the number of sequence products obtained for each of the normal (control), carrier, and affected PCR samples differed depending on the quality of the sequence obtained from the respective primers. These products were combined to create a consensus sequence for each animal (normal, carrier, and affected), and the three consensus sequences aligned. The entire length of the PCR product for exon 3 was not sequenced in any of the fragments. The reason for this is because certain regions of sequence, particularly around the primer region, were not good enough to use for mutation analysis. From the alignment in Figure 24 corresponding to 98.8 %, 87.8 %, and 97.8 % of the sequence of the PCR product for exon 3 for control, carrier, and affected, respectively, it can be seen that there are no nucleotide differences between the exonic DNA.

Name: Ex3Affected	= Exon 3 Affected consensus	Len: 1451
Name: Ex3Carrier	= Exon 3 Carrier consensus	Len: 1302
Name: Ex3Normal	= Exon 3 Control consensus	Len: 1465

	1				50
Ex3Normal	TTCTCAGTCT	ACCTCTCCGA	TGCCTTGCTG	GGTGGGTTTG	TCACTGGTGC
Ex3Carrier	~~~~~	~~~~~	~~~~~	~~~~~	~~~~~
Ex3Affected	~~~~~CAGTCT	ACCTCTCCGA	TGCCTTGCTG	GGTGGGTTTG	TCACTGGTGC

	51				100
Ex3Normal	CTCCTTCACT	ATTCTTACAT	CTCAAGTCAA	GTACCTCCTT	GGACTCAGCC
Ex3Carrier	~~~~~	~~~~~	~~~~~	~~~~~	~~~~~
Ex3Affected	CTCCTTCACT	ATTCTTACAT	CTCAAGTCAA	GTACCTCCTT	GGACTCAGCC

	101				150
Ex3Normal	TTCCTCGGAG	TGGTGGAGTG	GGATCACTCA	TCACTACTTG	GATACATATC
Ex3Carrier	~~~~~	~~~~~	~~~~~	~~~~~	~~~~~
Ex3Affected	TTCCTCGGAG	TGGTGGAGTG	GGATCACTCA	TCACTACTTG	GATACATATC

	151				200
Ex3Normal	TTCAGAAACA	TCCATAAGAC	CAATATCTGT	GATCTCATCA	CCAGCCTTTT
Ex3Carrier	~~~AGAAACA	TCCATAAGAC	CAATATCTGT	GATCTCATCA	CCAGCCTTTT
Ex3Affected	TTCAGAAACA	TCCATAAGAC	CAATATCTGT	GATCTCATCA	CCAGCCTTTT

	201				250
Ex3Normal	GTGCCTTTTG	GTTCTTTTGC	CAACCAAAGA	ACTCAATGAG	CGCTTCAAGT
Ex3Carrier	GTGCCTTTTG	GTTCTTTTGC	CAACCAAAGA	ACTCAATGAG	CGCTTCAAGT
Ex3Affected	GTGCCTTTTG	GTTCTTTTGC	CAACCAAAGA	ACTCAATGAG	CGCTTCAAGT

	251				300
Ex3Normal	CCAAGCTTAA	GGCACCGATT	CCTGTTGAAC	TCTTTGTTGT	TGTGGCAGCC
Ex3Carrier	CCAAGCTTAA	GGCACCGATT	CCTGTTGAAC	TCTTTGTTGT	TGTGGCAGCC
Ex3Affected	CCAAGCTTAA	GGCACCGATT	CCTGTTGAAC	TCTTTGTTGT	TGTGGCAGCC

	301				350
Ex3Normal	ACATTAGCCT	CTCATTTTGG	AAAACCTCTCT	GAGAAATATG	GCACCAGTAT
Ex3Carrier	ACATTAGCCT	CTCATTTTGG	AAAACCTCTCT	GAGAAATATG	GCACCAGTAT
Ex3Affected	ACATTAGCCT	CTCATTTTGG	AAAACCTCTCT	GAGAAATATG	GCACCAGTAT
	351				400
Ex3Normal	TGCTGGGCAT	ATTCCCACCTG	GGTTTATGCC	ACCCAAAGCA	CCTGACTGGA
Ex3Carrier	TGCTGGGCAT	ATTCCCACCTG	GGTTTATGCC	ACCCAAAGCA	CCTGACTGGA
Ex3Affected	TGCTGGGCAT	ATTCCCACCTG	GGTTTATGCC	ACCCAAAGCA	CCTGACTGGA
	401				450
Ex3Normal	ACTTAATTCC	TAGAGTGGCT	GTAGATGCAA	TAGCTATTGC	TATCATTGGG
Ex3Carrier	ACTTAATTCC	TAGAGTGGCT	GTAGATGCAA	TAGCTATTGC	TATCATTGGG
Ex3Affected	ACTTAATTCC	TAGAGTGGCT	GTAGATGCAA	TAGCTATTGC	TATCATTGGG
	451				500
Ex3Normal	TTTGCTATCA	CTGTATCACT	TTCTGAGATG	TTTGCCAAGA	AACATGGCTA
Ex3Carrier	TTTGCTATCA	CTGTATCACT	TTCTGAGATG	TTTGCCAAGA	AACATGGCTA
Ex3Affected	TTTGCTATCA	CTGTATCACT	TTCTGAGATG	TTTGCCAAGA	AACATGGCTA
	501				550
Ex3Normal	CACAGTCAAA	GCTAATCAGG	AAATGTACGC	TATCGGCTTT	TGCAATATCA
Ex3Carrier	CACAGTCAAA	GCTAATCAGG	AAATGTACGC	TATCGGCTTT	TGCAATATCA
Ex3Affected	CACAGTCAAA	GCTAATCAGG	AAATGTACGC	TATCGGCTTT	TGCAATATCA
	551				600
Ex3Normal	TCCCTTCCTT	CTTCCACAGC	TTCACTACTA	GCGCAGCTCT	TGCAAAGACA
Ex3Carrier	TCCCTTCCTT	CTTCCACAGC	TTCACTACTA	GCGCAGCTCT	TGCAAAGACA
Ex3Affected	TCCCTTCCTT	CTTCCACAGC	TTCACTACTA	GCGCAGCTCT	TGCAAAGACA
	601				650
Ex3Normal	CTGGTGAAGG	AATCCACAGG	CTGTCAAACCT	CAGGTTTCTG	GTGTGATGAC
Ex3Carrier	CTGGTGAAGG	AATCCACAGG	CTGTCAAACCT	CAGGTTTCTG	GTGTGATGAC
Ex3Affected	CTGGTGAAGG	AATCCACAGG	CTGTCAAACCT	CAGGTTTCTG	GTGTGATGAC
	651				700
Ex3Normal	AGCTCTGGTT	CTTTTGTGG	TCCTCTTGGT	CATAGCTCCT	TTGTCTTCT
Ex3Carrier	AGCTCTGGTT	CTTTTGTGG	TCCTCTTGGT	CATAGCTCCT	TTGTCTTCT
Ex3Affected	AGCTCTGGTT	CTTTTGTGG	TCCTCTTGGT	CATAGCTCCT	TTGTCTTCT
	701				750
Ex3Normal	CCCTGCAGAA	AAGTGTCTCT	GGTGTGATCA	CTATTGTAAA	TCTCCGGGGA
Ex3Carrier	CCCTGCAGAA	AAGTGTCTCT	GGTGTGATCA	CTATTGTAAA	TCTCCGGGGA
Ex3Affected	CCCTGCAGAA	AAGTGTCTCT	GGTGTGATCA	CTATTGTAAA	TCTCCGGGGA
	751				800
Ex3Normal	GCCCTATGTA	AATTTAAGGA	TCTGCCCCAG	ATGTGGAGGA	TTAGCAGAAT
Ex3Carrier	GCCCTATGTA	AATTTAAGGA	TCTGCCCCAG	ATGTGGAGGA	TTAGCAGAAT
Ex3Affected	GCCCTATGTA	AATTTAAGGA	TCTGCCCCAG	ATGTGGAGGA	TTAGCAGAAT
	801				850
Ex3Normal	GGACACAGTT	ATCTGGTTTG	TTACTATGCT	GTCCTCTGCA	CTGATCAGTA
Ex3Carrier	GGACACAGTT	ATCTGGTTTG	TTACTATGCT	GTCCTCTGCA	CTGATCAGTA
Ex3Affected	GGACACAGTT	ATCTGGTTTG	TTACTATGCT	GTCCTCTGCA	CTGATCAGTA
	851				900
Ex3Normal	CTGAAATAGG	CCTGCTTACT	GGGGTTTGGT	TTTCTATGTT	TTGTGTTATC
Ex3Carrier	CTGAAATAGG	CCTGCTTACT	GGGGTTTGGT	TTTCTATGTT	TTGTGTTATC
Ex3Affected	CTGAAATAGG	CCTGCTTACT	GGGGTTTGGT	TTTCTATGTT	TTGTGTTATC
	901				950
Ex3Normal	CTCCGCACCT	AGAAGCCAAA	GGCTTCATTG	CTTGGCTTGG	TGGAAGATTC
Ex3Carrier	CTCCGCACCT	AGAAGCCAAA	GGCTTCATTG	CTTGGCTTGG	TGGAAGATTC
Ex3Affected	CTCCGCACCT	AGAAGCCAAA	GGCTTCATTG	CTTGGCTTGG	TGGAAGATTC
	951				1000
Ex3Normal	TGAAGTCTTT	GAGTCCATGT	CTGCCTACAA	GAACCTTCAG	GCCAAGTCAG
Ex3Carrier	TGAAGTCTTT	GAGTCCATGT	CTGCCTACAA	GAACCTTCAG	GCCAAGTCAG
Ex3Affected	TGAAGTCTTT	GAGTCCATGT	CTGCCTACAA	GAACCTTCAG	GCCAAGTCAG

	1001				1050
Ex3Normal	GCATCAAGAT	TTTCCGCTTT	GTGGCCCCTC	TCTACTACGT	AAACAAAGAA
Ex3Carrier	GCATCAAGAT	TTTCCGCTTT	GTGGCCCCTC	TCTACTACGT	AAACAAAGAA
Ex3Affected	GCATCAAGAT	TTTCCGCTTT	GTGGCCCCTC	TCTACTACGT	AAACAAAGAA
	1051				1100
Ex3Normal	TATTTTAAAT	CTGTCTTATA	CAAAAAAACT	CTCAACCCAG	TCTTAGTAAA
Ex3Carrier	TATTTTAAAT	CTGTCTTATA	CAAAAAAACT	CTCAACCCAG	TCTTAGTAAA
Ex3Affected	TATTTTAAAT	CTGTCTTATA	CAAAAAAACT	CTCAACCCAG	TCTTAGTAAA
	1101				1150
Ex3Normal	AGCAGCTCAG	AGGAAGGCAG	CAAAGAAAAA	GATCAAAAAGG	GAAACGGTAA
Ex3Carrier	AGCAGCTCAG	AGGAAGGCAG	CAAAGAAAAA	GATCAAAAAGG	GAAACGGTAA
Ex3Affected	AGCAGCTCAG	AGGAAGGCAG	CAAAGAAAAA	GATCAAAAAGG	GAAACGGTAA
	1151				1200
Ex3Normal	CACCTCAGTGG	AATCCAGGAC	GAAGTTTCAG	TGCAACTTTC	CTATGATCCC
Ex3Carrier	CACCTCAGTGG	AATCCAGGAC	GAAGTTTCAG	TGCAACTTTC	CTATGATCCC
Ex3Affected	CACCTCAGTGG	AATCCAGGAC	GAAGTTTCAG	TGCAACTTTC	CTATGATCCC
	1201				1250
Ex3Normal	TTAGAGTTCC	ATACAATAGT	GATTGACTGT	AGTGCAATAC	AGTTTTTAGA
Ex3Carrier	TTAGAGTTCC	ATACAATAGT	GATTGACTGT	AGTGCAATAC	AGTTTTTAGA
Ex3Affected	TTAGAGTTCC	ATACAATAGT	GATTGACTGT	AGTGCAATAC	AGTTTTTAGA
	1251				1300
Ex3Normal	TACAGCAGGG	ATCCATACAC	TGAAAGAAGT	TCGCAGAGAT	TATGAAGCTA
Ex3Carrier	TACAGCAGGG	ATCCATACAC	TGAAAGAAGT	TCGCAGAGAT	TATGAAGCTA
Ex3Affected	TACAGCAGGG	ATCCATACAC	TGAAAGAAGT	TCGCAGAGAT	TATGAAGCTA
	1301				1350
Ex3Normal	TTGGCATCCA	GGTTCGCTG	GCTCAGTGCA	ATCCCTCTGT	GAGGGACTCC
Ex3Carrier	TTGGCATCCA	GGTTCGCTG	GCTCAGTGCA	ATCCCTCTGT	GAGGGACTCC
Ex3Affected	TTGGCATCCA	GGTTCGCTG	GCTCAGTGCA	ATCCCTCTGT	GAGGGACTCC
	1351				1400
Ex3Normal	CTGGCCAGGG	GAGAGTACTG	CAAAAAGGAT	GAAGAAAACC	TTCTCTTTTA
Ex3Carrier	CTGGCCAGGG	GAGAGTACTG	CAAAAAGGAT	GAAGAAAACC	TTCTCTTTTA
Ex3Affected	CTGGCCAGGG	GAGAGTACTG	CAAAAAGGAT	GAAGAAAACC	TTCTCTTTTA
	1401				1450
Ex3Normal	TAGTGTATAT	GAAGCCATGA	CTTTTGCAGA	AGATTCTCAG	AATCAAAAAG
Ex3Carrier	TAGTGTATAT	GAAGCCATGA	CTTTTGCAGA	AGATTCTCAG	AATCAAAAAG
Ex3Affected	TAGTGTATAT	GAAGCCATGA	CTTTTGCAGA	AGATTCTCAG	AATCAAAAAG
	1451	1465			
Ex3Normal	AGAGATATGT	CCAAT			
Ex3Carrier	AGAGA~~~~~	~~~~~			
Ex3Affected	AGAGA~~~~~	~~~~~			

Figure 24: Alignment of the sequenced regions of exon 3 from normal (Ex3Normal), carrier (Ex3Carrier), and affected (Ex3Affected) animals. There are no base pair polymorphisms present in any of the sequences.

4.4.3 Overall exon alignment

Figure 25 shows the alignment of the shortest sequences obtained for the two exons (Ex2/Ex3), these being from the normal animal (Ex2Normal) from the carrier animal (Ex3Carrier) for exon 2 and exon 3, respectively, aligned with the *Ovis aries* gene encoding sulfate transporter (NCBI accession # Y18558). The DNA sequence obtained from sequencing accounts for 85.4 % of the total *Ovis aries* sulfate transporter coding

region. The fact that there are no polymorphisms in the sequenced region does reduce the likelihood that this gene is involved in the disease. It does not however rule out the gene as a candidate for Texel chondrodysplasia, because a mutation may be present in the exonic region not sequenced or in the intron affecting splicing.

1		0	Ex2 /Ex3
1	ATGTCTTTGAAAAATGGAGAGCAAAATGACCTTTCACCCAAGGACTCAGT	50	Ovis aries
1		20	
	TGGGATCCATGTGGAGCATG		
51	TAAAGGAAATGACCAGTACAGATCTCCATCTGGGATCCATGTGGAGCATG	100	
21	AAGAGGAATCACGTAATGACTTCTGGCAGTTTGAGTCCAGTAATCTTTTT	70	
101	AAGAGGAATCACGTAATGACTTCTGGCAGTTTGAGTCCAGTAATCTTTTT	150	
71	AGACACCTTAGGATCCATTTGGAGCCTCAAGAGAAATCAGATAATAACCT	120	
151	AGACACCTTAGGATCCATTTGGAGCCTCAAGAGAAATCAGATAATAACCT	200	
121	CAAGAAGTTTGTATCAAAAACTAGAGAAGAGTTGCCAGTGTAGTTCAA	170	
201	CAAGAAGTTTGTATCAAAAACTAGAGAAGAGTTGCCAGTGTAGTTCAA	250	
171	CCAAAGCCAAAAATACCATTTTGGTTTCCTTCCTGTTTGCAGTGGCTC	220	
251	CCAAAGCCAAAAATACCATTTTGGTTTCCTTCCTGTTTGCAGTGGCTC	300	
221	CCAAAATATGATCTGAAGAAAAACATTTTAGGAGATATGATGCTGGCTT	270	
301	CCAAAATATGATCTGAAGAAAAACATTTTAGGAGATATGATGCTGGCTT	350	
271	GATTGTGGGCATCTTATTGGTGCCCAATCCATTGCTTATTCTCTCTTGG	320	
351	GATTGTGGGCATCTTATTGGTGCCCAATCCATTGCTTATTCTCTCTTGG	400	
321	CTGGCCAAGAACCTATCTATGGTCTGTACACATCTTTTTTTGCCAGCCTC	370	
401	CTGGCCAAGAACCTATCTATGGTCTGTACACATCTTTTTTTGCCAGCCTC	450	
371	ATTTATTTTCATTTTGGGTACCTCCCGTCACATCTCTGTGGGCATTTTGG	420	
451	ATTTATTTTCATTTTGGGTACCTCCCGTCACATCTCTGTGGGCATTTTGG	500	
421	AATACTGTGCCTTATGATTGGTGAAGTAGTTGACCGAGAACTATACATAG	470	
501	AATACTGTGCCTTATGATTGGTGAAGTAGTTGACCGAGAACTATACATAG	550	
471	CTGGCTATGACACTGTCCATGCCGCTTCAAATGAGAGCTCATTAGTAAAC	520	
551	CTGGCTATGACACTGTCCATGCCGCTTCAAATGAGAGCTCATTAGTAAAC	600	
521	CAGATGTCAAACCAGACATGTGACAGAAGTTGCTATGCAATTACAGTTGG	570	
601	CAGATGTCAAACCAGACATGTGACAGAAGTTGCTATGCAATTACAGTTGG	650	
571	CAGCACTGTAA-----	581	
651	CAGCACTGTAACTTTTGGGCTGGAGTTTATCAGGTAGCAATGGGCTTCT	700	
582	-----	581	
701	TTCAAGTGGGCTTTGTCTCAGTCTACCTCTCCGATGCCTTGCTGGGTGGG	750	
582	-----	581	
751	TTTGTCACTGGTGCCTCCTTCACTATTCTTACATCTCAAGTCAAGTACCT	800	
582	-----	581	
801	CCTTGGACTCAGCCTTCTCGGAGTGGTGGAGTGGGATCACTCATCACTA	850	

```

582 -----AGAAACATCCATAAGACCAATATCTGTGATCTC 614
      |||
851 CTTGGATACATATCTTCAGAAACATCCATAAGACCAATATCTGTGATCTC 900
      |||
615 ATCACCAGCCTTTTGTGCCTTTTGGTTCTTTTGCCAACCAAAGAACTCAA 664
      |||
901 ATCACCAGCCTTTTGTGCCTTTTGGTTCTTTTGCCAACCAAAGAACTCAA 950
      |||
665 TGAGCGCTTCAAGTCCAAGCTTAAGGCACCGATTCTGTGAACTCTTTG 714
      |||
951 TGAGCGCTTCAAGTCCAAGCTTAAGGCACCGATTCTGTGAACTCTTTG 1000
      |||
715 TTGTTGTGGCAGCCACATTAGCCTCTCATTTTGAAAACCTCTCTGAGAAA 764
      |||
1001 TTGTTGTGGCAGCCACATTAGCCTCTCATTTTGAAAACCTCTCTGAGAAA 1050
      |||
765 TATGGCACCAGTATTGCTGGGCATATCCCCTGGGTTTATGCCACCCAA 814
      |||
1051 TATGGCACCAGTATTGCTGGGCATATCCCCTGGGTTTATGCCACCCAA 1100
      |||
815 AGCACCTGACTGGAACCTTAATTCCTAGAGTGGCTGTAGATGCAATAGCTA 864
      |||
1101 AGCACCTGACTGGAACCTTAATTCCTAGAGTGGCTGTAGATGCAATAGCTA 1150
      |||
865 TTGCTATCATTTGGGTTTGTCTATCACTGTATCACTTTCTGAGATGTTTGCC 914
      |||
1151 TTGCTATCATTTGGGTTTGTCTATCACTGTATCACTTTCTGAGATGTTTGCC 1200
      |||
915 AAGAAACATGGCTACACAGTCAAAGCTAATCAGGAAATGTACGCTATCGG 964
      |||
1201 AAGAAACATGGCTACACAGTCAAAGCTAATCAGGAAATGTACGCTATCGG 1250
      |||
965 CTTTGTGCAATATCATCCCTCCTTCTTCCACAGCTTCACTACTAGCGCAG 1014
      |||
1251 CTTTGTGCAATATCATCCCTCCTTCTTCCACAGCTTCACTACTAGCGCAG 1300
      |||
1015 CTCTTGCAAAGACACTGGTGAAGGAATCCACAGGCTGTCAAACCTCAGGTT 1064
      |||
1301 CTCTTGCAAAGACACTGGTGAAGGAATCCACAGGCTGTCAAACCTCAGGTT 1350
      |||
1065 TCTGGTGTGATGACAGCTCTGGTCTTTTGTGGTCCCTCTTGGTCATAGC 1114
      |||
1351 TCTGGTGTGATGACAGCTCTGGTCTTTTGTGGTCCCTCTTGGTCATAGC 1400
      |||
1115 TCCTTTGTTCTTCTCCCTGCAGAAAAGTGCCTTGGTGTGATCACTATTG 1164
      |||
1401 TCCTTTGTTCTTCTCCCTGCAGAAAAGTGCCTTGGTGTGATCACTATTG 1450
      |||
1165 TAAATCTCCGGGGAGCCCTATGTAAATTTAAGGATCTGCCCCAGATGTGG 1214
      |||
1451 TAAATCTCCGGGGAGCCCTATGTAAATTTAAGGATCTGCCCCAGATGTGG 1500
      |||
1215 AGGATTAGCAGAATGGACACAGTTATCTGGTTTGTACTATGCTGTCTC 1264
      |||
1501 AGGATTAGCAGAATGGACACAGTTATCTGGTTTGTACTATGCTGTCTC 1550
      |||
1265 TGCACTGATCAGTACTGAAATAGGCTGCTTACTGGGTTTGTGTTTTCTA 1314
      |||
1551 TGCACTGATCAGTACTGAAATAGGCTGCTTACTGGGTTTGTGTTTTCTA 1600
      |||
1315 TGTTTTGTGTTATCCTCCGCACTCAGAAGCCAAAGGCTTCATTGCTTGGC 1364
      |||
1601 TGTTTTGTGTTATCCTCCGCACTCAGAAGCCAAAGGCTTCATTGCTTGGC 1650
      |||
1365 TTGGTGAAGATTCTGAAGTCTTTGAGTCCATGTCTGCCTACAAGAACCT 1414
      |||
1651 TTGGTGAAGATTCTGAAGTCTTTGAGTCCATGTCTGCCTACAAGAACCT 1700
      |||
1415 TCAGGCCAAGTCAGGCATCAAGATTTCCGCTTTGTGGCCCTCTCTACT 1464
      |||
1701 TCAGGCCAAGTCAGGCATCAAGATTTCCGCTTTGTGGCCCTCTCTACT 1750
      |||
1465 ACGTAAACAAAGAATATTTTAAATCTGTCTTATACAAAAAACTCTCAAC 1514
      |||
1751 ACGTAAACAAAGAATATTTTAAATCTGTCTTATACAAAAAACTCTCAAC 1800
      |||
1515 CCAGTCTTAGTAAAAGCAGCTCAGAGGAAGGCAGCAAAGAAAAAGATCAA 1564
      |||
1801 CCAGTCTTAGTAAAAGCAGCTCAGAGGAAGGCAGCAAAGAAAAAGATCAA 1850
      |||

```

```

1565 AAGGGAAACGGTAACACTCAGTGAATCCAGGACGAAGTTTCAGTGCAAC 1614
      |||
1851 AAGGGAAACGGTAACACTCAGTGAATCCAGGACGAAGTTTCAGTGCAAC 1900
      |||
1615 TTTCCTATGATCCCTTAGAGTTCATACAATAGTGATTGACTGTAGTGCA 1664
      |||
1901 TTTCCTATGATCCCTTAGAGTTCATACAATAGTGATTGACTGTAGTGCA 1950
      |||
1665 ATACAGTTTTTTAGATACAGCAGGGATCCATACTGAAAGAAGTTCGCAG 1714
      |||
1951 ATACAGTTTTTTAGATACAGCAGGGATCCATACTGAAAGAAGTTCGCAG 2000
      |||
1715 AGATTATGAAGCTATTGGCATCCAGGTTCTGCTGGCTCAGTGCAATCCCT 1764
      |||
2001 AGATTATGAAGCTATTGGCATCCAGGTTCTGCTGGCTCAGTGCAATCCCT 2050
      |||
1765 CTGTGAGGGACTCCCTGGCCAGGGGAGAGTACTGCAAAAAGGATGAAGAA 1814
      |||
2051 CTGTGAGGGACTCCCTGGCCAGGGGAGAGTACTGCAAAAAGGATGAAGAA 2100
      |||
1815 AACCTTCTCTTTTATAGTGATATGAAGCCATGACTTTTGCAGAAGATTC 1864
      |||
2101 AACCTTCTCTTTTATAGTGATATGAAGCCATGACTTTTGCAGAAGATTC 2150
      |||
1865 TCAGAATCAAAAAGAGAGA 1883
      |||
2151 TCAGAATCAAAAAGAGAGATATGTTCCAATGGTCCAAGTTTTTCCAGTG 2200
      |||
1884          1883
2201 ATTGA    2205

```

Figure 25: Complete alignment of the shortest sequence obtained for each of exon 2 (Ex2Normal), and exon 3 (Ex3Carrier), with the complete exonic sequence for the *Ovis aries* gene encoding sulfate transporter. The aligned region represents 85.4 % of the total exonic region.

5 – Summary and future direction

Based on the breeding trial results it is likely that inheritance of Texel chondrodysplasia is the result of a single autosomal recessive gene. This is in agreement with the observation that chondrodysplasias, in many animals, are commonly inherited in this manner.

Biochemical analysis of proteoglycans by SDS-PAGE analysis and sulfate-specific staining has provided a strong indication of the biochemical pathway, and therefore the genes/gene mutations, that may be involved in the disease. Analysis of collagen species, also using SDS-PAGE, from affected and normal animals revealed no difference, excluding a collagen defect as the cause of the disease. A number of genes (DTDST, SK2) that encode the proteins of the chondrocyte sulfate activation pathway have been implicated in skeletal diseases including the DTDST family of inherited chondrodysplasias in humans, the brachymorphic mouse, and a DTDST-related phenotype in Holstein cattle.

In terms of the candidate gene studied, DTDST, determination of its involvement was not definitive. While mutations were absent from the sequenced region of the gene, it can not be eliminated as a candidate because the regions unable to be sequenced, of which there is 14.6 %, may contain polymorphisms. In addition, there are several other genes for which candidate status may be given based on phenotypic and biochemical evidence.

Not only does this new chondrodysplasia of Texel sheep provide an important discovery for the agricultural industry in New Zealand, it has considerable potential as an animal model for studying various aspects of chondrodysplasia and resulting dwarfism in human patients. It will not only provide an opportunity to investigate aspects of cartilage metabolism, but there is also considerable potential for its use in assessing methods of drug and/or gene therapy. Sheep are an excellent species for studying skeletal diseases, not only because of their size and ease of containment but the fact that the lambs are born alive and appear relatively normal at that age, thus providing an opportunity for early

intervention (Thompson *et al*, 2005). It is of great importance that the cause of this disease is determined, because if left unchecked it has the potential to become a serious issue for the Texel industry in New Zealand. Given that it is likely to be caused by a single autosomal recessive gene, the gene frequency in the Texel population could be high, and therefore become detrimental very quickly.

The current study has provided an insight into what might be the underlying cause of the disease, provided a number of clues as to what biochemical and genetic factors may be involved, and given a clear direction for further investigation. Ultimately the aim would be to develop a diagnostic genetic test, which would be relatively inexpensive, for identification of diseased and carrier individuals and therefore allow the elimination of the undesired gene from the population by standard breeding regimes. It would be essential that the test be inexpensive as many animals would have to be tested. However in order to do this effectively, the gene and mutation involved needs to be known. Once a mutation in a gene is identified a causative relationship has to be proven i.e. the mutated gene proven to co-segregate with the disorder. This may be achieved by a simple analysis of mutation associated with phenotype. Linkage analysis or quantitative trait loci (QTL) analysis using markers that co-segregate with the disease phenotype could also be used if no defects were found on the selected candidate gene.

The focus of future work will revolve around continued investigation into the genes of the sulfate activation pathway. It would be imperative to sequence the remainder of the DTDST gene, including intron-exon boundaries and splice sites, to determine whether it is causative or not. This could involve direct PCR and some inverse PCR, followed by DNA sequencing to obtain the boundary regions.

With the development of chondrocyte cultures a possibility would arise to investigate the *in vitro* synthesis of sulfated proteoglycans in these cultures, using radio-labeling. This would be very useful in determining the level of under-sulfation, if indeed the defect is associated with this part of proteoglycan synthesis.

Chondrocyte cultures also provide an opportunity to study the activation of sulfate in affected animals. This can be done by a pulse chase experiment involving monitoring of radio-labeled sulfate and its conversion to the high energy APS and PAPS molecules, and would allow assessment of the conversion of inorganic sulfate by the respective enzymes involved. This information could be used to determine whether the reduced sulfation was the result of a reduction in the availability of the PAPS donor molecule.

A prospect may also be that of examining the sulfotransferase activity. This would allow distinction between impaired sulfation as a result of reduced PAPS availability or as a result of impaired transferase activities. This would involve the use of a radio-labeled PAPS donor molecule. The amount of radio-labeled sulfate transferred from PAPS to the macromolecular acceptors would indicate the activity of the sulfotransferase enzyme in normal and affected animals.

In addition to the aforementioned experiments, it would be valuable to determine the level of sulfation derived from sulfhydryl compounds. By incubating chondrocyte cultures, grown from affected animal tissue, in the presence of different concentrations of cysteine one could observe using HPLC analysis whether any recovery in impaired sulfation of proteoglycans occurs. This type of experiment may be used to determine whether the ability to use cytoplasmic thiols could explain the variation seen within the affected phenotype.

It appears that the currently studied condition is a new recessively inherited chondrodysplasia of the Texel breed of sheep. This is strongly supported by a number of notable factors, and the results of a breeding trial, albeit with a relatively small population size. The defect is likely associated with a reduction in the level of sulfation of proteoglycans in the ECM of cartilage in affected animals. The likelihood of a collagen defect being causative was eliminated by demonstration that collagen species show no differences between normal and affected animals. An exonic region of the candidate gene, *DTDST*, was sequenced from normal and affected animals, and comparisons showed no base pair differences. The involvement of this gene in the disease has

therefore not been definitive. There are a number of further candidate genes that may be assessed for involvement in the disease. Ultimately, the aim would be to identify a causative mutation and implement DNA-based diagnostic testing. This would allow identification of carriers and their elimination from breeding stock.

Reference list

Argaves, W. S. McKeown-Longo P. J. Goetinck P. F. Absence of Proteoglycan Core Protein in the Cartilage Mutant Nanomelia. *FEBS Letters* 131(2), 265-268. 1981.

Arikawa-Hirasawa, E. Alexander H. L. Nishino I. Nonaka I. Ho N. C. Francamano C. A. Govindraj P. Hassell J. R. Devaney J. M. Spranger J. Stevenson R. E. Iannaccone S. Dalakas M. C. Yamada Y. Structural and Functional Mutations of the Perlecan Gene Causes Schwartz-Jampel Syndrome, with Myotonic Myopathy and Chondrodysplasia. *American Journal of Medical Genetics* 70, 1368-1375. 2002.

Arikawa-Hirasawa, E. Watanabe H. Takami H. Hassell JR. Y. Perlecan is essential for cartilage and cephalic development. *Nature Genetics* 23(3), 354-358. 1999.

Aszódi, A. Chan D. Hunziker E. Bateman J. F. Fassler R. Collagen II is essential for the removal of the notochord and the formation of intervertebral discs. *Journal of Cell Biology* 30, 1399-1412. 1998.

Bateman, J. F. Freddi S. Nattrass G. Savarirayan R. Tissue-specific RNA surveillance? Nonsense-mediated mRNA decay causes collagen X haploinsufficiency in Schmid metaphyseal chondrodysplasia cartilage. *Human Molecular Genetics* 12(3), 217-225. 2003.

Bingel, S. A. Sande R. D. Wight T. N. Chondrodysplasia in the Alaskan Malamute. Characterisation of Proteoglycans Dissociatively Extracted from Dwarf Growth Plates. *Laboratory Investigation* 53(4), 479-485. 1985.

Bonaventure, J. Chaminade F. Maroteaux P. Mutations in three subdomains of the carboxy-terminal region of collagen type X account for most of the Schmid metaphyseal dysplasias. *Human Genetics* 96(1), 58-64. 1995.

Bonnemann, C. G. Cox G. F. Shapiro F. Wu J. J. Feener C. A. Thompson T. G. Anthony D. C. Eyre D. R. Darras B. T. Kunkel L. M. A mutation in the alpha 3 chain of type IX collagen causes autosomal dominant multiple epiphyseal dysplasia with mild myopathy. *Proceedings of the National Academy of Science of the United States of America* 97(5), 1212-1217. 2000.

Brenig, B. Baumgartner B. G. Kriegesmann B. Habermann F. Fries R. Swalve H. H. Molecular cloning, mapping, and functional analysis of the bovine sulfate transporter SLC26a2 gene. *Gene* 319, 161-166. 2003.

Brennan, M. J. Oldberg A. Ruoslathi E. Brown K. Schwartz N. Immunological Evidence for Two Distinct Chondroitin Sulfate Proteoglycan Core Proteins: Differential Expression in Cartilage Matrix Deficient Mice . *Developmental Biology* 98, 139-147. 1983.

Cavanagh, J. A. L. Tammen I. Windsor P. A. Nicholas F. W. Raadsma H. W. Identification of the gene causing chondrodysplasia in Dexter cattle. *Proceedings of the 7th World Congress on Genetics Applied to Livestock Production* 22, 1-4. 2002.

Chan, D. Freddi S. Weng Y. M. Bateman J. F. Interaction of Collagen $\alpha 1(X)$ Containing Engineered NCI Mutations with Normal $\alpha 1(X)$ *in Vitro* . *The Journal of Biological Chemistry* 274(19), 13091-13097. 1999.

Cockett, N. E. Shay T. L. Beever J. E. Nielsen D. Albreetsen J. Georges M. Peterson K. Stephens A. Vernon W. Timofeevskaja O. South S. Mork J. Maciulis A. Bunch T. D. Localization of the locus causing spider lamb syndrome to the distal end of ovine chromosome 6 . *Mammalian Genome* 10(1), 35-38. 1999.

Corsi, A. Riminucci M. Fisher L. W. Bianco P. Achondrogenesis Type 1B Agenesis of Cartilage Interterritorial Matrix as the Link Between Gene Defect and Pathological Skeletal Phenotype. *Archives of Pathology and Laboratory Medicine* 125, 1375-1378. 2001.

Costell, M. Gustafsson E. Aszodi A. Morgelin M. Bloch W. Hunziker E. Addicks K. Timpl R. Fassler R. Perlecan Maintains the Integrity of Cartilage and Some Basement Membranes. *The Journal of Cell Biology* 147(5), 1109-1122. 1999.

Crombrughe, B. Lefebvre V. Nakashima K. Regulatory mechanisms in the pathways of cartilage and bone formation. *Current Opinion in Cell Biology* 13, 721-727. 2001.

Dertinger, S. Soeder S. Bosch H. Aigner T. Matrix composition of cartilaginous anlagen in achondrogenesis type II (Langer-Saldino). *Frontiers in Bioscience* 10, 446-453. 2005.

Diab, M. Wu J. J. Shapiro F. Eyre D. Abnormality of type IX collagen in a patient with diastrophic dysplasia. *American Journal of Medical Genetics* 49(4), 402-409. 1994.

Duffell, S. J. Lansdown A. B. G. Richardson C. Skeletal abnormalities of sheep: Clinical radiological and pathological account of occurrence of dwarf lambs. *The Veterinary Record* 117, 571-576. 1985.

Eck, D., Ryan, J. The Chi Square Statistic.
<http://math.hws.edu/javamath/ryan/ChiSquare.html>, 2005.

- Epstein, D. L. Polifka J. E. Omoy A. Beckman D. A. Carbone J. P. Brent R. L. Evaluation of bone mineralization using the brachymorphic mouse (bm/bm) model. *Teratology* 37(5), 453-454. 1988.
- Eyre, D. Collagen of articular cartilage. *Arthritis Research* 4, 30-35. 2002.
- Eyre D. R., Weis M. A. Moskowitz R. W. Cartilage Expression of a Type II Collagen Mutation in an inherited Form of Osteoarthritis Associated with a Mild Chondrodysplasia. *Journal of Clinical Investigation* 87, 357-361. 1991.
- Fernandes, R. J. Schmid T. M. Eyre D. R. Assembly of collagen types II, IX and XI into nascent hetero-fibrils by a rat chondrocyte cell line. *European Journal of Biochemistry* 270, 3243-3250. 2003.
- Francamano, C. A. McIntosh I. Wilkin D. J. Bone dysplasias in man: molecular insights. *Current Opinion in Genetics and Development* 6, 301-308. 1996.
- French, M. M. Smith S. E. Akanbi K. Sanford T. Hecht J. Farach-Carson M. C. Carson D. D. Expression of the Heparin Sulfate Proteoglycan, Perlecan, during Mouse Embryogenesis and Perlecan Chondrogenic Activity In Vitro. *The Journal of Cell Biology* 145(5), 1103-1115. 1999.
- Gundlach, M. W. Conrad H. E. Glycosyl transferases in chondroitin sulfate biosynthesis. *Biochemical Journal* 226, 705-714. 1985.
- Hyttinen, M. M. Toyras J. Lapvetelainen T. Lindblom J. Prockop D. J. Li S-W. Arita M. Jurvelin J. S. Helminen H. J. Inactivation of one allele of the type 2 collagen gene alters the collagen network in murine articular cartilage and makes cartilage softer. *Annals of Rheumatic Disease* 60(3), 262-268. 2001.
- Ichimura, S. Wu J. J. Eyre D. R. Two-Dimensional Peptide Mapping of Cross-Linked Type IX Collagen in Human Cartilage. *Archives of Biochemistry and Biophysics* 378(1), 33-39. 2000.
- Ikegawa, S. Nakamura K. Nagano A. Haga N. Nakamura Y. Mutations in the N-terminal globular domain of the type X collagen gene (COL10A1) in patients with Schmid metaphyseal chondrodysplasia. *Human Mutation* 9(2), 131-135. 1997.
- Ikegawa, S. Nishimura G. Nagai T. Hasegawa T. Ohashi H. Nakamura Y. Mutations of the Type X Collagen Gene (*COL11A1*) Causes Spondylometaphyseal Dysplasia. *American Journal of Human Genetics* 63, 1659-1662. 1998.

- Ito, K. Kimata K. Sonue M. Suzuki S. Altered proteoglycan synthesis by epiphyseal cartilages in culture at low sulfate concentration. *Journal of Biological Chemistry* 257, 917. 1982.
- Jacenko, O. Chan D. Franklin A. Ito Susumu Underhill C. B. Bateman J. F. Campbell M. R. A Dominant Interference Collagen X Mutation Disrupts Hypertrophic Chondrocyte Pericellular Matrix and Glycosaminoglycan and Proteoglycan Distribution in Transgenic Mice. *American Journal of Pathology* 159(6), 2257-2269. 2001.
- Jones, J. M. Jolly R. D. Dwarfism in Hereford cattle: a genetic morphological and biochemical study. *New Zealand Veterinary Journal* 30, 185-189. 1982.
- Karniski, L. P. Mutations in the diastrophic dysplasia sulfate transporter (DTDST) gene: correlation between sulfate transport activity and chondrodysplasia phenotype. *Human Molecular Genetics* 10(14), 1485-1490. 2001.
- Kikukawa, K. Suzuki K. Histochemical and Immunological Distribution of Glycosaminoglycans, Type 2 Collagen, and Fibronectin in Developing Fetal Cartilage of Congenital Osteochondrodysplasia Ray (ocd/ocd). *Teratology* 46, 509-523. 1992.
- Kimata, K. Barrach H. J. Brown K. S. Pennypacker J. P. Absence of Proteoglycan Core Protein in Cartilage from the cmd/cmd (Cartilage Matrix Deficient) Mouse. *The Journal of Biological Chemistry* 256(13), 6961-6968. 1981.
- Kimura, K. Warman M. L. Krishnan S. Domowicz M. Krueger Jr R. C. Deyrup A. Schwartz N. B. A member of a family of sulfate-activating enzymes causes murine brachymorphism. *Proceedings of the National Academy of Science of the United States of America* 95(15), 8681-8685. 1998.
- Krueger, R. C. Kurima K. Schwartz N. B. Completion of the mouse aggrecan gene structure and identification of the defect in the cmd-Bc mouse as a near complete deletion of the murine aggrecan gene. *Mammalian Genome* 10(12), 1119-1125. 1999.
- Kuivaniemi, H. Tromp G. Prockop D. J. Mutations in Fibrillar Collagens (Type I, II, III, And XI), Fibril-Associated Collagen (Type IX), And Network-Forming Collagen (Type X) Cause a spectrum Of Disease of Bone, Cartilage, and Blood Vessels. *Human Mutation* 9, 300-315. 1997.
- Kwan, K. M. Pang M. K. M. Zhou S. Cowen S. K. Kong R. Y. C. Pfordte T. Olsen B. R. Sillence D. O. Tam P. P. L. Cheah K. S. E. Abnormal Compartmentalization of Cartilage Matrix Components in Mice Lacking Collagen X: Implications for Function. *The Journal of Cell Biology* 136(2), 459-471. 1997.

Landauer, L. Chang T. K. The Ancon or Otter Sheep History and Genetics. *The Journal of Heredity* 40, 105-112. 1949.

Leach Jr, R. M. Role of manganese in mucopolysaccharide metabolism. *Federation Proceedings* 30, 991-994. 1971.

Li, S. Takanosu M. Arita M. Bao Y. Ren Z. Maier A. Prockop D. J. Mayne R. Targeted disruption of *Coll11a2* produces a mild cartilage phenotype in transgenic mice: Comparison with the human disorder otospondylomegaphyseal dysplasia (OSMED). *Developmental Dynamics* 222(2), 141-152. 2001.

Li, Y. Lacerda D. A. Warman M. L. Beier D. R. Yoshioka H. Ninomiya Y. Oxford J. T. Morris N. P. Andrikopoulos K. Ramirez F. Wardell B. B. Lifferth G. D. Teuscher C. Woodward S. R. Taylor B. A. Seegmiller R. E. Olsen B. R. A fibrillar collagen gene, *Coll1A1*, is essential for skeletal morphogenesis. *Cell* 80, 423-430. 1995.

Liu, A. C. H. Heinrichs B. S. Leach JR. R. M. Influence of Manganese Deficiency on the Characteristics of Proteoglycans in Avian Epiphyseal Growth Plate Cartilage. *Poultry Science* 73, 663-669. 1994.

Lozzo, R. V. Murdoch A. D. Proteoglycans of the extracellular environment: Clues from the gene and protein side offer novel perspectives in molecular diversity and function. *FASEB Journal* 10, 598-614. 1996.

Luo, W. Kuwada T. S. Chandrasekaran L. Zheng J. Tanzer M. L. Divergent Secretory Behaviour of the Opposite Ends of Aggrecan. *The Journal of Biological Chemistry* 271(28), 16447-16450. 1996.

Maddox, B. K. Garofalo S. Keene D. R. Smith C. Horton W. A. Type II Collagen Pro- α -Chains Containing a Gly574Ser Mutation Are Not Incorporated into the Cartilage Matrix of Transgenic Mice. *Matrix Biology* 16, 93-103. 1997.

Melkonniemi, M. Brunner H. G. Manouvrier S. Hennekam R. Superti-Furga A. Kääriäinen H. Pauli R. M. van Essen T. Warman M. L. Bonaventure J. Miny P. Alla-Kokko L. Autosomal Recessive Disorder Otospondylomegaepiphyseal Dysplasia Is Associated with Loss-of-Function Mutations in the *COL11A2* Gene. *American Journal of Human Genetics* 66, 368-377. 2000.

Minor, R. R. Famum C. E. Animal Models with Chondrodysplasia/Osteochondrodysplasia. *Pathology and Immunopathology Research* 7, 62-67. 1988.

Mortier, G. R. Weis M. A. Nuytinck L. King L. M. Wilkin D. J. De Paepe A. Lachman R. S. Rimoin D. L. Eyre D. R. Cohn D. H. Report of five novel and one recurrent *COL2A1* mutations with analysis of genotype-phenotype correlation in patients with a lethal type II collagen disorder. *Journal of Medical Genetics* 37, 263-271. 2000.

Muragaki, M. Mariman E. C. M. van Beersum S. E. C. perälä M. van Mourik J. B. A. Warman M. J. Olsen B. R. Hamel B. C. J. A mutation in the gene encoding the $\alpha 2$ chain of the fibril-associated collagen IX, *COL9A2*, causes multiple epiphyseal dysplasia (EDM2). *Nature Genetics* 12, 103-105. 1996.

Murray, L. W. Bautista J. James P. L. Rimoin D. L. Type II collagen defects in the chondrodysplasias. I. Spondyloepiphyseal dysplasias. *American Journal of Human Genetics* 45(1), 5-15. 1989.

Mäkitie, O. Savarirayan R. Bonafé L. Robertson S. Susic M. Superti-Furga A. Cole W. G. Autosomal recessive multiple epiphyseal dysplasia with homozygosity for C653S in the *DTDST* gene: Double-layer patella as a reliable sign. *American Journal of Medical Genetics* 122A, 187-192. 2003.

Nakano, T. Walker B. Young B. A. Analysis of tissues from normal lambs and those with spider syndrome. *Canadian Journal of Animal Science* 74(3), 583-585. 1994.

Nakashima, E. Kitoh H. Haga N. Kosaki R. Mabuchi A. Nashimura G. Ohashi H. Ikegawa S. Novel *COL9A3* Mutation in a Family With Multiple Epiphyseal Dysplasia. *American Journal of Medical Genetics* 132A, 181-184. 2005.

Oberbauer, A. M. East N. E. Pool R. Rowe J. D. BonDurant R. H. Developmental progression of the Spider Lamb Syndrome. *Small Ruminant Research* 18, 179-184. 1995.

Oldberg, A. Antonsson P. Hedbom E. Heinegard D. Structure and function of extracellular matrix proteoglycans. *Biochemical Society Transactions* 18, 789-792. 1990.

Olsen, B. R. Mutations in Collagen Genes Resulting in Metaphyseal and Epiphyseal Dysplasias. *Bone* 17(2 Supplement), 45S-49S. 1995.

Orkin, R. W. Williams B. R. Cranley R. E. Poppke D. C. Brown K. S. Defects in the cartilaginous growth plates of brachymorphic mice. *Journal of Cell Biology* 73, 287-297. 1977.

Paasilta, P. Lohiniva J. Annunen S. Bonaventure J. Le Merrer M. Pai L. Ala-kokko L. *COL9A3*: A Third Locus for Multiple epiphyseal Dysplasia. *American Journal of Human Genetics* 64, 1036-1044. 1999.

- Richards, A. J. Yates J. R. W. Williams R. Payne S. J. Pope F. M. Scott J. D. Snead M. P. A family with Stickler syndrome type 2 has a mutation in the *COL11A1* gene resulting in the substitution of glycine 97 by valine in $\alpha 1$ (XI collagen. *Human Molecular Genetics* 5(9), 1339-1343. 1996.
- Rook, J. S. Trapp A. L. Krehbiel J. Yamini B. Benson M. Diagnosis of hereditary chondrodysplasia (spider lamb syndrome) in sheep. *Journal of the American Veterinary Medical Association* 193(6), 713-718. 1988.
- Rossi, A. Bonaventure J. Delezoide A. Cetta G. Superti-Furga A. Undersulfation of Proteoglycans Synthesized by Chondrocytes from a Patient with Achondrogenesis Type 1B Homozygous for an L483P Substitution in the Diastrophic Dysplasia Sulfate Transporter. *The Journal of Biological Chemistry* 271(31), 18456-18464. 1996.
- Rossi, A. Cetta G. Piazza R. *In Vitro* Proteoglycan Sulfation Derived from Sulfhydryl Compounds in Sulfate Transporter Chondrodysplasias. *Pediatric Pathology and Molecular Medicine* 22, 311-321. 2003.
- Rossi, A. Kaitila I. Wilcox W. R. Rimoin D. L. Steinmann B. Cetta G. Superti-Furga A. Proteoglycan sulfation in cartilage and cell cultures from patients with sulfate transporter chondrodysplasias: Relationship to clinical severity and indications on the role of intracellular sulfate production. *Matrix Biology* 17(5), 361-369. 1998.
- Rossi, A. Superti-Furga A. Mutations in the Diastrophic Dysplasia Sulfate Transporter (DTDST) Gene (SLC26A2): 22 Novel Mutations, Mutation Review, Associated Skeletal Phenotypes, and Diagnostic Relevance. *Human Mutation* 17, 159-171. 2001.
- Sahlman, J. Pitkänen M. T. Prockop D. J. Arita M. Li S. Helminen H. J. Langsjö T. K. Puustjarvi K. Lammi M. J. A Human *COL2A1* Gene With an Arg519Cys Mutation Causes Osteochondrodysplasia in Transgenic Mice. *Arthritis & Rheumatism* 50(10), 3153-3160. 2004.
- Satoh, H. Susaki M. Shukunami C. Iyama K. Negoro T. Hiraki Y. Functional Analysis of Diastrophic Sulfate Transporter. *The Journal of Biological Chemistry* 273(20), 12307-12315. 1998.
- Sawai, H. Ida A. Nakata Y. Koyama K. Noval missense mutation resulting in the substitution of tyrosine by cysteine at codon 597 of the type X collagen gene associated with Schmid metaphyseal chondrodysplasia. *Human Genetics* 43(4), 259-261. 1998.
- Shelton, M. A Recurrence of the Ancon Dwarf in Marino Sheep. *The Journal of Heredity* 59, 267-268. 1968.

- Singh, B. Schwartz N. B. Identification and Functional Characterization of the Novel BM-motif in the Murine Phosphoadenosine Phosphosulfate (PAPS) Synthetase. *The Journal of Biological Chemistry* 278(1), 71-75. 2003.
- So, C. L. Kaluarachchi K. Tam P. P. Cheah K. S. Impact of mutations of cartilage matrix genes on matrix structure, gene activity and chondrogenesis. *Osteoarthritis Cartilage* 9 Supplement A, S160-173. 2001.
- Sokal, R. R. Rohlf F. J. *Biometry: The principles and practice of statistics in biological research*. W. H. Freeman and company, San Fransisco, 1969.
- Spranger, J. The type XI collagenopathies. *Pediatric Radiology* 28, 745-750. 1998.
- Steinmann, B. Rao V. H. Vogel A. Bruckner P. Gitzelmann R. Byers P. H. Cysteine in the Triple-helical Domian of One Allelic Product of the alpha1 (1) Gene of Type I Collagen Produces a Lethal Form of Osteogenesis Imperfecta . *The Journal of Biological Chemistry* 259(17), 11129-11138. 1984.
- Stirpe, N. S. Argraves W. S. Goetinck P. F. Chondrocytes from the Cartilage Proteoglycan-Deficient Mutant, Nanomelia, Synthesize Greatly Reduced Levels of the Proteoglycan Core Protein Transcript. *Developmental Biology* 124, 77-81. 1987.
- Subramaniam, S. *Biology Workbench*. 2005. <http://workbench.sdsc.edu/>
- Sugahara, K. Schwartz N. B. Defect in 3'-phosphoadensine 5'-phosphosulfate formation in brachymorphic mice. *Proceedings of the National Academy of Science of the United States of America* 76(12), 6615-6618. 1979.
- Superti-Furga, A. A Defect in the Metabolic Activation of Sulfate in a Patient with Achondrogenesis Type 1B. *American Journal of Human Genetics* 55, 1137-1145. 1994.
- Superti-Furga, A. *The Metabolic and Molecular Bases of Inherited Disease: Defects in Sulfate Meatabolism and Skeletal Dysplasias*. McGraw Hill, New York (2001).
- Superti-Furga, A. Hastbacka J. Wilcox W. R. Cohn D. H. van der Harten H. J. Rossi A. Blau N. Rimoin D. L. Steinmann B. Lander E. S. Gitzelmann R. Achondrogenesis type 1B is caused by mutations in the diastrophic dysplasia sulfate transporter gene. *Nature Genetics* 12, 100-102. 1996.
- Sykes, B. Puddle B. Francis M. Smith R. The estimation of two collagens from human dermis by interrupted gel electrophoresis. *Biochemical and Biophysical Research Communications* 72(4), 1472-1480. 1976.

- Thompson, K. G. Blair H. T. Linney L. E. West D. M. Byrne T. J. Inherited chondrodysplasia in Texel sheep. *New Zealand Journal of Veterinary Pathology*. 2005 (in press).
- Tiller, G. E. Polumbo P. A. Weis M. A. Bogaert R. Lachman R. S. Cohn D. H. Rimoin D. L. Eyre D. R. Dominant mutations in the type II collagen gene, COL2A1, produce spondyloepimetaphyseal dysplasia, Strudwick type. *Nature Genetics* 11(1), 87-90. 1995.
- Troyer, D. L. Thomas D. L. Stein L. E. A Morphological and Biochemical Evaluation of Spider Syndrome in Suffolk Sheep. *Anat. Histol. Embryol.* 17, 289-300. 1988.
- ul Haque, M. F. King L. M. Krakow D. Cantor R. M. Rusiniak M. E. Swank R. T. Superti-Furga A. Haque S. Abbas H. Ahmad W. Ahmad M. Cohn D. H. Mutations in Orthologous Genes in Human Spondyloepimetaphyseal Dysplasia and the Brachymorphic Mouse. *Nature Genetics* 20, 157-162. 1998.
- Valero, G. Alley M. R. Badcoe L. M. Manktelow B. W. Merral M. Lawes G. S. Chondrodystrophy in calves associated with manganese deficiency. *New Zealand Veterinary Journal* 38, 161-167. 1990.
- Vanek, J. A. Alstad A. D. Berg I. E. Misek A. R. Moore B. L. Limesand W. Spider syndrome in lambs: A clinical and postmortem analysis. *Veterinary Medicine* 81(7), 663-668. 1986.
- Vanek, J. A. Walter P. A. Alstad A. D. Radiographic diagnosis of hereditary chondrodysplasia in newborn lambs. *Journal of the American Veterinary Medical Association* 194(2), 244-248. 1989.
- Vertel, B. M. Grier B. L. Li H. Schwartz N. B. The Chondrodystrophy, nanomelia: biosynthesis and processing of the defective aggrecan precursor. *Biochemical Journal* 301, 211-216. 1994.
- Vertel, B. M. Walters L. M. Grier B. Maine N. Nanomelic chondrocytes synthesize, but fail to translocate, a truncated aggrecan precursor. *Journal of Cell Science* 104, 939-948. 1993.
- Weis, M. A. Wilkin D. J. Kim H. J. Wilcox W. R. Lachman R. S. Rimoin D. L. Cohn D. H. Eyre D. R. Structurally Abnormal Type II Collagen in a Severe Form of Kniest Dysplasia Caused by an Exon 24 skipping Mutation. *The Journal of Biological Chemistry* 273(8), 4761-4768. 1998.

West, D. M. Burbidge H. M. Vermunt J. J. Aurther D. G. Hereditary chondrodysplasia ("spider syndrome") in a New Zealand Suffolk lamb of American origin. *New Zealand Veterinary Journal* 43, 118-122. 1995.

Wisconsin Package Version 9.1, Genetics Computer Group (GCG), Madison, Wisconsin, 2005.

Wray, C. Mathieson. A. O. An Achondroplastic Syndrome in South Country Cheviot Sheep. *The Veterinary Record* 88, 521-522. 1971.

Yanagishita, M. *Glycoforum: Proteoglycan*. 2005.

<http://www.glycoforum.gr.jp/science/word/proteoglycan/PGA06E.html>

Yang, P. Klimis-Tavantzis D. J. Manganese deficiency alters arteial glycosaminoglycan structure in the Sprague-Dawley rat. *Journal of Nutritional Biochemistry* 9, 324-331. 1998.

Appendix A

Ewe parturition data (pilot trial – year 1)

Born	Lamb ID	Dam ID	Sex	Rank	Birth weight (kg)	Status
24-Aug						
	3-Jan	14 Affected	f	Single	4.5	Affected
27-Aug						
	3-Feb	10	f	Twin to 3-03	4.1	Affected
	3-Mar	10	m	Twin to 2-03	4	Carrier
1-Sep						
	3-Apr	1	f	Single	4	Carrier
	3-May	21 Affected	m	Single	5	Affected
	3-Jun	6	f	Twin to 7-03	3.5	Carrier
	3-Jul	6	f	Twin to 6-03	3.1	Carrier
	3-Aug		f	Single	3.6	Carrier
2-Sep						
	3-Sep	9262	m	Twin to 10-03	4.1	Carrier
	3-Oct	9262	f	Twin to 9-03	6	Carrier
3-Sep						
	3-Nov	9055	m	Twin to 12-03	5	Affected
	3-Dec	9055	m	Twin to 11-03	5	Affected
4-Sep						
	13-03	11	m	Twin to 14-03	5.1	Carrier
	14-03	11	f	Twin to 13-03	4.6	Affected
	15-03	8	f	Single	5	Carrier
	16-03	5	m	Twin to 17-03	6.5	Carrier
	17-03	5	f	Twin to 16-03	5.1	Affected
6-Sep						
	18-03	22 Affected	f	Single	5.5	Affected
	19-03	9011	f	Single	6.8	Affected
7-Sep						
	20-03	174	m	Twin to 21-03	5.5	Carrier
	21-03	174	f	Twin to 20-03	4.5	Carrier
8-Sep						
	22-03	2	m	Twin to 23-03	5	Carrier
	23-03	2	m	Twin to 22-03	6	Affected
	24-03	26 Affected	m	Single	6	Affected
	25-03	12	m	Twin to 26-03	5.1	Carrier
	26-03	12	f	Twin to 25-03	4.5	Affected
9-Sep						
	27-03	15 Affected	m	Single	7.1	Affected
14-Sep						
	28-03	3	f	Single	5.5	Carrier
23-Sep						
	29-03	3081	f	Single	6.2	Carrier
	30-03	3220	m	Twin to 31-03	5.5	Affected
	31-03	3220	m	Twin to 30-03	6.1	Carrier
	32-03	9159	m	Single	7.5	Carrier
	33-03	9155	f	Single	5.5	Affected

	34-04	9285	f	Single	7	Affected
1-Oct						
	35-03	9	m	Twin to 36-03	5	Affected
	36-03	9	m	Twin to 35-03	4.7	Affected
20-Oct						
	201-03	4	m	Twin to 202-03	4.5	Carrier
	202-03	4	f	Twin to 201-03	4.6	Carrier

Appendix B

Ewe scanning data (pilot trial – year 2)

ewe ID	ewe weight (kg) 03/05/2004	status	scanned (# lambs) (29/07/2004)	period
1	70.5	in lamb	2	E
R2	71	in lamb	2	E
R1	68.5	in lamb	2	E
9285	71.5	in lamb	1	E
9262	81	in lamb	2	E
9155	72	in lamb	1	L
9055	71	in lamb	2	E
9011	82.5	in lamb	2	E
3220	76.5	dry	0	N/A
3081	57.5	in lamb	2	E
1212	75	in lamb	1	E
174	80.5	in lamb	3	E
26	59.5	in lamb	2	E
22	58.5	in lamb	1	E
12	83	in lamb	2	E
10	75	in lamb	2	E
8	50	in lamb	1	E
6	81.5	in lamb	2	E
5	86.5	in lamb	3	E
4	84.5	dry	0	N/A
3	81	in lamb	2	E
2	75	in lamb	2	E
22	73.273		37	

Period refers to the cycle that the ewe was expected to give birth in, based on the age and size of the foetus at scanning. E refers to lambs that expected to be born early, and were conceived in the first oestrous cycle. While L refers to lambs expected to be born late, and were conceived in the second oestrous cycle.

Appendix C

Ewe parturition data (pilot trial – year 2)

Bom	Lamb ID	Sex	Rank	Birth weight (kg)	Status
9/26/2004	2-04	F	Single	5.2	
9/28/2004	9-04	F	Single	5.5	Carrier
	10-04	M	Single	5.3	Affected
9/29/2004	19-04	F	Triplet to 20-04 and 20a-04	4.1	Carrier
	20-04	F	Triplet to 19-04 and 20a-04	3.5	Carrier
	20a-04	M	Triplet to 19-04 and 20-04	3.8	
9/30/2004	22-04	F	Triplet to 23-04 and 24-04	3.7	Affected
	23-04	M	Triplet to 22-04 and 24-04	4.6	Carrier
	24-04	M	Triplet to 22-04 and 23-04	4.0	Affected
10/1/2004	30b-04	F	Twin to 30c-04	3.0	Obligate affected
	30c-04	F	Twin to 30b-04	4.4	Obligate affected
10/2/2004	32-04	M	Single	5.0	Obligate affected
10/3/2004	35-04	F	Twin to 36-04	4.5	Affected
	36-04	F	Twin to 35-04	4.2	Carrier
10/5/2004	39-04	M	Single	5.8	Carrier
10/10/2004	45-04	F	Twin to 46-04	4.2	Carrier
	46-04	F	Twin to 45-04	4.3	Carrier
	47-04	M	Twin to 48-04	5.6	Affected
	48-04	F	Twin to 47-04	4.5	Carrier
	50-04	M	Single	6.8	Carrier
10/13/2004	58-04	M	Single	5.5	Carrier
10/14/2004	60-04	F	Twin to 61-04	3.3	
	61-04	M	Twin to 60-04	3.6	
	62-04	F	Twin to 63-04	3.1	Carrier
	63-04	F	Twin to 62-04	4.3	Carrier
10/21/2004	79-04	F	Single	6.1	Affected

Appendix D

Hogget scanning data (backcross – year 2)

hogget ID	hogget weight (kg) 3/5/2004	status	scanned (# lambs) (29/07/04)	period
4	38	pilot (dry)	0	N/A
10	29.5	pilot (in lamb)	1	L
15	24	pilot (dry)	0	N/A
21	42	pilot (dry)	0	N/A
28	38	pilot (in lamb)	1	E
29	39.5	pilot (in lamb)	1	E
41	36.5	in lamb	1	E
42	36	dry	0	N/A
43	27	dry	0	N/A
44	34	in lamb	1	E
46	30.5	in lamb	2	L
47	36.5	in lamb	1	E
48	47.5	dry	0	N/A
49	44	in lamb	1	E
50	39.5	dry	0	N/A
51	40	in lamb	1	E
52	46.5	dry	0	N/A
53	38	dry	0	N/A
54	36.5	in lamb	1	E
55	40	in lamb	1	E
56	34	in lamb	1	E
57	33	in lamb	1	E
59	30.5	dry	0	N/A
60	35	in lamb	2	E
61	31	in lamb	1	L
62	43	dry	0	N/A
63	34	culled (2/6/04)	0	N/A
64	24.5	dry	0	N/A
65	39.5	dry	0	N/A
66	31	culled (2/6/04)	0	N/A
67	26.5	in lamb	1	L
68	23.5	in lamb	1	E
69	29.5	in lamb	1	E
70	38.5	dry	0	N/A
71	34.5	in lamb	1	E
72	32	in lamb	1	L
73	39	dry	0	N/A
74	35.5	in lamb	2	E
76	33	in lamb	1	L
77	36	in lamb	1	E
78	35	in lamb	1	L
79	28	in lamb	1	L
80	33.5	in lamb	1	E

82	39.5	in lamb	1	L
84	30.5	in lamb	1	E
85	33	culled (2/6/04)	0	N/A
86	26	dry	0	N/A
87	27	in lamb	1	E
88	25.5	in lamb	1	E
89	31	in lamb	1	L
90	42.5	dry	0	N/A
91	40	in lamb	2	E
93	30	in lamb	1	L
94	45	in lamb	1	E
95	34.5	in lamb	1	L
96	33.5	in lamb	1	E
97	34.5	dry	0	N/A
98	41.5	dry	0	N/A
99	34.5	in lamb	1	L
100	38.5	in lamb	1	E
101	41.5	in lamb	1	E
102	33.5	culled (2/6/04)	0	N/A
103	30	in lamb	1	L
104	33	in lamb	1	E
105	35.5	in lamb	1	E
106	33	in lamb	1	L
107	32	in lamb	1	E
108	40.5	in lamb	1	E
109	37.5	in lamb	2	L
110	32	in lamb	1	E
111	31	in lamb	2	L
112	35	in lamb	1	L
113	37.5	dry	0	N/A
114	34	dry	0	N/A
116	40.5	in lamb	1	E
117	35	in lamb	2	L
118	34.5	in lamb	1	E
119	37	dry	0	N/A
120	36.5	dry	0	N/A
121	24.5	dry	0	N/A
122	34	in lamb	1	E
124	31.5	in lamb	1	E
126	37.5	in lamb	1	E
127	36.5	in lamb	1	E
128	29	culled (2/6/04)	0	N/A
129	41.5	in lamb	2	E
130	41	dry	0	N/A
131	40	in lamb	1	E
132	43.5	in lamb	1	E
133	37	in lamb	1	L
135	30	dry	0	N/A
136	34	in lamb	1	E
137	32	in lamb	1	E

138	30.5	dry	0	N/A
139	26.5	culled (2/6/04)	0	N/A
141	28.5	in lamb	1	L
142	41	in lamb	1	E
144	38.5	in lamb	1	L
145	25	culled (2/6/04)	0	N/A
147	39.5	in lamb	1	E
148	29.5	dry	0	N/A
150	33.5	in lamb	1	E
151	36	in lamb	1	E
152	38.5	in lamb	1	E
153	36	dry	0	N/A
154	31	dry	0	N/A
155	41	in lamb	1	E
156	28.5	dry	0	N/A
157	33	culled (2/6/04)	0	N/A
158	36	in lamb	1	E
159	36	in lamb	2	E
161	37	dry	0	N/A
163	30	dry	0	N/A
164	31	dry	0	N/A
166	40.5	in lamb	2	E
167	31	dry	0	N/A
168	31	dry	0	N/A
169	39	in lamb	1	L
170	32.5	in lamb	1	E
171	32	in lamb	1	E
172	28.5	culled (2/6/04)	0	N/A
174	34	in lamb	1	L
175	29.5	in lamb	1	L
	34.6		88	

Period refers to the cycle that the ewe was expected to give birth in, based on the age and size of the foetus at scanning. E refers to lambs that expected to be born early, and were conceived in the first oestrous cycle. While L refers to lambs expected to be born late, and were conceived in the second oestrous cycle.

Appendix E

Hogget parturition data (backcross – year 2)

Born	Lamb ID	Sex	Rank	Birth weight (kg)	Status
9/26/2004					
d	1-04	M	Single	3.7	Carrier
d	3-04	F	Single	3.6	Affected
9/27/2004					
d	4-04	F	Single	4.0	Carrier
d	5-04	F	Single	3.5	Affected
d	6-04	F	Single	4.1	Carrier
9/28/2004					
	7-04	F	Twin to 8-04	3.2	
	8-04	M	Twin to 7-04	3.3	
9/29/2004					
d	11-04	F	Single	3.2	Carrier
d	12-04	F	Single	4.5	Carrier
d	13-04	F	Single	3.4	Carrier
d	14-04	M	Twin to 15-04	3.9	Carrier
d	15-04	F	Twin to 14-04	3.9	Affected
d	16-04	M	Twin to 17-04	4.0	Affected
d	17-04	M	Twin to 16-04	4.8	Carrier
d	18-04	F	Single	3.8	Affected
d	21-04	F	Single	4.6	Carrier
9/30/2004					
d	25-04	M	Twin to 25a-04	3.5	Carrier
	25a-04	M	Twin to 25-04	2.7	
d	26-04	M	Single	4	Carrier
d	27-04	F	Single	3.8	Affected
10/1/2004					
d	28-04	M	Twin to 29-04	3.1	Carrier
d	29-04	M	Twin to 28-04	3.9	Carrier
d	30-04	F	Single	4.3	Affected
	30a-04	F	Single	4.3	
10/2/2004					
d	31-04	M	Single	5.0	Affected
d	33-04	M	Single	3.9	Carrier
	34-04	M	Single	6.3	
10/3/2004					
d	37-04	M	Single	3.1	Affected
	38-04	M	Single	4.3	
	38a-04	M	Single	6.7	
	38b-04	F	Single	5.8	
	38c-04	F	Single	4.6	
	38d-04	M	Single	5.3	
	38e-04	F	Single	4.0	
	38f-04	F	Single	4.7	
10/4/2004					

	38g-04	M	Single	6.6	
10/5/2004					
d	40-04	M	Single	5.1	Affected
10/6/2004					
d	40a-04	M	Twin to 40b-04	2.2	Affected
	40b-04	M	Twin to 40a-04	1.8	
	41-04	M	Twin to 41a-04	6.1	
	41a-04	M	Twin to 41-04	1.1	
	42-04	F	Single	3.7	
10/8/2004					
	43-04	F	Single	3.0	
10/10/2004					
d	44-04	F	Single	3.7	Carrier
d	49-04	M	Single	5.1	Affected
10/11/2004					
d	51-04	F	Single	2.1	Carrier
10/12/2004					
d	52-04	F	Single	4.1	Affected
d	53-04	M	Single	3.0	Carrier
d	54-04	F	Single	4.0	Carrier
	54a-04	F	Single	5.0	
	55-04	F	Single	3.1	
d	56-04	F	Twin to 57-04	4.2	
	57-04	M	Twin to 58-04	3.5	Affected
10/13/2004					
d	57a-04	M	Single	4.7	
	59-04	M	Single	5.0	Affected
10/14/2004					
d	64-04	F	Single	4.2	Carrier
	66-04	M	Single	4.5	
10/15/2004					
d	65-04	M	Single	3.8	Carrier
	67-04	M	Single	3.7	
	67a-04	F	Single	4.8	
10/16/2004					
d	68-04	F	Twin to 69-04	3.7	Affected
	69-04	F	Twin to 68-04	2.1	
	70-04	M	Single	4.4	
	71-04	F	Single	2.3	
d	72-04	M	Single	3.8	
10/17/2004					
d	73-04	F	Single	2.7	Carrier
	74-04	F	Single	2.0	
	75-04	M	Twin to 75a-04	2.0	
	75a-04	M	Twin to 75-04	2.3	
10/18/2004					
d	76-04	F	Twin to 77-04	3.7	Carrier
d	77-04	F	Twin to 76-04	3.7	Affected
	77a-04	M	Single	5.0	
10/19/2004					

	77b-04	M	Single	5.0	
10/20/2004					
d	78-04	M	Single	4.9	Affected
	78a-04	M	Single	3.9	
10/22/2004					
d	80-04	F	Single	4.6	Affected
	80a-04	M	Single	5.2	
10/24/2004					
d	81-04	F	Single	3.2	Carrier
d	No tag		Single		Carrier
10/25/2004					
	81a-04	F	Single	4.8	
	81b-04	M	Single	3.9	
10/26/2004					
d	82-04	F	Single	4.1	Affected
10/27/2004					
d	83-04	F	Single	3.7	Affected

Those lambs which were unable to be diagnosed because they died at birth or too soon after to allow diagnosis based on clinical signs, of which there are 37, are the individuals in the table above that lack the letter d in the “born” column

Appendix F

Protein (BSA) quantification for standard curve

Standard (µg)	abs. triplicates			Absorbance
0	0.262	0.272	0.266	0.267
0.4	0.32	0.311	0.335	0.322
0.6	0.345	0.333	0.353	0.344
0.8	0.389	0.396	0.384	0.390
1	0.406	0.41	0.418	0.411
1.5	0.488	0.487	0.503	0.493
2	0.545	0.556	0.558	0.553
2.5	0.607	0.633	0.641	0.627

Protein (collagen) quantification

Sample	abs	Conc.	abs	Conc.	abs	Conc.	Average conc. (2-fold)	undilute (µg/5µL)	(µg/µL)
C1	0.536	1.858	0.578	2.147	0.573	2.113	2.039	4.079	0.816
C2	0.581	2.168	0.600	2.298	0.578	2.147	2.204	4.409	0.882
C3	0.647	2.622	0.620	2.436	0.636	2.546	2.535	5.069	1.014
C4	0.598	2.285	0.593	2.250	0.591	2.237	2.257	4.514	0.903
C5	0.613	2.388	0.658	2.697	0.618	2.422	2.503	5.005	1.001
A1	0.571	2.099	0.576	2.133	0.582	2.175	2.136	4.271	0.854
A2	0.586	2.202	0.580	2.161	0.561	2.030	2.131	4.262	0.852
A3	0.619	2.429	0.607	2.347	0.520	1.748	2.175	4.349	0.870
A4	0.570	2.092	0.595	2.264	0.501	1.618	1.991	3.983	0.797

The table above represents absorbance's obtained from a dilution of the collagen extract.

In each case the fold dilution is converted back to a concentration per microlitre in the undiluted sample. Control animal samples are represented by C1, C2..... While affected animal samples are represented by A1, A2..... Absorbance (abs) was measured at 595nm. Conc. = concentration

Protein (BSA) quantification for standard curve

Standard (μg)	abs. triplicates			Absorbance
0	0.245	0.253	0.25	0.249
0.4	0.264	0.298	0.316	0.293
0.6	0.339	0.307	0.369	0.338
0.8	0.349	0.362	0.392	0.368
1	0.413	0.432	0.427	0.424
1.5	0.485	0.506	0.514	0.502
2	0.508	0.536	0.542	0.529
2.5	0.602	0.603	0.625	0.610

Protein (proteoglycan) quantification

Sample	abs	Conc.	abs	Conc.	abs	Conc.	Average conc. (2-fold)	undiluted ($\mu\text{g}/5\mu\text{L}$)	($\mu\text{g}/\mu\text{L}$)
C1	0.489	1.612	0.323	0.478	0.424	1.168	1.086	2.172	0.434
C2	0.399	0.997	0.378	0.854	0.388	0.922	0.924	1.849	0.370
C3	0.479	1.543	0.472	1.496	0.471	1.489	1.509	3.018	0.604
C4	0.419	1.134	0.395	0.970	0.395	0.970	1.025	2.049	0.410
A1	0.401	1.011	0.386	0.909	0.386	0.909	0.943	1.885	0.377
A2	0.385	0.902	0.397	0.984	0.392	0.949	0.945	1.890	0.378
A3	0.398	0.990	0.406	1.045	0.358	0.717	0.918	1.835	0.367
A4	0.383	0.888	0.352	0.676	0.353	0.683	0.749	1.499	0.300
	abs	Conc.	abs	Conc.	abs	Conc.	Average conc. (5-fold)	undiluted ($\mu\text{g}/5\mu\text{L}$)	($\mu\text{g}/\mu\text{L}$)
C1	0.297	0.301	0.298	0.308	0.304	0.349	0.319	1.596	0.319
C2	0.32	0.458	0.316	0.431	0.291	0.260	0.383	1.915	0.383
C3	0.369	0.792	0.351	0.670	0.344	0.622	0.695	3.473	0.695
C4	0.327	0.506	0.313	0.410	0.314	0.417	0.444	2.222	0.444
A1	0.319	0.451	0.327	0.506	0.325	0.492	0.483	2.415	0.483
A2	0.356	0.704	0.343	0.615	0.324	0.485	0.601	3.007	0.601
A3	0.318	0.444	0.285	0.219	0.307	0.369	0.344	1.721	0.344
A4	0.312	0.403	0.296	0.294	0.31	0.390	0.362	1.812	0.362
	abs	Conc.	abs	Conc.	abs	Conc.	Average conc. (10-fold)	undiluted ($\mu\text{g}/5\mu\text{L}$)	($\mu\text{g}/\mu\text{L}$)
C1	0.296	0.294	0.293	0.274	0.278	0.171	0.246	2.464	0.493
C2	0.284	0.212	0.276	0.158	0.281	0.192	0.187	1.873	0.375
C3	0.315	0.424	0.311	0.397	0.304	0.349	0.390	3.898	0.780
C4	0.29	0.253	0.292	0.267	0.285	0.219	0.246	2.464	0.493
A1	0.304	0.349	0.301	0.328	0.287	0.233	0.303	3.033	0.607
A2	0.3	0.322	0.299	0.315	0.286	0.226	0.287	2.874	0.575
A3	0.289	0.246	0.286	0.226	0.287	0.233	0.235	2.350	0.470
A4	0.289	0.246	0.292	0.267	0.304	0.349	0.287	2.874	0.575

The table above represents absorbance's obtained from differing dilutions of the proteoglycan extracts. In each case the fold dilution is converted back to a concentration per microlitre in the undiluted sample, and then the average taken from the three calculated undiluted concentration, for each sample. Control animal samples are represented by C1, C2..... While affected animal samples are represented by A1, A2..... Absorbance (abs) was measured at 595nm. Conc. = concentration.

Appendix G

PCR primers

Primer name	Exon primed	Sequence (5' – 3')
exon2-for	2	CATCTGGGATCCATGTGGAGCATGA
exon2-rev	2	CTCCAGCCACAAAGGTTACAGTGCT
exon3-for	3	AAGTGGGCTTTGTCTCAGTCTACCT
exon3-rev	3	GGACCATTGGGAACATATCTCTCTT

Sequencing primers

Primer name	Exon sequenced	Sequence (5' – 3')
exon2-for	2	CATCTGGGATCCATGTGGAGCATGA
exon2-rev	2	CTCCAGCCACAAAGGTTACAGTGCT
exon3-for	3	AAGTGGGCTTTGTCTCAGTCTACCT
exon3-rev	3	GGACCATTGGGAACATATCTCTCTT
exon3-for1	3	GCCTCCTTCACTATTCTT
exon3-for2	3	ATGTGGAGGATTAGCAGA
exon3-rev1	3	TCATGGCTTCATATACACTA
exon3-rev2	3	GAGGACAGCATAGTAACA